ISTANBUL TECHNICAL UNIVERSITY ★ GRADUATE SCHOOL OF SCIENCE

BCS-BEC CROSSOVER WITH MODEL SQUARE WELL INTERACTION IN 2D AND 3D

M.Sc. THESIS

Hasan Hüseyin SÖMEK

Department of Physics Engineering

Physics Engineering Programme

DECEMBER 2015

ISTANBUL TECHNICAL UNIVERSITY ★ GRADUATE SCHOOL OF SCIENCE

BCS-BEC CROSSOVER WITH MODEL SQUARE WELL INTERACTION IN 2D AND 3D

M.Sc. THESIS

Hasan Hüseyin SÖMEK
(509121105)

Department of Physics Engineering

Physics Engineering Programme

Thesis Advisor: Assoc. Prof. Dr. A. Levent SUBAŞI

DECEMBER 2015

İSTANBUL TEKNİK ÜNİVERSİTESİ ★ FEN BİLİMLERİ ENSTİTÜSÜ

İKİ VE ÜÇ BOYUTTA MODEL KARE KUYU POTANSİYELİ ETKİLEŞİMİYLE BCS-BEY GEÇİŞİ

YÜKSEK LİSANS TEZİ

Hasan Hüseyin SÖMEK
(509121105)

Fizik Mühendisliği Anabilim Dalı

Fizik Mühendisliği Programı

Tez Danışmanı: Doç. Dr. A. Levent SUBAŞI

ARALIK 2015

Hasan Hüseyin SÖMEK, a M.Sc. student of ITU Graduate School of ScienceEngineering and Technology with ID number 509121105 successfully defended the thesis entitled "BCS-BEC CROSSOVER WITH MODEL SQUARE WELL INTERACTION IN 2D AND 3D", which he prepared after fulfilling the requirements specified in the associated legislations, before the jury whose signatures are below.

Thesis Advisor :	**Assoc. Prof. Dr. A. Levent SUBAŞI** Istanbul Technical University	.....
Jury Members :	**Prof. Dr. Mehmet Nazmi POSTACIOĞLU** Istanbul Technical University	.....
	Assoc. Prof. Dr. Menderes IŞKIN Koç University	.....

Date of Submission : **27 November 2015**
Date of Defense : **24 December 2015**

To my parents,

FOREWORD

I would like to thank everyone in the Faculty of Science and Letters and the Physics Department. First I would like to express my gratitude to my supervisor A. Levent Subaşı for his suggestions, encouragement and guidance in writing the thesis and approaching different challenges and Nazmi Postacıoğlu for his help. Also, I would like to thank Tuğrul Hakioğlu for his advice, encouragement and his many-body course.

Finally, I would like to thank my parents for their constant support during the time of my studies.

December 2015

Hasan Hüseyin SÖMEK
(Research Assistant)

TABLE OF CONTENTS

Page

ABBREVIATIONS

BCS : Bardeen Cooper Schrieffer
BEC : Bose Einstein Condensation
B-V : Bogoliubov-Valatin
App : Appendix

LIST OF TABLES

Page

LIST OF FIGURES

Page

BCS-BEC CROSSOVER WITH MODEL SQUARE WELL INTERACTION IN 2D AND 3D

SUMMARY

Superfluidity is one of the most remarkable phenomena that we come across in many distinct fields of physics. It was first observed by H. K. Onnes in 1911 when he cooled a mercury sample below 4.2 Kelvin. He found that the sample conducts electricity without any dissipation. Both bosonic and fermionic systems can exhibit superfluidity. We focus on the fermionic superfluidity in this thesis. The crossover from weak coupling Bardeen-Cooper-Schrieffer (BCS) pairing to a Bose-Einstein condensate (BEC) of tightly bound pairs, as a function of the attractive interaction has long been of interest to theoretical physicists. The past decade has seen a series of remarkable experimental developments in ultracold Fermi gases that has realized the BCS-BEC crossover in the laboratory, bringing with it fresh new insights into the very strongly interacting unitary regime in the middle of this crossover. In this thesis we study the crossover from the BCS state to BEC in a Fermionic gas interacting with a model square well potential at zero temperature by tuning the interaction between fermions and using mean field approximation. The possibility to change the interaction strength allows the ground state of the system to evolve from a weakly interacting BCS limit to the strongly interacting BCS limit. The thesis consists of two parts. In the first part we examine the the BCS-BEC crossover in a 3-dimensional fermionic gas. We show that there is a crossover between two limits and calculate the physical quantities such as momentum distribution, energy per particle, excitation energies, changing of the chemical potential and superconducting gap parameter with respect to the interaction parameter or scattering length. In the second part we repeat the all process for the two-dimensional and quasi-two-dimensional system. We show that the crossover occurs at weaker interaction strength with respect to the three-dimensional system. We obtain strictly two-dimensional and three-dimensional limits by changing the thickness of the quasi-two-dimensional system. Within the developed formalism and numerical implementation it is possible to study different systems having different interaction or dispersion relations in which there is different interaction potential and linear energy dispersion with the numerical implementation given in the thesis.

İKİ VE ÜÇ BOYUTTA MODEL KARE KUYU POTANSİYELİ ETKİLEŞİMİYLE BCS-BEY GEÇİŞİ

ÖZET

Son yüz yıl içerisinde fiziğin bir çok alanında farklı fenomenlerle karşılaştık. Bunların en göz alıcı olanlarından biri de *süperiletkenlik* olayıdır. Hollandalı fizikçi Heike Kamerlingh Onnes 1908 yılında Helyum gazını sıvı hale dönüştürmeyi başardı. Bu başarı $4,2$ K'e kadar olan düşük sıcaklıklardaki fiziksel olayların özelliklerinin araştırılmasını mümkün hale getirdi. Metallerin elektriksel dirençlerinin bu düşük sıcaklık bölgelerindeki değişimi yine ilk defa Onnes tarafından incelendi. Onnes, sıvı Helyum'un keşfinden 3 yıl sonra, civa metalinde doğru akım elektriksel direncin kritik sıcaklık T_c diye adlandırdığı sıcaklık ve altındaki sıcaklıklarda ölçülemeyecek kadar küçük bir değere düştüğünü gözlemledi. Bu heyecan verici gözlem süperiletkenliğin keşfi olarak bilinmektedir. Bu çalışmadan dolayı Kamerling Onnes 1913 yılında Nobel Fizik ödülünü kazandı. O yıllarda kuantum kuramı daha oluşmamıştı. Bu yüzden süperiletkenliğin arkasındaki mekanizma anlaşılamamıştı ve süperiletkenliğin mikroskopik teorisi yaklaşık elli yıl sonra oluşturuldu.

Genel olarak doğada fermiyonlar ve bozonlar olmak üzere iki tip temel parçacık vardır. Bozonlar spini tam sayı olan parçacıklardır. Dalga fonksiyonları herhangi iki bosonun yerdeğiştirmesi durumda simetrik kalır ve bozonlar Bose-Einstein istatisiğine uyarlar. Bozonlar belli bir kritik sıcaklığın altında en düşük enerjili seviyede Bose-Einstein yoğuşması (BEY) gösterebilirler ve bu limitte tek bir "dev" dalga fonksiyonu ile temsil edilebilirler. Öte yandan fermiyonlar spini buçuklu olan parçacıklardır ve Fermi-Dirac istatistiğine uyarlar. Fermiyonların dalga fonksiyonları ise anti-simetriktir. Başka bir deyişle iki fermiyonun yer değiştirmesi durumunda dalga fonksiyonu işaret değiştirir. Bu sebepten fermiyonlar Pauli dışarlama ilkesine uyarlar, yani bütün kuantum mekaniksel özellikleri aynı olan iki fermiyon aynı enerji seviyesinde bulunamazlar.

Hem bozonik hem de fermiyonik sistemler süperiletkenlik veya süperakışkanlık gösterebilir. Fermiyonik süperakışkanlık nötron yıldızlarında, nükleer maddelerde, ve aşırı soğuk gazlarda görülmektedir. Helium-4'de bozonik süperakışkanlık gözlemlendikten sonra Alman fizikçi Fritz Wolfgang London BEC ile süperakışkanlığın arasında bir bağlantı olduğunu öne sürdü. Daha sonra akıllara femiyonik sistemlerde fermiyonların Pauli dışarlama ilkesini çiğnemeden nasıl en düşük enerjili seviyeye yoğuştuğu sorusu düşünülmeye başlandı. Fizikçiler sıkı bağlı elektron çiftlerinin bozonlar olarak düşünülebileceği ve böylelikle sistemin taban durumuna çökebilceğini hayal ettiler. Ancak, iki elektronun arasında çekici bir etkileşim bilinmiyordu. 1950'de bir kristalin içerisinde örgü titreşimlerinden dolayı elektronlar arasında efektif bir çekici etkileşim (elektron-fonon etkileşimi aracılığı ile) olduğu bulundu. Daha sonra 1956'da Leon Cooper elektron çifti problemini çözerek Fermi yüzeyinin üzerinde iki fermiyonun çekici bir etkileşimle bozonumusu yapılar oluşturabileceğini gösterdi. Bu bozonumsu yapılara "Cooper çifti" adı verilir. Ancak tek bir Cooper çifti fermiyonik süperakışkanlığı açıklayamaz. Cooper'ın çalışmalarından bir yıl sonra

John Bardeen, Leon Cooper ve Robert Schrieffer (BCS) üçlüsü, süperiletkenliğin mikroskopik teorisini tasvir ettikleri bir makale yayınladılar. Bu ünlü teori BCS teorisi olarak bilinir ve çok parçacıklı bir sistemin dalga foksiyonunun, üst üste binmiş sıfır kütle merkezi mometumuna, sıfır açısal momentuma (s-dalgası) ve sıfır spine sahip fermiyon çiftlerine karşılık geldiğini ileri sürer. BCS teorisinde parçacıklar arasındaki etkileşim zayıf ve çiftlerin boyutu parçacıklar arası ortalama mesafeden çok fazladır. 1986 yılında yüksek sıcaklık (100 K üzeri) süperiletkenliği gündeme geldi ve daha sonra bilim insanlarının en önemli amaçlardan biri oda sıcaklığında süperiletkenlik bulmak oldu. Ancak görüldü ki; yüksek sıcaklık süper iletkenlerinde Cooper çiftleri parçacıklar arası mesafeye göre çok küçükler. Bu yüzden BCS teorisi fermiyonların sıkıca bağlı olduğu ve güçlüce etkileşip Bose-Einstein yoğuşması gerçekleştirdiği bölgeyi de içerecek şekilde genelleştirilmek zorundaydı. Dolayısıyla bu teorinin bir limitinde BCS diğer limitinde BEY durumu olmalıydı.

BCS-BEY geçişini ilk çalışan kişilerden biri olan Anthony Legett; etkileşim zayıf olduğu durumda BCS türü bir süperiletken ve güçlü olduğu durumda BEC türü süperiletken ortaya çıktığını gösterdi. BCS teorisinin aksine, BCS-BEY geçişinde bütün fermiyonlar Cooper çiftleri oluşturabilirler. Etkileşimi arttıkça fermiyonlar zayıfça bağlı Cooper çiftlerinin olduğu BCS limitinden güçlü etkileşime sahip çiflerin olduğu limite (BEY) geçerler. Bugün deneysel olarak bu yapılmaktadır. Atomik BEY deneysel olarak ilk defa Eric Cornell ve Carl Wieman tarafından 1995 yılında gerçekleştirilmiştir. Rubidium atomlarını lazerle soğutma ve buharlaştırma tekniklerini kullanarak nano-Kelvin mertebesinde sıcaklıklara kadar soğutmayı başardılar. Bu başarıdan sonra, aşırı soğuk gaz üzerine yapılan çalışmalarda ani bir artış yaşandı. Helium-4 gibi yoğun ve güçlü etkileşen bir sistem yerine daha basit bir sistemle uğraşmak zekice bir fikirdi. Aşırı soğuk gazlar seyrektirler ve bu yüzden 3-cisim çarpışmaları ele alınmaz. Aşırı soğuk gazların yoğunlukları düşük olduğu için kritik sıcaklıkları da çok düşüktür.

Aşırı soğuk gazlar fiziksel niceklikleri deneysel olarak kontrol edebilmemizi sağladıkları için, maddenin yeni fazlarını incelemek açısından oldukça uygun ortamlardır. Atomik sistemler Feshbach rezonansı ile atomlar arasındaki etkileşimi ayarlayabilme avantajına sahiptirler. Böylelikle bütün BCS-BEY geçişi deneysel olarak incelenebilir. Ayrıca bu sistemlerin yoğunluğu da kontrol edilebilmektedir. Bu yüzden, aşırı soğuk atomlar üzerine araştırmalar yaklaşık 20 yıldır çok ilgi çekmektedir. Fizikçiler bu tür sistemlerin yeni fazlarını bulmaya çalışıyorlar. 2003 yılında, üç farklı deney grubu sıkı bağlı fermiyonların Bose-Einstein yoğuşmasını keşfetti ve nihayet 2004 yılında MIT' da aşırı soğuk gazlarda vortekslerin gözlemlenmesiye fermiyonik süperakışkanlık da gözlemlenmiş oldu.

İlk çalışmaların çoğunluğu "spin-yukarı" ve "spin-aşağı" olarak adlandırılan atomların sayısının eşit olduğu "dengeli" Fermi gazına yönelik oldu. Dengeli Fermi gazında etkileşimi arttırdıkça BCS durumundan BEC durumuna faz değişiminden (phase transition) ziyade bir geçiş (crossover) vardır. İki limitin arasında etkileşimin en yüksek olduğu noktaya "teklik" (unitarity) denir. Sistem tam üniterlik anında sadece tek bir uzunluk ifadesiyle (etkileşim mesafesi) anlatılabilir. Sistem bütün bu geçiş süreci boyunca süperakışkandır. Bu sonuç deneylerle de gözlemlenmiştir. RF (radyo frekansı) dalgaları dengeli olmayan Fermi gazı sistemleri oluşturmak için kullanılır. Bu tür gazlarda BCS-BEY evriminin bir geçiş (crossover) olmadığı ve maddenin yeni fazlarının olduğu bulundu. Bu fazlar; normal faz, faz ayrımı ve süperiletken

faz bazı deneylerde gözlemlendi. Optik örgülerin varlığında fermiyonik sistemler, üç inceyapı durumlu fermiyonik karışımlar ve tuzaklanmış fermiyonik karışımlar fazlaca ilgi görmüş çalışma alanlarıdır. Bu fermiyonik karışımlar farklı titreşim frekansınlarında harmonik potansiyeller ile tuzaklandığında dengeli olmayan durumlar için yeni fazların oluştuğu gözlemlendi. Üç farklı aşırı ince durumlu fermiyon karışımı ilginç sonuçlar doğurabilir. Nötron yıldızlarının merkezindeki quarklardaki duruma benzer üç farklı Cooper çiftleri olabilir.

Bu tezde ilk olarak Cooper probleminden ve bazı süperiletkenlerin mikroskopik özelliklerini tasvir eden ünlü BCS teorisinden bahsettik. Daha sonra sistemin Gibbs serbest enerjisini varyasyonel yöntem kullanarak minimize ettik ve öz tutarlı denklemleri oluşturduk. Bir sonraki adımda ortalama alan teorisi yaklaşımıyla bu denklem setini farklı etkileşimlerde öz tutarlı bir şekilde 3 boyutlu femiyon gazı için çözdük. Daha sonra elde ettiğimiz sonuçları grafiğe dökerek BCS-BEY geçisi esnasında momentum dağılımının, süperiletken düzen parametresinin, sistemin uyarılma enerjilerinin, parçacık başına enerjinin ve kimyasal potansiyelin etkileşim arttıkça nasıl değiştiğini inceledik. BCS limitinde düzen parametresi sıfır iken, BEY limitine yaklaştıkça düzen parametresi giderek arttığını gözlemledik. Öte yandan, BCS limitinde kimyasal potasiyel Fermi enerjisine eşittir, ancak etkileşim arttıkça giderek azalmaya başlar. Etkileşim yeterince arttırıldığı zaman kimyasal potasiyelin ve parçacık başına enerjinin bağlanma enerjisinin yarısına yaklaştığı gördük. Bir sonraki bölümde 2 boyutta BCS-BEY geçişini inceledik. İki boyutta geçiş sürecinin, çok daha zayıf etkileşim şiddetinde gerçekleştiğini saptadık. Benzer şekilde quasi-2D (z-yönünde sonlu ince bir kalınlığı olan) sistem için tüm bu süreci tekrar ettik. Kalınlığı yeterince küçük alındığı zaman sonuçların iki boyutlu sistem için olan sonuçlarla tutarlı olduğunu gösterdik. Benzer şekilde kalınlığı fazla seçtiğimiz sonuçların üç boyutlu sistemin sonuçlarına yaklaştığını saptadık.

1. INTRODUCTION

In physics, a fermion named after Enrico Fermi is a particle characterized by Fermi – Dirac statistics. These particles which have half-integer spin quantum number obey the Pauli exclusion principle. As a consequence of the Pauli exclusion principle, only one fermion can occupy a particular quantum state at any given time. If multiple fermions have the same spatial probability distribution, then at least one property of each fermion, such as its spin, must be different. Fermions are usually associated with matter, whereas bosons are generally force carrier particles. Fermions include all quarks and leptons, as well as any composite particle made of an odd number of these, such as all baryons and many atoms and nuclei. They differ from bosons, which obey Bose – Einstein statistics and have integer spin and can condense into the same quantum state. This property of bosons is exemplified by Helium-4 when it is cooled to become a superfluid. A fermion can be an elementary particle, such as the electron, or it can be a composite particle, such as the proton. Bosons are particles with integer spin. The wave function for a system of identical bosons is symmetric under interchange of any two particles. They obey Bose-Einstein statistic [1]. In Fig. 1.1 it is shown that unlike fermions which have odd integer spin and antisymmetric wave functions non-interacting bosons may occupy the same single particle energy state in the ground state at zero temperature.

1.1 Bose-Einstein Condensation

Bose-Einstein (BEC) is a phase of a dilute gas of bosons cooled to temperatures very close to absolute zero. Under such conditions, below a critical temperature (T_c) the bosons start to condensate in lowest energy state. After bosons condense to the lowest energy state, they can be described by one wave function. This is predicted long ago by Bose (1924) and by Einstein (1925). They claimed that a finite fraction of bosons should occupy a single quantum state below a critical transition temperature (T_c)

$$T_c \propto \frac{\hbar^2 n^{2/3}}{m k_B} \tag{1.1}$$

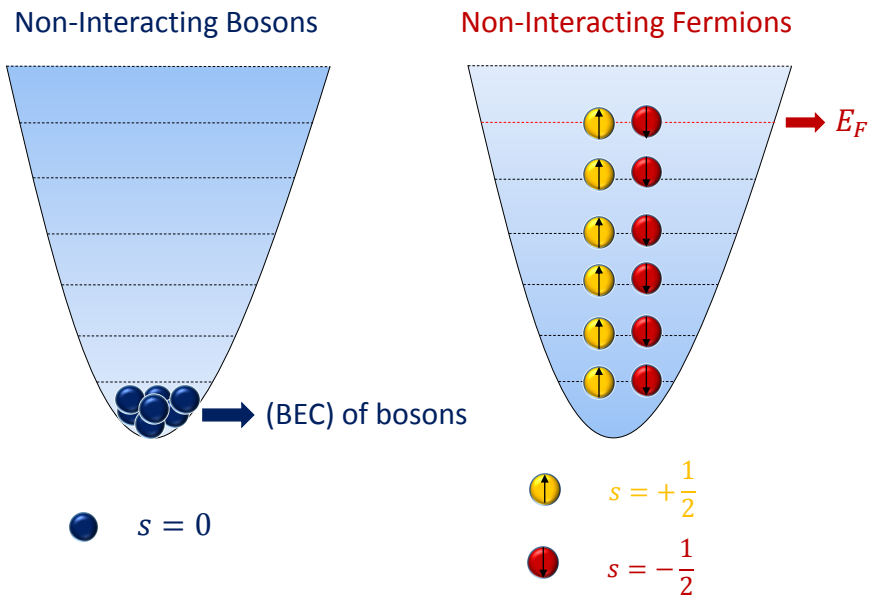

Figure 1.1 : Demonstration of quantum statistics of identical non-interacting bosons and fermions at zero temperature for the many-body ground state.

where m is the mass of the bosons, $h = 2\pi\hbar$ is the Planck constant, k_B is the Boltzmann constant, and n is the number of particles per unit volume. The lowest quantum state of the system should be separated from the the excited states. This is the essential requirement for superfluidity. So far, Bose - Einstein condensation has been realized experimentally in dilute gases of hydrogen, lithium, sodium, rubidium (etc.). From a theoretical point of view, atomic gas are appealing because at low energies the effective interaction between particles may be characterized by a single quantity, the *scattering length*. The gases are dilute in the sense that the scattering length much less than the interparticle separation. This make it possible to calculate the properties of the system with very high precision. For a uniform dilute gas the relevant theoretical framework was developed in the 1950s and 60s, but the presence of a confining potential gives rise to new features that are absent for uniform systems. The non-uniform systems, however, is outside the scope of this thesis. The possibility of adjusting the interatomic interaction, for instance, by changing the magnitude of the external potential experimentally (Feshbach resonance) [2] [3] makes it possible to study the regime where the scattering length is much larger than the interparticle

spacing. Under these conditions the atomic clouds constitute strongly interacting many-body systems.

1.2 Cooper Problem

Fermions can not occupy the same quantum state due to the Pauli exclusion principle. In 1938, F. London proposed that superfluidity was related to a quantum emergent phenomenon called "Bose-Einstein condensation" (BEC) [4]. This was one of the important moments in physics. This is an example where quantum mechanics is not only at play at the microscopic scale of atoms or molecules, but also at the macroscopic scale of our visible world. A clue for the explanation of superconductivity in a fermionic system was provided by Leon Cooper, who showed that the noninteracting Fermi sea is unstable towards the addition of a single pair of electrons with attractive interactions. He examined a situation in which two fermions are placed on a Fermi surface and found that if they interact attractively, they form a bound state regardless of however weak the interaction is [5]. This result is very different from the case of two fermions in free space. On the one hand, it is known that there is always a bound state between two fermions in one and two dimension if even there exists very weak interaction, on the other hand, there must be a minimum threshold interaction in three dimension should be overcame to form a bound state for two fermions. However, the fermions' momenta is in a narrow shell on the top of the Fermi sea. This is why the problem can be imaged effectively two dimensional. In three dimensional free space the attractive interaction must be sufficiently strong to overcome the zero-point kinetic pressure in order to form a bound state.

1.3 BCS Theory of Superconductivity

Superconductivity is the frictionless motion of the charge carriers. In 1911, the superconductivity was first observed in mercury by Dutch physicist Heike Kamerlingh Onnes of Leiden University. There existed no consistent microscopic theory that described why superconductivity arose and there was only macroscopic theories to calculate certain thermodynamic and electrodynamic quantities. It remained unexplained up to 1957 when the first satisfactory microscopic theory explaining the conceptual and mathematical structure of the conventional superconductivity was

developed by Bardeen, Cooper, and Scrieffer(BCS) [6, 7]. They later received the Nobel Prize in 1972. The essential ingredient of the BCS theory is the idea of Cooper pair-a dimer of up-spin and down-spin electron which exist an attractive interaction between them. The basic opinion of Cooper that was the even very weak attraction can turn pairs of fermions into bound pairs in the presence of the Fermi sea which is unstable to the formation of such Cooper pairs. A variational wave function is used to give an explanation to the superconductivity of the metals at the absolute zero temperature.

1.4 Crossover: From BCS to BEC

Ultracold atomic vapors provide a unique and tunable experimental system to explore pairing phenomena particularly in the context of Fermi gases. The crossover from weak coupling BCS pairing to BEC of tightly bound pairs, as a function of the attractive interaction has long been of interest to theoretical physicists. The past decade has seen a series of remarkable experimental developments in ultracold Fermi gases that has realized the BCS-BEC crossover in the laboratory. The aim of this section is to review the basic concepts of this BCS-BEC crossover in atomic Fermi gases. The idea of the BCS-BEC crossover preceeds cold atom experiments by several decades [8]. It is a generic feature of attractively interacting Fermi gases and can thus occur in a variety of systems ranging from superconductors and excitons in semiconductors, to neutron stars. However, so far, it has only been observed experimentally in the dilute atomic gases. The crossover is realized by varying the pairing correlations according to the interparticle separations as depicted in Fig.1.2. Instead of tuning the interactions at fixed density it is also possible to change the particle density at fixed interactions. The former "interaction-driven" crossover is achieved in atomic gases via use of the Fesbach resonance. The latter "density-driven" crossover occurs in a Coulomb system such as excitons [9] where the interactions cannot be changed easily. The fact that there is a crossover between two states rather than a phase transition is not easy to prove theoretically but can be intuitively predicted on the ground that both limits are obtained by the same wave function. The BCS-BEC crossover has more recently been reviewed in [10–12]. There are three important limits in the BCS-BEC crossover problem. In the BCS limit, the scattering length is small and negative, and the interparticle

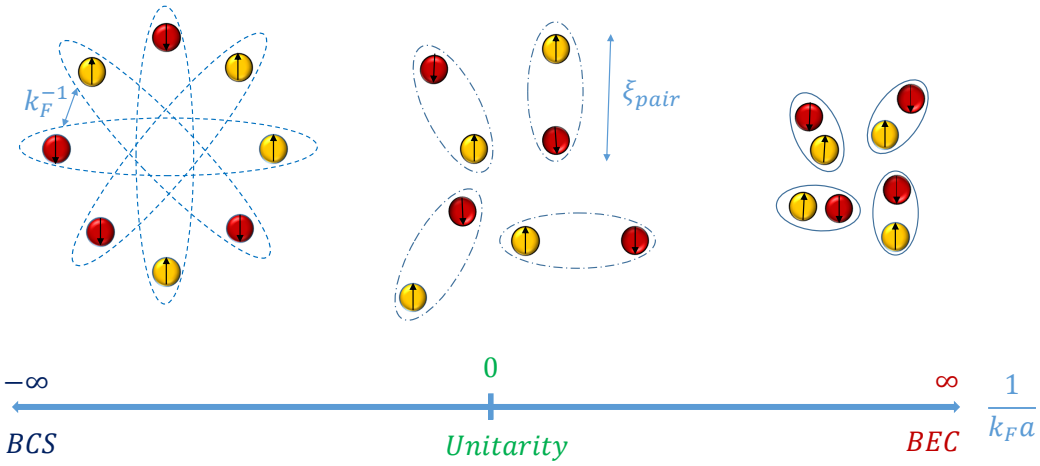

Figure 1.2 : Illustration of the weakly bound and largely overlapping Cooper pairs in the BCS regime and the small tightly bound and strongly interacting local pairs in the BEC regime, where ξ_{pair} is the size of the pair and k_F^{-1} is inverse of the Fermi momentum and it is proportional to interparticle distance in unitarity.

fermion-fermion interaction is small and attractive. In the BEC limit, the scattering length is small but positive, and although the interparticle fermion-fermion interaction is large and attractive, the interparticle composite boson-boson interaction is small and repulsive. At unitarity limit, the scattering length diverges, and the interparticle fermion-fermion interaction is very large and attractive. In this limit, for dilute systems, the superfluid properties does not depend on the actual value of the diverging scattering length, and the inverse of the Fermi momentum k_F is the only relevant length scale in the problem. In this regime the superfluid properties are universal.

2. BCS-BEC CROSSOVER in 3D

Much of the theoretical work on systems of two types of fermions interacting via an adjustable, attractive potential have focussed on interactions that are governed by a single parameter, namely the s-wave scattering length "a". [12]. Such a description is valid as long as we have $|a| \gg \langle r \rangle$ and $k_F \langle r \rangle \ll 1$, where $\langle r \rangle$ is the range of the potential and k_F is the Fermi momentum of the non-interacting system, so that the only independent dimensionless variable in the problem is $(ak_F)^{-1}$. The potential supports a two-body bound state for $(ak_F)^{-1} > 0$, but this molecular state passes through zero energy and vanishes into the continuum at $(ak_F)^{-1} = 0$, the position of the Feshbach resonance. The BCS and BEC limits correspond respectively to $(ak_F)^{-1} \to -\infty$ and $(ak_F)^{-1} \to \infty$. In this chapter we introduce a framework to describe the BCS-BEC crossover starting with the description of the non-interacting system.

2.1 Non-Interacting Fermi Gas in 3D

The ground state of a non-interacting unpolarized Fermi gas at $T = 0$ corresponds to a completely filled Fermi sea (or sphere) of the single particle states up to Fermi momentum ($k \leq k_F$) in the momentum space and the absence of the particles or hole sea in ($k > k_F$) states. The Hamiltonian for a free particle in a box is

$$\hat{H} = -\frac{\hbar^2}{2m}\nabla^2 \tag{2.1}$$

where m is the mass of the particle. The time-independent Schrödinger equation can be written as

$$\hat{H}\Psi_{\mathbf{k}}(x,y,z)\chi(\sigma) = \varepsilon_{\mathbf{k}}\Psi_{\mathbf{k}}(x,y,z)\chi(\sigma) \tag{2.2}$$

the solutions for this equation are plane waves.

$$\Psi_{\mathbf{k}}(x,y,z) = \frac{1}{\sqrt{L_x L_y L_z}} e^{i(k_x x + k_y y + k_z z)} \tag{2.3}$$

where L_i $(i = x, y, z)$ is the length in i^{th} of i of the box. Considering the periodic boundary conditions

$$\Psi_{\mathbf{k}}(x+L_x, y, z) = \Psi_{\mathbf{k}}(x, y, z) \tag{2.4}$$

$$\Psi_{\mathbf{k}}(x, y+L_y, z) = \Psi_{\mathbf{k}}(x, y, z) \tag{2.5}$$

$$\Psi_{\mathbf{k}}(x, y, z+L_z) = \Psi_{\mathbf{k}}(x, y, z) \tag{2.6}$$

we find that the momenta are quantized as

$$k_x = \frac{2\pi}{L_x} n_x, \qquad k_y = \frac{2\pi}{L_y} n_y, \qquad k_z = \frac{2\pi}{L_z} n_z \tag{2.7}$$

where n_i are integers. The eigenvalues is also quantized.

$$\varepsilon_{\mathbf{k}} = \frac{\hbar^2 k^2}{2m} = \frac{2\hbar^2 \pi^2}{m} \left(\frac{n_x^2}{L_x^2} + \frac{n_y^2}{L_y^2} + \frac{n_z^2}{L_z^2} \right) \tag{2.8}$$

2.1.1 Balanced populations

For equal number of spin-up and spin-down particles we can easily calculate particle density and energy density. In the thermodynamic limit, $(N \to \infty,\ V \to \infty,\ n = N/V \to constant)$ the discrete energies and momenta turn into continuous variables. These states will be filled up to Fermi energy level which is

$$\varepsilon_F = \frac{\hbar^2 k_F^2}{2m} \tag{2.9}$$

determined by the density of electrons (see Table2.1) and the volume of the Fermi sphere is $4\pi k_F^3/3$ where k_F is the Fermi momentum. Each quantum state in the momentum space occupies the volume $(2\pi)^3/V$ which comes from the Heisenberg's uncertainty principle. The number of total particles is given by

$$N = 2\frac{4\pi k_F^3/3}{(2\pi/L)^3} = V\frac{k_F^3}{3\pi^2} \tag{2.10}$$

where the factor of two comes from spin and the particle density is

$$n = \frac{N}{V} = \frac{k_F^3}{3\pi^2} \tag{2.11}$$

The total internal energy of the Fermi gas can be calculated as

$$E = 2\sum_{\mathbf{k}<\mathbf{k}_F} \frac{\hbar^2 k^2}{2m} \tag{2.12}$$

	1D	2D	3D
k_F	$n\pi$	$(2\pi n)^{1/2}$	$(3\pi^2 n)^{1/3}$
ε_F	$(\hbar n\pi)^2/2m$	$\hbar^2 n\pi/m$	$\hbar^2(3\pi^2 n)^{2/3}/2m$
E/N	$\varepsilon_F/3$	$\varepsilon_F/2$	$3\varepsilon_F/5$
$g(E)$	$L(m/2\varepsilon)^{1/2}/\pi\hbar$	$mL^2/\pi\hbar^2$	$L^3/2\pi^2(2m/\hbar^2)^{3/2}\varepsilon^{1/2}$

Table 2.1 : Fermi momentum, Fermi energy, enegy per particle and density of states in 1D, 2D, 3D

In the thermodynamic limits the summation can be written as an integral

$$\sum_{\mathbf{k}} \quad \rightarrow \quad \frac{V}{(2\pi)^3}\int d^3k \tag{2.13}$$

$$E = \frac{V}{m\pi^2}\int_0^{k_F} k^4 dk \tag{2.14}$$

$$= \frac{V}{m\pi^2}\frac{k_F^5}{5} = V\frac{3}{5}n\varepsilon_F \tag{2.15}$$

The energy density

$$e = \frac{E}{V} = \frac{3}{5}n\varepsilon_F \tag{2.16}$$

and the energy per particle is

$$\frac{e}{n} = \frac{E}{N} = \frac{3}{5}\varepsilon_F \tag{2.17}$$

2.1.2 Imbalanced populations

For different number of between spin-up and spin-down particles, particle densities and energy per particle values will be modified. The particle densities for spin up and down particles respectively is,

$$n_\uparrow = \frac{k_{F\uparrow}^3}{6\pi^2} \qquad n_\downarrow = \frac{k_{F\downarrow}^3}{6\pi^2} \tag{2.18}$$

and the total number of particles

$$n = n_\uparrow + n_\downarrow = \frac{1}{6\pi^2}(k_{F\uparrow}^3 + k_{F\downarrow}^3) \tag{2.19}$$

from Eq. (2.11)

$$k_F^3 = \frac{1}{2}(k_{F\uparrow}^3 + k_{F\downarrow}^3) \tag{2.20}$$

Because of this imbalanced situation we can define the polarization of the system as

$$\eta = \frac{n_\uparrow - n_\downarrow}{n_\uparrow + n_\downarrow} = \frac{n_\uparrow - n_\downarrow}{n} \tag{2.21}$$

By solving Eq. (2.19) and Eq. (2.21) we find that

$$n_\uparrow = \frac{n}{2}(1+\eta) \qquad n_\downarrow = \frac{n}{2}(1-\eta) \tag{2.22}$$

also from Eq. (2.18) and Eq. (2.22)

$$k_{F\uparrow} = k_F(1+\eta)^{1/3} \qquad k_{F\downarrow} = k_F(1-\eta)^{1/3} \tag{2.23}$$

The single particle energies of the spin-up particles is given by

$$E_\uparrow = \frac{V}{2\pi^2 m}\int_0^{k_{F\uparrow}} k^4 dk \tag{2.24}$$

$$= \frac{V}{2\pi^2 m}\frac{k_{F\uparrow}^5}{5} \tag{2.25}$$

energy density for spin-up particles

$$e_\uparrow = \frac{3}{10} n\varepsilon_F (1+\eta)^{5/3} \tag{2.26}$$

and similarly for spin-down particles

$$e_\downarrow = \frac{3}{10} n\varepsilon_F (1-\eta)^{5/3} \tag{2.27}$$

so from Eq. (2.26) and Eq. (2.27) the energy per total particle is

$$\frac{e}{n} = \frac{E}{N} = \frac{3}{10}\varepsilon_F \left[(1+\eta)^{5/3} + (1-\eta)^{5/3}\right] \tag{2.28}$$

2.2 Model Interaction

To model the interaction between the two particles we take a spherical square well potential with U_0 depth and range r_0 as the pair potential.

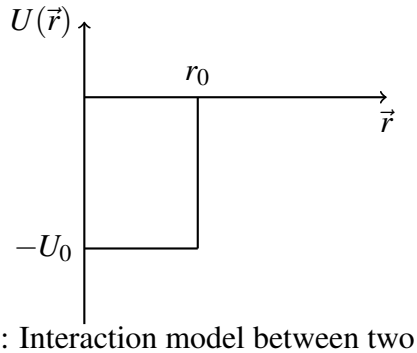

Figure 2.1 : Interaction model between two particles.

$$U(\vec{r}) = \begin{cases} -U_0 & ; \quad |\vec{r}| \le r_0 \\ 0 & ; \quad |\vec{r}| > r_0 \end{cases} \tag{2.29}$$

The Fourier transform of this potential is

$$U_q = \int_0^\infty U(\mathbf{r}) e^{-i\mathbf{qr}}\, d\mathbf{r} \tag{2.30}$$

$$= -U_0 \int_0^{r_0} r^2\, dr \int_0^\pi e^{-iqr\cos\theta} sin\theta\, d\theta \int_0^{2\pi} d\phi \tag{2.31}$$

after the substitution

$$-cos\theta = u \tag{2.32}$$

$$sin\theta\, d\theta = du \tag{2.33}$$

becomes

$$U_q = -2\pi U_0 \int_0^{r_0} r^2 \frac{1}{iqr}(e^{iqr} - e^{-iqr})\, dr \tag{2.34}$$

$$= -\frac{4\pi U_0}{q} \int_0^{r_0} r \sin qr\, dr \tag{2.35}$$

$$= -\frac{4\pi U_0}{q} \int_0^{r_0} \frac{\partial}{\partial q}(-\cos qr)\, dr \tag{2.36}$$

$$= \frac{4\pi U_0}{q} \frac{\partial}{\partial q}\left(\frac{\sin qr_0}{q}\right) \tag{2.37}$$

$$= \frac{4\pi U_0}{q}\left[\frac{r_0 \cos qr_0}{q} - \frac{\sin qr_0}{q^2}\right] \tag{2.38}$$

2.3 Two-Body Problem

Consider a system of two particles interacting with each other without external fields. The Hamiltonian of the system is given by

$$H = -\frac{\hbar^2}{2m_1}\nabla_1^2 - \frac{\hbar^2}{2m_2}\nabla_2^2 + V(\mathbf{r}_1 - \mathbf{r}_2) \tag{2.39}$$

where $V(\mathbf{r}_1 - \mathbf{r}_2)$ is the interaction potential energy of the particles and the Schrödinger equation is

$$H\Psi(\mathbf{r}_1, \mathbf{r}_2) = E\Psi(\mathbf{r}_1, \mathbf{r}_2) \tag{2.40}$$

We can define the center of mass and relative coordinates as

$$\mathbf{r} = \mathbf{r}_1 - \mathbf{r}_2 \tag{2.41}$$

$$\mathbf{R} = \frac{m_1\mathbf{r}_1 + m_2\mathbf{r}_2}{m_1 + m_2} \tag{2.42}$$

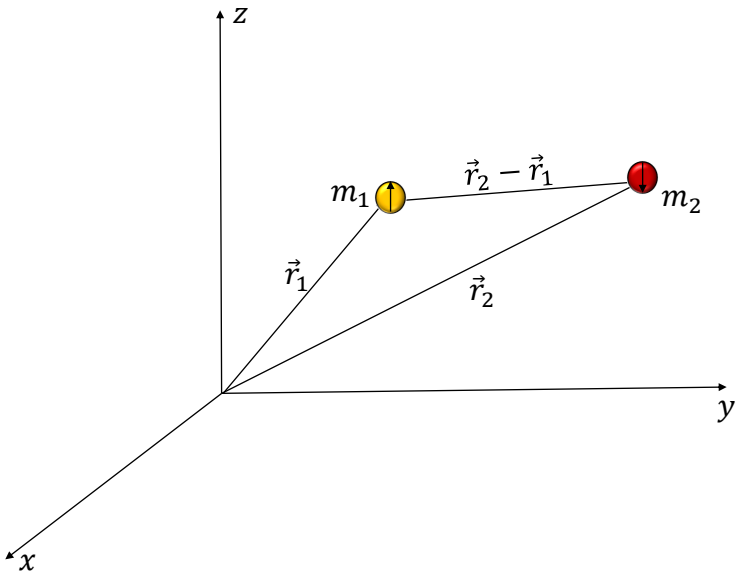

Figure 2.2 : The two parcticle system with masses m_1, m_2 and spins $\uparrow$, $\downarrow$ respectively.

and introduce the total and reduced masses

$$m_r = \frac{m_1 m_2}{m_1 + m_2} \tag{2.43}$$

$$M = m_1 + m_2 \tag{2.44}$$

where r, R represent the relative and center of mass coordinates respectively. The Hamiltonian becomes

$$H = \frac{-\hbar^2}{2M}\nabla_R^2 + \frac{-\hbar^2}{2m_r}\nabla_r^2 + V(\mathbf{r}) \tag{2.45}$$

$$H = H_{cm} + H_{rel} \tag{2.46}$$

and the Scrödinger equation is written as

$$(H_{cm} + H_{rel})\Psi(\mathbf{R},\mathbf{r}) = (E_{cm} + E_{rel})\Psi(\mathbf{R},\mathbf{r}) \tag{2.47}$$

The solution of this equation with spin wave function included can be written as

$$\Psi(\mathbf{R},\mathbf{r},\sigma_1,\sigma_2) = \phi(\mathbf{r})e^{i\mathbf{k}_{cm}.\mathbf{R}}\chi(\sigma_1,\sigma_2) \tag{2.48}$$

where $\chi(\sigma)$ is the spin state which can be singlet (total spin is zero) or triplet (total spin is one) such as,

$$\chi^2(\sigma_1,\sigma_2) = \frac{|\uparrow\rangle|\downarrow\rangle - |\downarrow\rangle|\uparrow\rangle}{\sqrt{2}} \tag{2.49}$$

$$\chi^T(\sigma_1,\sigma_2) = \begin{cases} (|\uparrow\rangle|\downarrow\rangle + |\downarrow\rangle|\uparrow\rangle)/\sqrt{2} \\ |\uparrow\rangle|\uparrow\rangle \\ |\downarrow\rangle|\downarrow\rangle \end{cases} \tag{2.50}$$

The Cooper pairs do have not center of mass momentum. This is why the center of mass energy is taken to be zero. The excitation energy of the system will be just relative energy. The equation for the relative motion can be rewritten the Eq. (2.47) as

$$\frac{-\hbar^2}{2m_r}\nabla_r^2\phi(\mathbf{r}) + V(\mathbf{r})\phi(\mathbf{r}) = E\Psi(\mathbf{r}) \tag{2.51}$$

We need to Fourier transformation of this equation to solve the two-body problem numerically. The Fourier transformation of the Eq. (2.51) is

$$\frac{\hbar^2 k^2}{2m_r}\phi(\mathbf{k}) + \frac{1}{(2\pi)^3}\int d\mathbf{k}' V(\mathbf{k}-\mathbf{k}')\phi(\mathbf{k}') = E\phi(\mathbf{k}) \tag{2.52}$$

In order to solve this Schrödinger equation numerically, we should diagonalize the Hamiltonian and calculate eigenvalues and eigenvectors. After choosing a suitable grid of $\mathbf{k}$ with Gaussian quadrature method, the integral will be reduced to a discrete summation over $\mathbf{k}$.

2.3.1 Basic scattering theory

In this section we review some aspects of scattering theory for a single channel and introduce the scattering length, which characterizes low-energy interactions between a pair of particles. Consider the scattering of two particles with masses m_1 and m_2 with no internal degrees of freedom. As usual, we transform to center of mass and relative coordinates. The wave function for the center of mass motion is a plane wave, while that for the relative motion satisfies a Schrödinger equation with the mass equal to the reduced mass Eq. (2.43). In order to describe the scattering, the wave function for the relative motion is written as the sum of an incoming plane wave and a scattered wave[1].

$$\psi(\mathbf{r}) = e^{i\mathbf{k}.\mathbf{r}} + \psi_{sc}(\mathbf{r}) \tag{2.53}$$

At large interatomic distances, the scattered wave is an outgoing spherical wave $f(\mathbf{k}')\exp(ikr)/r$, where $f(\mathbf{k}')$ is the "scattering amplitude" and $\mathbf{k}'$, which has

[1]Plane wave-states are written as $e^{i\mathbf{k}.\mathbf{r}}$ without the factor of $1/V^{1/2}$

magnitude k, specifies the wave vector of the scattered wave. Since the interaction between atoms is spherically symmetric, the scattering amplitude $f(\mathbf{k}')$ depends on direction only through the scattering angle θ, which is the angle between the directions of the relative momentum of the atoms before and after scattering. The wave function for large r is thus

$$\psi = e^{ikz} + f(\theta)\frac{e^{ikr}}{r} \tag{2.54}$$

where the relative velocity of the coming wave is taken to be in the z direction. The scattering amplitude f depends on θ and on the magnitude k of the wave vector of the incoming wave. It is sufficient to take s-wave scattering at very low temperature. In this limit the scattering amplitude $f(\theta)$ approaches a constant, which is denoted by a. The wave function can be written as

$$\psi = 1 - \frac{a}{r} \tag{2.55}$$

where the constant a is the *scattering length*.

The scattering length depends on the details of the inter-atomic potential model. In order to illustrate this in a simple case, let us consider the relative motion of the two particles interacting with a spherically symmetric square well potential. Since the potential is spherically symmetric, the solution of the Schrödinger equation has axial symmetry with respect to the direction of the incident particle. The wave function for the relative motion therefore may be expanded in terms of Legendre polynomials $P_l(\cos\theta)$

$$\psi = \sum_{l=0}^{\infty} A_l P_l(\cos\theta) R_{nl}(r) \tag{2.56}$$

where $R_{kl}(r)$ is the radial part of the wave function and it satisfies the equation

$$\frac{\partial^2 R_{nl}(r)}{\partial r^2} + \frac{2}{r}\frac{\partial R_{nl}(r)}{\partial r} + \left[k^2 - \frac{l(l+1)}{r^2} - \frac{2m_r}{\hbar^2}V(r)\right] R_{nl}(r) = 0 \tag{2.57}$$

At very low temperatures it will be sufficient to take $l = 0$ s-wave part of the Eq. (2.57) and the equation is

$$-\frac{\hbar^2}{2m_r}\frac{d^2u(r)}{dr^2} + V(r)u(r) = Eu(r) \tag{2.58}$$

where $u(r) = rR(r)$ and the potential term is written as

$$V(r) = \begin{cases} -\frac{\hbar^2 k_0^2}{2m_r} & ; \quad r < r_0 \\ 0 & ; \quad r > r_0 \end{cases} \tag{2.59}$$

We must use the Bessel function near the origin and the inside solution is

$$R_{nl}^{in}(r) = A j_0(kr) \tag{2.60}$$

where $k = 2m_r(E+V_0)/\hbar^2$ and for large r the solutions must be Hankel function of the first type

$$R_{nl}^{out}(r) = B h_0^{(1)}(i\kappa r) \tag{2.61}$$

where $\kappa = \left(-2Em_r/\hbar^2\right)^{1/2}$. To solve the problem, we should match the solutions and their derivatives at the boundary which is often called matching of the logarithmic derivatives. After matching the boundary conditions we obtain

$$k \cot kr_0 = -\kappa \tag{2.62}$$

Now let us determine the scattering length a for this potential. We consider solutions to Eq. (2.58) with positive energy and let E tend to zero. Then according to Eq. (2.55) the exterior solution has the form $u \approx (r-a)$, while the interior solution is given by $u \approx \sin k_0 r$ [1, 13]. By matching the logarithmic derivatives [1] we obtain

$$k_0 \cot k_0 d = \frac{1}{r_0 - a} \tag{2.63}$$

For the solution of this equation see App. B.

2.4 BCS Theory of Superconductivity

The BCS theory is the first microscopic theory of superconductivity since its discovery in 1911. The theory describes superconductivity as microscopic effect caused by a condensation of Cooper pairs into boson-like state. It was proposed by John Bardeen, Leon Cooper and John Robert Schrieffer (BCS) in 1957 and they received the Nobel Prize in Physics for their theory in 1972.

At sufficiently low temperatures, electrons near the Fermi surface become unstable against the formation of Cooper pairs. Cooper showed that such a bound state will occur by an attractive potential no matter how weak in the existence of a Fermi sea. In conventional superconductors, an is attraction generally provided by electron-phonon interaction. The basic idea is that an electron moving through a conductor will attract nearby positive ion cores and polarize its vicinity in the lattice. This polarization moves a second electron, with opposite spin and momentum, into the region of higher positive

charge density. Thus, two electrons become correlated and construct a pair called "Cooper pair". In the BCS framework superconductivity is a macroscopic effect which results from the condensation of the Cooper pairs.

2.4.1 Pairing mechanism

One of the most fascinating consequences of quantum mechanics is that in spite of the exclusion principle, fermions confined to a metal or a nucleus sometimes bind into stable pairs. These pairs are known as Cooper pairs [14] and lead to the phenomenon of superconductivity in metals and pairing in nuclei. The BCS theory relies on the assumption that superconductivity arises when the attractive Cooper pair interaction dominates over the repulsive Coulomb force [5]. The electrons in a metal occupy the Fermi sea and those electrons that can change their behaviours in order to give rise to some kind of a condensation have energies of order $k_B T_c$ (T_c-Critical Temperature of Superconductivity). Two electrons can be attractive to each other with electron-phonon interaction [15]. If they have,

- momentums in opposite direction
- same energy state k (one$\uparrow$ the other$\downarrow$)
- k in a shell whose radius is order of the inverse coherence length ξ^{-1} nearby the Fermi level k_F and its thickness determined by Debye energy.

When $+\mathbf{k}$ and $-\mathbf{k}$ states can be combined it is possible to obtain standing waves so-called "Cooper Pairs" having a net zero wave vector. These objects is "Bose-like" particles. A Cooper pair is a weak electron-electron bound pair mediated by a phonon interaction. Although quite ambiguous, one can imagine this pairing by the following explanation. Visualize an electron moving within a material. There is a Coulomb attraction between the electron and the positively charged cores of ions which will leave a net positive charge at their vicinities. A *paired* electron is one with opposite momentum and spin that is attracted to this force. Cooper's wonderful work in 1956 showed that due to the Fermi statistics of the electron, this paired state can have energy less than that of the Fermi-energy of the material [5]. Thus, bound states can form at adequately low temperatures where the thermal energy is not an important factor.

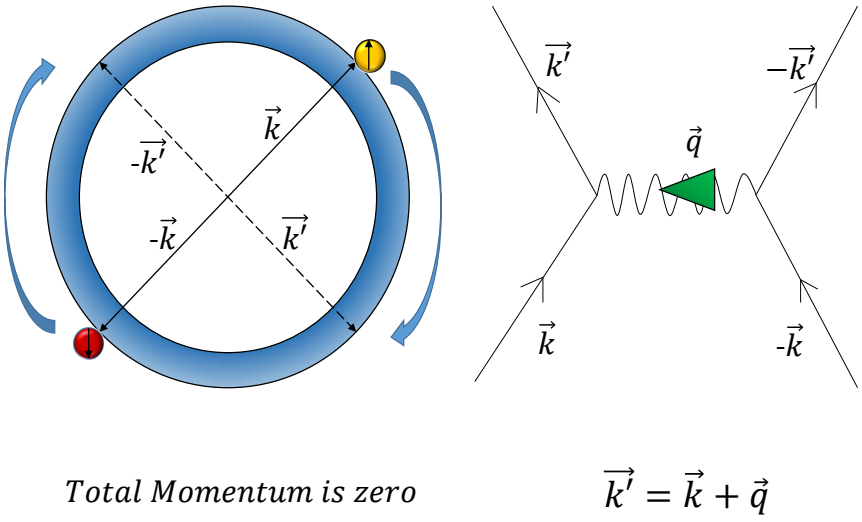

Figure 2.3 : The process which binds two electrons into a Cooper pair. It is an interaction between the two electrons, which are in initial states with wave-vectors $\mathbf{k}$ and $-\mathbf{k}$, via exchange of a virtual phonon of wavevector $\mathbf{q}$. The electrons go into new states $\mathbf{k}'$ and $-\mathbf{k}'$

.

2.4.2 The BCS wave function

Let us define the pair creation operator in $\mathbf{k}$ space by,

$$\hat{P}^{\dagger}_{\mathbf{k}} = c^{\dagger}_{\mathbf{k}\uparrow} c^{\dagger}_{-\mathbf{k}\downarrow} \tag{2.64}$$

This creates a pair of fermion of zero total momentum, and opposite spins. In terms of this operator Schrieffer proposed the following coherent state many-body wave function [16],

$$\left|\Psi_{\mathbf{BCS}}\right\rangle = N \exp\left(\sum_{\mathbf{k}} \alpha_{\mathbf{k}} \hat{P}^{\dagger}_{\mathbf{k}}\right) \left|0\right\rangle \tag{2.65}$$

where N is the normalization constant and the complex numbers, $\alpha_{\mathbf{k}}$ are parameters which can be adjusted to minimize the total energy. Here the vacuum state, $\left|0\right\rangle$ is the state with no electrons at all in the band of Bloch states at Fermi surface. The commutation relations between the pair creation operators are

$$\left[\hat{P}_{\mathbf{k}}, \hat{P}^{\dagger}_{\mathbf{k}}\right] \neq 1, \tag{2.66}$$

$$\left[\hat{P}^{\dagger}_{\mathbf{k}}, \hat{P}^{\dagger}_{\mathbf{k}'}\right] = 0. \tag{2.67}$$

On the other hand, for the same $\mathbf{k}$ point, $\mathbf{k} = \mathbf{k}'$, the product $\hat{P}^{\dagger}_{\mathbf{k}}\hat{P}^{\dagger}_{\mathbf{k}}$ contains $\hat{c}^{\dagger}_{\mathbf{k}\uparrow}\hat{c}^{\dagger}_{\mathbf{k}\uparrow}$ term which is zero. Therefore,

$$\left(\hat{P}^{\dagger}_{\mathbf{k}}\right)^2 = 0. \tag{2.68}$$

We can rewrite the coherent state as a product of exponentials, one for each $\mathbf{k}$ point,

$$\left|\Psi_{\mathbf{BCS}}\right\rangle = N\prod_{\mathbf{k}}\exp(\alpha_{\mathbf{k}}\hat{P}^{\dagger}_{\mathbf{k}})\left|0\right\rangle \tag{2.69}$$

We can also expand out each of the operator exponentials. In the expansion all terms containing $\hat{P}^{\dagger}_{\mathbf{k}}$ to quadratic or higher powers are zero. Therefore we obtain

$$\left|\Psi_{\mathbf{BCS}}\right\rangle = N\prod_{\mathbf{k}}(1+\alpha_{\mathbf{k}}\hat{P}^{\dagger}_{\mathbf{k}})\left|0\right\rangle \tag{2.70}$$

If we normalize the coherent state,

$$\left\langle 0\right|(1+\alpha^{*}_{\mathbf{k}}\hat{P}_{\mathbf{k}})(1+\alpha_{\mathbf{k}}\hat{P}^{\dagger}_{\mathbf{k}}\left|0\right\rangle = 1+|\alpha_{\mathbf{k}}|^2\left\langle 0\right|\hat{P}_{\mathbf{k}}\hat{P}^{\dagger}_{\mathbf{k}}\left|0\right\rangle \tag{2.71}$$

Since

$$\begin{aligned}
\left\langle 0\right|\hat{P}_{\mathbf{k}}\hat{P}^{\dagger}_{\mathbf{k}}\left|0\right\rangle &= \left\langle 0\right|\hat{c}_{-\mathbf{k}\downarrow}\hat{c}_{\mathbf{k}\uparrow}\hat{c}^{\dagger}_{\mathbf{k}\uparrow}\hat{c}^{\dagger}_{-\mathbf{k}\downarrow}\left|0\right\rangle && \textbf{(2.72)}\\
&= \left\langle 0\right|\hat{c}_{-\mathbf{k}\downarrow}(1-\hat{c}^{\dagger}_{\mathbf{k}\uparrow}\hat{c}_{\mathbf{k}\uparrow})\hat{c}^{\dagger}_{-\mathbf{k}\downarrow}\left|0\right\rangle && \textbf{(2.73)}\\
&= \left\langle 0\right|\hat{c}_{-\mathbf{k}\downarrow}\hat{c}^{\dagger}_{-\mathbf{k}\downarrow}\left|0\right\rangle - \left\langle 0\right|\hat{c}_{-\mathbf{k}\downarrow}\hat{c}^{\dagger}_{\mathbf{k}\uparrow}\hat{c}_{\mathbf{k}\uparrow}\hat{c}^{\dagger}_{-\mathbf{k}\downarrow}\left|0\right\rangle && \textbf{(2.74)}\\
&= 1+\left\langle 0\right|\hat{c}_{-\mathbf{k}\downarrow}\hat{c}^{\dagger}_{\mathbf{k}\uparrow}\hat{c}^{\dagger}_{-\mathbf{k}\downarrow}\hat{c}_{\mathbf{k}\uparrow}\left|0\right\rangle && \textbf{(2.75)}\\
&= 1 && \textbf{(2.76)}
\end{aligned}$$

we can finally write the normalized BCS state as

$$\left|\Psi_{\mathbf{BCS}}\right\rangle = \prod_{\mathbf{k}}(u^{*}_{\mathbf{k}}+v^{*}_{\mathbf{k}}\hat{P}^{\dagger}_{\mathbf{k}})\left|0\right\rangle \tag{2.77}$$

where

$$u^{*}_{\mathbf{k}} = \frac{1}{1+|\alpha_{\mathbf{k}}|^2} \qquad v^{*}_{\mathbf{k}} = \frac{\alpha_{\mathbf{k}}}{1+|\alpha_{\mathbf{k}}|^2} \tag{2.78}$$

and

$$|u_{\mathbf{k}}|^2 + |v_{\mathbf{k}}|^2 = 1. \tag{2.79}$$

Finally, the way the BCS state was originally written, as described above, treats electrons and holes in a relatively unsymmetrical manner. We start with a vacuum $\left|0\right\rangle$ and add pairs of electrons. But what about pairs of holes? In fact these are also included in the theory. We just have to see that by a suitable redefinition of the original

reference state $\big|0\big\rangle$ we can write the BCS state in a form which treats electrons and holes more evenly,

$$\big|\Psi_{\mathbf{BCS}}\big\rangle = \prod_{k>k_F} (u^*_{\mathbf{k}} + v^*_{\mathbf{k}} \hat{P}^\dagger_{\mathbf{k}}) \prod_{k'<k_F} (u^*_{\mathbf{k}'} \hat{P}_{\mathbf{k}'} + v^*_{\mathbf{k}'}) \big|\psi_0\big\rangle \tag{2.80}$$

Here $\big|\psi_0\big\rangle$ is the zero temperature Fermi sea, in which all states with $k < k_F$ are occupied and the rest are unoccupied. One can equally well view the BCS state as a condensate of electron pairs above a filled electron Fermi sea, of a condensate of the hole pairs below an empty "hole sea".

2.4.3 The BCS hamiltonian

In order to take interactions between particles into account we use the following second quantized model Hamiltonian

$$\hat{H} = \sum_{ik} H^{(1)}_{ik} \hat{c}^\dagger_{\mathrm{i}} \hat{c}_{\mathrm{k}} + \frac{1}{2} \sum_{iklm} U^{(2)}_{iklm} \hat{c}^\dagger_{\mathrm{i}} \hat{c}^\dagger_{\mathrm{k}} \hat{c}_{\mathrm{l}} \hat{c}_{\mathrm{m}} + \ldots \tag{2.81}$$

where the two - body matrix element associated with the inter particle potential $U^{(2)}(\mathbf{r}_1 - \mathbf{r}_2)$ is

$$U^{(2)}_{iklm} = \big\langle ik|U^{(2)}|lm\big\rangle \tag{2.82}$$

$$= \int\int d^3r_1 d^3r_2 \psi^*_i(\mathbf{r}_1)\psi^*_k(\mathbf{r}_2) U^{(2)}(\mathbf{r}_1 - \mathbf{r}_2)\psi_l(\mathbf{r}_1)\psi_m(\mathbf{r}_2) \tag{2.83}$$

The $\psi_i(\mathbf{r})$ represents the wave functions of the single particle states with quantum number i, which is associated with the (destruction) operators $\hat{c}_i$. Since we are here dealing with a uniform gas, plane waves of the form $\psi_k(\mathbf{r}) = L^{-3/2} e^{i\mathbf{k}.\mathbf{r}}$ will be suitable basis functions. We can write

$$\begin{aligned} U^{(2)}_{k_1' k_2' k_2 k_1} &= \frac{1}{L^6} \int\int e^{-i\mathbf{k}_1'.\mathbf{r}_1} e^{-i\mathbf{k}_2'.\mathbf{r}_2} U^{(2)}(\mathbf{r}_1 - \mathbf{r}_2) e^{i\mathbf{k}_2.\mathbf{r}_2} e^{i\mathbf{k}_1.\mathbf{r}_1} d^3r_1 d^3r_2 \\ &= \frac{1}{L^6} \int\int e^{-i\mathbf{k}_1'.(\mathbf{r}_1 - \mathbf{r}_2)} e^{-i(\mathbf{k}_2' + \mathbf{k}_1').\mathbf{r}_2} U^{(2)}(\mathbf{r}_1 - \mathbf{r}_2) e^{i(\mathbf{k}_2 + \mathbf{k}_1).\mathbf{r}_2} e^{i\mathbf{k}_1.(\mathbf{r}_1 - \mathbf{r}_2)} \\ & d(\mathbf{r}_1 - \mathbf{r}_2) d^3r_2 \\ &= \frac{1}{L^6} \int U^{(2)}(\mathbf{k}_1 - \mathbf{k}_1') e^{i(\mathbf{k}_2 + \mathbf{k}_1 - \mathbf{k}_2' - \mathbf{k}_1').\mathbf{r}_2} d^3r_2 \end{aligned}$$

where in the third step we have introduced the Fourier transform of the two body potential and the last integral vanishes unless $\mathbf{k}_2 + \mathbf{k}_1 - \mathbf{k}_2' - \mathbf{k}_1' = 0$ (corresponding to momentum conservation in our translational invariant system in the presence of the

two body interactions only). If this condition is satisfied, the integral gives a factor L^3 and hence,

$$U^{(2)}_{k_1' k_2' k_2 k_1} = \frac{1}{L^3} U^{(2)}(\mathbf{k}_1 - \mathbf{k}_1') \delta_{\mathbf{k}_2 + \mathbf{k}_1 - \mathbf{k}_2' - \mathbf{k}_1'} \tag{2.84}$$

Similarly, our single particle energies can be written as

$$H^{(1)}_{kk'} = \varepsilon_{\mathbf{k}} \delta_{kk'} \tag{2.85}$$

where

$$\varepsilon_{\mathbf{k}} = \frac{\hbar^2 k^2}{2m} \tag{2.86}$$

is the single particle energies and after defining $\mathbf{k}_1' = \mathbf{k}_1 + \mathbf{q}$ and $\mathbf{k}_2' = \mathbf{k}_2 - \mathbf{q}$ our Hamiltonian becomes

$$\hat{H} = \sum_k \varepsilon_{\mathbf{k}} \hat{c}^\dagger_{\mathrm{k}} \hat{c}_{\mathrm{k}} + \frac{1}{2L^3} \sum_{\mathbf{k}_1, \mathbf{k}_2, \mathbf{q}} U(\mathbf{q}) \hat{c}^\dagger_{\mathrm{k}_1 + \mathbf{q}} \hat{c}^\dagger_{\mathrm{k}_2 - \mathbf{q}} \hat{c}_{\mathrm{k}_2} \hat{c}_{\mathrm{k}_1} \tag{2.87}$$

Taking the spin quantum numbers into account we finally get the spin dependent Hamiltonian

$$\hat{H} = \sum_{k,\sigma} \varepsilon_{\mathbf{k}} \hat{c}^\dagger_{\mathrm{k}\sigma} \hat{c}_{\mathrm{k}\sigma} + \frac{1}{2V} \sum_{\mathbf{k}_1, \mathbf{k}_2, \mathbf{q}, \sigma, \sigma'} U(\mathbf{q}) \hat{c}^\dagger_{\mathrm{k}_1 + \mathbf{q}, \sigma} \hat{c}^\dagger_{\mathrm{k}_2 - \mathbf{q}, \sigma'} \hat{c}_{\mathrm{k}_2, \sigma'} \hat{c}_{\mathrm{k}_1, \sigma} \tag{2.88}$$

where $V = L^3$ is the volume of the system. The interaction part of the Hamiltonian can be rewritten by explicitly summing over the spins

$$\hat{U} = \frac{1}{2V} \sum_{\mathbf{k}_1, \mathbf{k}_2, \mathbf{q}} U(\mathbf{q}) (\hat{c}^\dagger_{\mathrm{k}_1 + \mathbf{q}, \uparrow} \hat{c}^\dagger_{\mathrm{k}_2 - \mathbf{q}, \uparrow} \hat{c}_{\mathrm{k}_2, \uparrow} \hat{c}_{\mathrm{k}_1, \uparrow} + \hat{c}^\dagger_{\mathrm{k}_1 + \mathbf{q}, \downarrow} \hat{c}^\dagger_{\mathrm{k}_2 - \mathbf{q}, \downarrow} \hat{c}_{\mathrm{k}_2, \downarrow} \hat{c}_{\mathrm{k}_1, \downarrow}) \tag{2.89}$$

$$+ \frac{1}{V} \sum_{\mathbf{k}_1, \mathbf{k}_2, \mathbf{q}} U(\mathbf{q}) \hat{c}^\dagger_{\mathrm{k}_1 + \mathbf{q}, \uparrow} \hat{c}^\dagger_{\mathrm{k}_2 - \mathbf{q}, \downarrow} \hat{c}_{\mathrm{k}_2, \downarrow} \hat{c}_{\mathrm{k}_1, \uparrow} \tag{2.90}$$

2.4.4 The Bogoliubov transformation

Before calculating the expectation value of the Hamiltonian, it is very useful to introduce the Bogolioubov operators through the following *canonical* transformation which transforms particles into quasiparticles denoted by the operators $\hat{\alpha}_{\mathbf{k}}$ and $\hat{\beta}_{\mathbf{k}}$.

$$\hat{\alpha}_{\mathbf{k}\uparrow} = u_{\mathbf{k}} \hat{c}_{\mathbf{k}\uparrow} - v_{\mathbf{k}} \hat{c}^\dagger_{-\mathbf{k}\downarrow} \qquad \hat{\beta}_{-\mathbf{k}\downarrow} = u_{\mathbf{k}} \hat{c}_{-\mathbf{k}\downarrow} + v_{\mathbf{k}} \hat{c}^\dagger_{\mathbf{k}\uparrow} \tag{2.91}$$

This transformation is known as Bogoliubov-Valatin (B-V) transformation

$$\hat{\alpha}^\dagger_{\mathbf{k}\uparrow} = u^*_{\mathbf{k}} \hat{c}^\dagger_{\mathbf{k}\uparrow} - v^*_{\mathbf{k}} \hat{c}_{-\mathbf{k}\downarrow} \qquad \hat{\beta}^\dagger_{-\mathbf{k}\downarrow} = u^*_{\mathbf{k}} \hat{c}^\dagger_{-\mathbf{k}\downarrow} + v^*_{\mathbf{k}} \hat{c}_{\mathbf{k}\uparrow} \tag{2.92}$$

The inverse transformations are,

$$\hat{c}_{\mathbf{k}\uparrow} = u^*_{\mathbf{k}}\hat{\alpha}_{\mathbf{k}\uparrow} + v_{\mathbf{k}}\hat{\beta}^\dagger_{-\mathbf{k}\downarrow} \qquad \hat{c}_{-\mathbf{k}\downarrow} = u^*_{\mathbf{k}}\hat{\beta}_{-\mathbf{k}\downarrow} - v_{\mathbf{k}}\hat{\alpha}^\dagger_{\mathbf{k}\uparrow} \tag{2.93}$$

$$\hat{c}^\dagger_{\mathbf{k}\uparrow} = u_{\mathbf{k}}\hat{\alpha}^\dagger_{\mathbf{k}\uparrow} + v^*_{\mathbf{k}}\hat{\beta}_{-\mathbf{k}\downarrow} \qquad \hat{c}^\dagger_{-\mathbf{k}\downarrow} = u_{\mathbf{k}}\hat{\beta}^\dagger_{-\mathbf{k}\downarrow} - v^*_{\mathbf{k}}\hat{\alpha}_{\mathbf{k}\uparrow} \tag{2.94}$$

Since quasi-particles should also satisfy fermionic anti-commutation relations

$$\{\hat{\alpha}_{\mathbf{k}\sigma}, \hat{\alpha}^\dagger_{\mathbf{k}'\sigma'}\} = \delta_{\mathbf{k}\mathbf{k}'}\delta_{\sigma\sigma'} \tag{2.95}$$

$$\{\hat{\beta}_{\mathbf{k}\sigma}, \hat{\beta}^\dagger_{\mathbf{k}'\sigma'}\} = \delta_{\mathbf{k}\mathbf{k}'}\delta_{\sigma\sigma'} \tag{2.96}$$

the functions $u_{\mathbf{k}}$ and $v_{\mathbf{k}}$ also obey the orthogonality relation

$$u^*_{\mathbf{k}}u_{\mathbf{k}'} + v^*_{\mathbf{k}}v_{\mathbf{k}'} = \delta_{\mathbf{k}\mathbf{k}'} \tag{2.97}$$

The BCS state given by Eq. (2.77) is the vacuum state for the Bogolioubov destruction operators.

$$\hat{\alpha}_{\mathbf{k}\uparrow}\big|\Psi_{\mathbf{BCS}}\big\rangle = 0 \tag{2.98}$$

$$\hat{\beta}_{-\mathbf{k}\downarrow}\big|\Psi_{\mathbf{BCS}}\big\rangle = 0 \tag{2.99}$$

For example, Eq. (2.98) can be rewritten as

$$\begin{aligned}\hat{\alpha}_{\mathbf{k}\uparrow}\big|\Psi_{\mathbf{BCS}}\big\rangle &= (u^*_{\mathbf{k}}\hat{c}^\dagger_{\mathbf{k}\uparrow} - v^*_{\mathbf{k}}\hat{c}_{-\mathbf{k}\downarrow})\prod_{\mathbf{k}}(u^*_{\mathbf{k}} + v^*_{\mathbf{k}}\hat{c}^\dagger_{\mathbf{k}\uparrow}a^\dagger_{-\mathbf{k}\downarrow})\big|0\big\rangle \\ &= (u^*_{\mathbf{k}}\hat{c}^\dagger_{\mathbf{k}\uparrow} - v^*_{\mathbf{k}}\hat{c}_{-\mathbf{k}\downarrow})(u^*_{\mathbf{1}} + v^*_{\mathbf{1}}a^\dagger_{\mathbf{1}\uparrow}a^\dagger_{-\mathbf{1}\downarrow})(u^*_{\mathbf{2}} + v^*_{\mathbf{2}}\hat{c}^\dagger_{\mathbf{2}\uparrow}\hat{c}^\dagger_{-\mathbf{2}\downarrow}) \\ &\ldots(u^*_{\mathbf{m}} + v^*_{\mathbf{m}}\hat{c}^\dagger_{\mathbf{m}\uparrow}\hat{c}^\dagger_{-\mathbf{m}\downarrow})\ldots\big|0\big\rangle\end{aligned}$$

If we use the anti-commutation relations for the creation and annihilation operators,

$$\{\hat{c}_{\mathbf{k}\sigma}, \hat{c}^\dagger_{\mathbf{k}'\sigma'}\} = \delta_{\mathbf{k}\mathbf{k}'}\delta_{\sigma\sigma'} \tag{2.100}$$

$$\{\hat{c}_{\mathbf{k}\sigma}, \hat{c}_{\mathbf{k}'\sigma'}\} = 0 \tag{2.101}$$

$$\{\hat{c}^\dagger_{\mathbf{k}\sigma}, \hat{c}^\dagger_{\mathbf{k}'\sigma'}\} = 0 \tag{2.102}$$

we can easily see that the terms in brackets commute and for the m^{th} term the multiplication is

$$\begin{aligned}&(u^*_{\mathbf{k}}\hat{c}_{\mathbf{k}\uparrow} - v^*_{\mathbf{k}}\hat{c}^\dagger_{-\mathbf{k}\downarrow})(u^*_{\mathbf{m}} + v^*_{\mathbf{m}}\hat{c}^\dagger_{\mathbf{m}\uparrow}\hat{c}^\dagger_{-\mathbf{m}\downarrow}) \\ &= u^*_{\mathbf{k}}u^*_{\mathbf{m}}\hat{c}_{\mathbf{k}\uparrow} + u^*_{\mathbf{k}}v^*_{\mathbf{m}}\hat{c}_{\mathbf{k}\uparrow}\hat{c}^\dagger_{\mathbf{m}\uparrow}\hat{c}^\dagger_{-\mathbf{m}\downarrow} - v^*_{\mathbf{k}}u^*_{\mathbf{m}}\hat{c}^\dagger_{-\mathbf{k}\downarrow} - v^*_{\mathbf{k}}v^*_{\mathbf{m}}\hat{c}_{-\mathbf{k}\downarrow}\hat{c}^\dagger_{\mathbf{m}\uparrow}\hat{c}^\dagger_{-\mathbf{m}\downarrow} \\ &= u^*_{\mathbf{k}}u^*_{\mathbf{m}}a_{\mathbf{k}\uparrow} + u^*_{\mathbf{k}}v^*_{\mathbf{m}}\delta_{\mathbf{k}\mathbf{m}}\hat{c}^\dagger_{-\mathbf{m}\downarrow} - u^*_{\mathbf{k}}v^*_{\mathbf{m}}a^\dagger_{\mathbf{m}\uparrow}a_{\mathbf{k}\uparrow}\hat{c}^\dagger_{-\mathbf{m}\downarrow} - v^*_{\mathbf{k}}u^*_{\mathbf{m}}\hat{c}^\dagger_{-\mathbf{k}\downarrow} - v^*_{\mathbf{k}}v^*_{\mathbf{m}}\hat{c}^\dagger_{-\mathbf{k}\downarrow}\hat{c}^\dagger_{\mathbf{m}\uparrow}\hat{c}^\dagger_{-\mathbf{m}\downarrow} \\ &= u^2_{\mathbf{k}}\hat{c}_{\mathbf{k}\uparrow} + u^*_{\mathbf{k}}v^*_{\mathbf{k}}\hat{c}^\dagger_{\mathbf{k}\uparrow}\hat{c}^\dagger_{-\mathbf{k}\downarrow}\hat{c}_{\mathbf{k}\uparrow}\end{aligned}$$

Provided that we apply the result terms to the vacuum state $\big|0\big\rangle$, we obtain zero. The B-V operators are useful even in the absence of superconductivity. Consider the ground state $\big|\psi_{gnd}\big\rangle$ of a free Fermi gas, which in terms of the $\hat{c}^{\dagger}_{\mathbf{k}\sigma}$ can be written

$$\big|\psi_{gnd}\big\rangle = \prod_{|\mathbf{k}|<k_F,\sigma} \hat{c}^{\dagger}_{\mathbf{k}\sigma}\big|\psi_{vac}\big\rangle \tag{2.103}$$

where $\big|\psi_{vac}\big\rangle$ is the vacuum or empty state. Now assume the special case of

$$u_{\mathbf{k}} = \theta(\varepsilon_{\mathbf{k}} - \varepsilon_F) \qquad v_{\mathbf{k}} = \theta(\varepsilon_F - \varepsilon_{\mathbf{k}}) \tag{2.104}$$

here $\theta(x)$ is the heaviside step funciton whose value is zero for negative argument and one for positive argument. For this specific case we have

$$\hat{\alpha}^{\dagger}_{\mathbf{k}\uparrow} = \begin{cases} \hat{c}^{\dagger}_{\mathbf{k}\uparrow} & ; \qquad k > k_F \\ -\hat{c}_{-\mathbf{k}\downarrow} & ; \qquad k < k_F \end{cases} \tag{2.105}$$

$$\hat{\beta}^{\dagger}_{-\mathbf{k}\downarrow} = \begin{cases} \hat{c}^{\dagger}_{-\mathbf{k}\downarrow} & ; \qquad k > k_F \\ \hat{c}_{\mathbf{k}\uparrow} & ; \qquad k < k_F \end{cases} \tag{2.106}$$

To make an electron excitation like $\big|\mathbf{k},\uparrow\big\rangle$ when $k > k_F$, one would insert an electron with quantum numbers, $\mathbf{k}\uparrow$, whereas to create an excitation with quantum numbers $\mathbf{k}\uparrow$ when $k < k_F$ we should destroy the existing electron state with quantum numbers $-\mathbf{k}\downarrow$ by creating a hole state. These two states can be obtained by the form $\alpha^{\dagger}_{\mathbf{k}\uparrow}\big|\psi_{gnd}\big\rangle$. From Eq. (2.79) it is obvious that we can select

$$u_{\mathbf{k}} = \cos\theta_{\mathbf{k}} \qquad v_{\mathbf{k}} = \sin\theta_{\mathbf{k}} \tag{2.107}$$

With this definition we can rewrite the transformation as

$$\begin{bmatrix} \hat{\alpha}^{\dagger}_{\mathbf{k}\uparrow} \\ \hat{\beta}_{-\mathbf{k}\downarrow} \end{bmatrix} = \begin{bmatrix} \cos\theta_{\mathbf{k}} & -\sin\theta_{\mathbf{k}} \\ \sin\theta_{\mathbf{k}} & \cos\theta_{\mathbf{k}} \end{bmatrix} \begin{bmatrix} \hat{c}^{\dagger}_{\mathbf{k}\uparrow} \\ \hat{c}_{-\mathbf{k}\downarrow} \end{bmatrix} \tag{2.108}$$

and from this aspect we can say that the B-V transformation correspond to a *rotation* in particle - hole space. The inverse transformation also is equivalent to a rotation in the opposite direction.

2.5 The Self Consistent Set of Equations

The next step is to rewrite the Hamiltonian of our system in terms of the B-V operators. In order to do this we substitute Eqs.(2.93) and (2.94) into Eq. (2.88). For the fist part of the BCS Hamiltonian we need to calculate the expectation values for spin-up and spin-down respectively. For the spin-up states the expectation value of the single particle energies

$$\left\langle \Psi_{BCS}\right| \hat{c}^{\dagger}_{\mathbf{k}\uparrow}\hat{c}_{\mathbf{k}\uparrow}\left|\Psi_{BCS}\right\rangle \tag{2.109}$$

$$= \left\langle \Psi_{BCS}\right| (u_{\mathbf{k}}\hat{\alpha}^{\dagger}_{\mathbf{k}\uparrow} + v^{*}_{\mathbf{k}}\hat{\beta}_{-\mathbf{k}\downarrow})(u^{*}_{\mathbf{k}}\hat{\alpha}_{\mathbf{k}\uparrow} + v_{\mathbf{k}}\hat{\beta}^{\dagger}_{-\mathbf{k}\downarrow})\left|\Psi_{BCS}\right\rangle \tag{2.110}$$

$$= \left|v_{\mathbf{k}}\right|^2 \tag{2.111}$$

and for the spin-down states

$$\left\langle \Psi_{BCS}\right| \hat{c}^{\dagger}_{-\mathbf{k}\downarrow}\hat{c}_{-\mathbf{k}\downarrow}\left|\Psi_{BCS}\right\rangle \tag{2.112}$$

$$= \left\langle \Psi_{BCS}\right| (u_{\mathbf{k}}\beta^{\dagger}_{-\mathbf{k}\downarrow} - v^{*}_{\mathbf{k}}\hat{\alpha}_{\mathbf{k}\uparrow})(u^{*}_{\mathbf{k}}\hat{\beta}_{-\mathbf{k}\downarrow} - v_{\mathbf{k}}\hat{\alpha}^{\dagger}_{\mathbf{k}\uparrow})\left|\Psi_{BCS}\right\rangle \tag{2.113}$$

$$= \left|v_{\mathbf{k}}\right|^2 \tag{2.114}$$

where we ignore the terms that do not pair a creation operator with a destruction operator and use Eq. (2.100). The expectation values for the second part or interaction part of the Hamiltonian can be calculated in the same way and using Wick's theorem. Similar calculations can be found in any book discussing (BCS) superconductivity [17].

2.5.1 Minimization of the Energy

In this section we will minimize the free energy and then apply variational method to obtain the self-consistent set of equations that describe the BCS ground state. The expectation value of the free energy

$$\left\langle \Psi_{BCS}\right| H - \mu N \left|\Psi_{BCS}\right\rangle = \langle f \rangle \tag{2.115}$$

$$= 2\sum_{\mathbf{k}} (\varepsilon_{\mathbf{k}} - \mu)\left|v_{\mathbf{k}}\right|^2 + \frac{1}{V}\sum_{\mathbf{k},\mathbf{k}'} U_q u_{\mathbf{k}'} v^{*}_{\mathbf{k}'} u^{*}_{\mathbf{k}} v_{\mathbf{k}} + 4\frac{1}{2V}\sum_{\mathbf{k},\mathbf{k}'} U_{q=0}\left|v_{\mathbf{k}}\right|^2\left|v_{\mathbf{k}'}\right|^2 \tag{2.116}$$

where $q = |\mathbf{k} - \mathbf{k}'|$ and the last term is just a constant. It will not have an effect on the minimization. After performing the change of variables,

$$u_{\mathbf{k}} = \sin\theta_k \qquad v_{\mathbf{k}} = \cos\theta_k \tag{2.117}$$

The expectation value of the free energy operator is

$$\langle f \rangle = 2\sum_{\mathbf{k}}(\varepsilon_{\mathbf{k}} - \mu)\sin^2\theta_k + \frac{1}{4V}\sum_{\mathbf{k}\mathbf{k}'}U_{\mathbf{k}\mathbf{k}'}\sin 2\theta_k \sin 2\theta_{k'} \tag{2.118}$$

and if we minimize with respect to θ_k using $\delta\langle f \rangle/\delta\theta_k = 0$, we get

$$(\varepsilon_{\mathbf{k}} - \mu)\sin 2\theta_k + \left[\frac{1}{2V}\sum_{\mathbf{k}'}U_{\mathbf{k}\mathbf{k}'}\sin 2\theta'_k\right]\cos 2\theta_k = 0 \tag{2.119}$$

or

$$\tan 2\theta_k = \frac{-\frac{1}{2V}\sum_{\mathbf{k}'}U_{\mathbf{k}\mathbf{k}'}\sin 2\theta'_k}{\varepsilon_{\mathbf{k}} - \mu} \equiv \frac{\Delta_{\mathbf{k}}}{\xi_{\mathbf{k}}} \tag{2.120}$$

and it follows that

$$\sin 2\theta_k = \frac{\Delta_{\mathbf{k}}}{\sqrt{\Delta_{\mathbf{k}}^2 + \xi_{\mathbf{k}}^2}} \equiv \frac{\Delta_{\mathbf{k}}}{E_{\mathbf{k}}} \tag{2.121}$$

and

$$\sin^2\theta_k = \frac{\Delta_{\mathbf{k}}^2}{2(\Delta_{\mathbf{k}}^2 + \xi_{\mathbf{k}}^2 + \xi_{\mathbf{k}}E_{\mathbf{k}})} = \frac{1}{2}\left(1 - \frac{\xi_{\mathbf{k}}}{E_{\mathbf{k}}}\right) \tag{2.122}$$

After the definitions of $\Delta_{\mathbf{k}}, \xi_{\mathbf{k}}$ and $E_{\mathbf{k}}$, we obtain the following set of equations. These equations should be solved self consistently. For simplicity we neglected the interaction between particles that have the same spin.

$$\Delta_{\mathbf{k}} = -\frac{1}{2V}\sum_{\mathbf{k}'}U_{\mathbf{q}}\frac{\Delta_{\mathbf{k}'}}{E_{\mathbf{k}'}} \tag{2.123}$$

$$\xi_{\mathbf{k}} = \varepsilon_{\mathbf{k}} - \mu \tag{2.124}$$

$$E_{\mathbf{k}}^2 = \xi_{\mathbf{k}}^2 + \Delta_{\mathbf{k}}^2 \tag{2.125}$$

The connection between $v_{\mathbf{k}}$ and $\Delta_{\mathbf{k}}$ is established using "pair wavefunction" which is associated with the eigenvectors in Eq. (2.52).

$$\phi_{\mathbf{k}} \equiv v_{\mathbf{k}}u_{\mathbf{k}} = \frac{\Delta_{\mathbf{k}}}{2E_{\mathbf{k}}} \tag{2.126}$$

The relations between quasi-particle excitation energies, gap function and momentum distribution is depicted in Fig. 2.4.

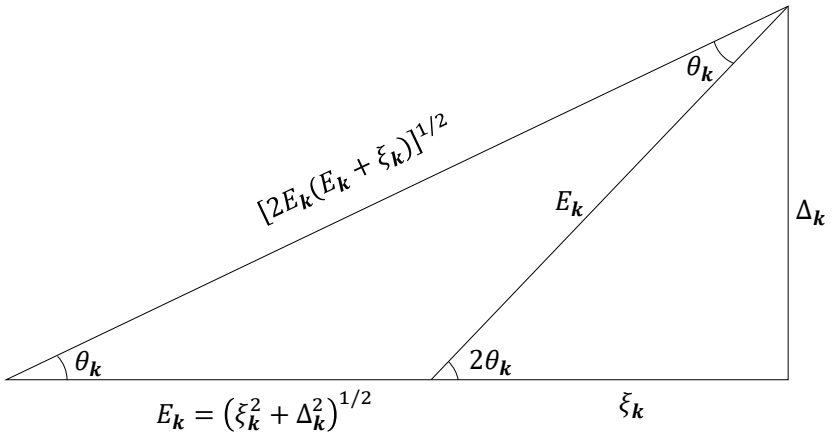

Figure 2.4 : Relations between $E_{\mathbf{k}}, \Delta_{\mathbf{k}}, \xi_{\mathbf{k}}$ and $\sin\theta_{\mathbf{k}}$.

2.5.2 Numerical solution of the gap equation

In this section we present our implementation of a numerical solution to the set of equations by iteration. We fix the range of the potential and the scattering length. Given these values we can calculate the depth of the potential U_0 (see App. B). The remaining part is to search for the right chemical potential that gives the correct density. The calculation boils down to finding the density of the system given a chemical potential, which, for a system with fixed number of particles will only be true if the density is equal to $k_F/3\pi^2$. In order to find a solution to the set of equations, we start with an initial guess of gap function, feed it to the right hand side and calculate the new values of the quantities $\Delta_{\mathbf{k}}$. This procedure is repeated until convergence to a desired degree is reached. For the gap energy we have

$$\Delta_{\mathbf{k}} = -\frac{1}{2V}\sum_{\mathbf{k}'} U_{\mathbf{q}} \frac{\Delta_{\mathbf{k}'}}{E_{\mathbf{k}'}} \tag{2.127}$$

where $\mathbf{q} = \mathbf{k} - \mathbf{k}'$. In the thermodynamic limit $(N \to \infty, V \to \infty, N/V \to n)$ we can bring the sum to an integral.

$$\sum_{\mathbf{k}} \quad \to \quad \frac{V}{(2\pi)^3}\int d^3k$$

In the calculation of $\Delta_{\mathbf{k}}$, we have to perform sums of the form

$$\frac{1}{V}\sum_{\mathbf{k}'} U_{\mathbf{k}\mathbf{k}'} F(k') \quad \to \quad \frac{1}{(2\pi)^3}\int dk' k'^2 U(k,k') F(k')$$

where we assume that $\xi_{\mathbf{k}}, \Delta_{\mathbf{k}}$ only depends on the magnitude of $\mathbf{k}$ and $U(k,k^{'})$ is the $U_{\mathbf{k}\mathbf{k}^{'}}$ integrated over the angles. (see Eq. 2.38)

$$U(k,k^{'}) = \int_0^{2\pi} d\phi \int_{\pi}^{0} d(\cos\theta) U(|\mathbf{k}-\mathbf{k}^{'}|) \tag{2.128}$$

$$= 2\pi \int_{-1}^{1} dx\, U(|\mathbf{k}-\mathbf{k}^{'}|) \tag{2.129}$$

$$= 8\pi^2 U_0 \int_{-1}^{1} dx \left[\frac{r_0 \cos\sqrt{k^2+k'^2-2kk'x}\, r_0}{k^2+k^{'}-2kk'x} - \frac{\sin\sqrt{k^2+k'^2-2kk'x}\, r_0}{(k^2+k'^2-2kk'x)^{3/2}} \right] \tag{2.130}$$

where $x = \cos\theta$. If we substitute

$$\beta = (k^2+k^{'2}-2kk^{'}x)^{1/2}$$

$$d\beta = -\frac{kk^{'}}{\beta} dx$$

it gives

$$U(k,k^{'}) = \frac{8\pi^2 U_0}{kk^{'}} \int_{k-k^{'}}^{k+k^{'}} d\beta \left[\frac{r_0 \cos\beta r_0}{\beta} - \frac{\sin\beta r_0}{\beta^2} \right] \tag{2.131}$$

We can integrate the second term by parts,

$$\int \sin\beta r_0 \, d\left(\frac{1}{\beta}\right) = \frac{\sin\beta r_0}{\beta} - \int r_0 \frac{\cos\beta r_0}{\beta} d\beta \tag{2.132}$$

so that

$$U(k,k^{'}) = \frac{8\pi^2 U_0}{kk^{'}} \left[\frac{\sin r_0(k+k^{'})}{k+k^{'}} - \frac{\sin r_0(k-k^{'})}{k-k^{'}} \right] \tag{2.133}$$

therefore the gap energy can be rewritten as

$$\Delta_k = -\frac{1}{2} \frac{1}{(2\pi)^3} \frac{8\pi^2 U_0}{k} \int dk^{'} k^{'} \left[\frac{\sin r_0(k+k^{'})}{k+k^{'}} - \frac{\sin r_0(k-k^{'})}{k-k^{'}} \right] \frac{\Delta_{k'}}{\sqrt{\xi_{k'}^2+\Delta_{k'}^2}} \tag{2.134}$$

$$= -\frac{1}{2\pi} \int dk^{'} k^{'} \frac{U_0}{k} \left[\frac{\sin r_0(k+k^{'})}{k+k^{'}} - \frac{\sin r_0(k-k^{'})}{k-k^{'}} \right] \frac{\Delta_{k'}}{\sqrt{\xi_{k'}^2+\Delta_{k'}^2}} \tag{2.135}$$

In dimensionless units,

$$\tilde{U}(\tilde{k},\tilde{k'}) = \frac{1}{8\pi^2} \frac{k_F^2}{\varepsilon_F} U(k,k^{'}) k^{'} \tag{2.136}$$

$$= \frac{\tilde{U}_0}{\tilde{k}} \left[\frac{\sin\tilde{r}_0(\tilde{k}+\tilde{k}^{'})}{\tilde{k}+\tilde{k}^{'}} - \frac{\sin r_0(\tilde{k}-\tilde{k}^{'})}{\tilde{k}-\tilde{k}^{'}} \right] \tag{2.137}$$

$$\tilde{\Delta}_k = -\frac{1}{2\pi} \int d\tilde{k^{'}}\ \tilde{k}^{'} \tilde{U}(\tilde{k},\tilde{k^{'}}) \frac{\tilde{\Delta_{k'}}}{\sqrt{(\tilde{k}'^2-\tilde{\mu})^2+\tilde{\Delta}_{k'}^2}} \tag{2.138}$$

$$\tilde{\Delta}_i = -\frac{1}{2\pi} \sum_j \omega_j \tilde{k_j^{'}} \tilde{U}(\tilde{k}_i,\tilde{k_j^{'}}) \tilde{F}(\tilde{k_j^{'}}) \tag{2.139}$$

where the last equation represents the Gaussian integration with

$$\tilde{F}(\tilde{k_j'}) = \frac{\tilde{\Delta}_j}{\sqrt{(\tilde{k}_j'^2 - \tilde{\mu})^2 + \tilde{\Delta}_j^2}}. \tag{2.140}$$

The Gaussian weight and abscissa are given by w_j and k_j.

2.6 Gap Function and Momentum Distribution

After the iteration converges to a desired degree of precision we can calculate other quantities of interest using

$$v_k = \sqrt{\frac{1}{2}\left(1 - \frac{\xi_k}{E_k}\right)} \qquad \text{and} \qquad {u_k}^2 = 1 - {v_k}^2 \tag{2.141}$$

$$\tilde{v}_k = \sqrt{\frac{1}{2}\left(1 - \frac{\tilde{\xi}_k}{\tilde{E}_k}\right)} \qquad \text{and} \qquad \tilde{u}_k^2 = 1 - \tilde{v}_k^2 \tag{2.142}$$

the expectation value of the particle number operator can be found as

$$\langle \hat{\mathrm{N}} \rangle = 2\sum_k \left|v_k\right|^2 \tag{2.143}$$

$$\langle \hat{\mathrm{n}} \rangle = \frac{2}{V}\sum_k \left|v_k\right|^2 \tag{2.144}$$

$$= \frac{2}{V}\frac{V}{(2\pi)^3} 4\pi \int_0^\infty dk\, k^2 \left|v_k\right|^2 \tag{2.145}$$

$$= \frac{1}{\pi^2}\sum_i \omega_i {k_i}^2 \left|v_i\right|^2 \tag{2.146}$$

$$\langle \tilde{\hat{\mathrm{n}}} \rangle = \frac{1}{\pi^2}\sum_i \omega_i \tilde{k}_i^2 \left|\tilde{v}_i\right|^2 \tag{2.147}$$

When this number is equal to $n = 1/3\pi^2$, we have found the right value chemical potential μ which is an input to our calculation. The expectation value of the Hamiltonian is found to be

$$\langle \hat{\mathrm{H}} \rangle = \sum_{\mathbf{k}} \left[2\varepsilon_{\mathbf{k}} \left|v_{\mathbf{k}}\right|^2 + \frac{\Delta_{\mathbf{k}}}{E_{\mathbf{k}}} \frac{1}{4V} \sum_{\mathbf{k}'} U_{\mathbf{k}\mathbf{k}'} \right] + 4\frac{1}{2V} \sum_{\mathbf{k}\mathbf{k}'} U_{\mathbf{k}-\mathbf{k}'=0} \left|v_{\mathbf{k}}\right|^2 \left|v_{\mathbf{k}'}\right|^2 \tag{2.148}$$

Using Eq. (2.125) this can be rewritten as

$$\langle \hat{\mathrm{h}} \rangle = \frac{1}{V}\sum_{\mathbf{k}} \left[2\varepsilon_{\mathbf{k}} \left|v_{\mathbf{k}}\right|^2 - \frac{1}{2}\frac{{\Delta_{\mathbf{k}}}^2}{E_{\mathbf{k}}} \right] + \frac{1}{2} Nn \int d\mathbf{r}\, U(\mathbf{r}) \tag{2.149}$$

$$= \frac{1}{V}\frac{V}{(2\pi)^3} 4\pi \int_0^\infty dk\, k^2 \left[2\varepsilon_{\mathbf{k}} \left|v_{\mathbf{k}}\right|^2 - \frac{1}{2}\frac{{\Delta_{\mathbf{k}}}^2}{E_{\mathbf{k}}} \right] - \frac{N}{2}\frac{1}{3\pi^2}\frac{4\pi}{3} {r_0}^3 U_0 \tag{2.150}$$

$$= \frac{1}{2\pi^2}\sum_i \omega_i {k_i}^2 \left[2\varepsilon_i \left|v_i\right|^2 - \frac{1}{2}\frac{{\Delta_{\mathrm{i}}}^2}{E_{\mathrm{i}}} \right] - N\frac{2}{9\pi} U_0 {r_0}^3 \tag{2.151}$$

Therefore

$$\langle\tilde{\hat{\mathrm{h}}}\rangle = \frac{1}{2\pi^2}\sum_i \omega_i \tilde{k_i}^2 \left[2\tilde{k}_i^2\left|\tilde{v}_i\right|^2 - \frac{1}{2}\frac{\tilde{\Delta}_i^2}{\tilde{E}_i}\right] - N\frac{2}{9\pi}\tilde{U}_0\tilde{r}_0^3 \tag{2.152}$$

and the energy per particle is

$$\frac{\langle\tilde{\hat{\mathrm{h}}}\rangle}{\langle\tilde{\hat{\mathrm{n}}}\rangle} = \frac{\sum_i \omega_i \tilde{k_i}^2 \left[2\tilde{k}_i^2\left|\tilde{v}_i\right|^2 - \frac{1}{2}\frac{\tilde{\Delta}_i^2}{\tilde{E}_i}\right]}{2\sum_i \omega_i \tilde{k}_i^2\left|\tilde{v}_i\right|^2} - \frac{2}{9\pi}\tilde{U}_0\tilde{r}_0^3 \tag{2.153}$$

2.7 Ground-State Fidelity

A quantum phase transition is an abrupt change of the ground-state of a many-body system when a controlling parameter like $\lambda = (k_F a)^{-1}$ of the Hamiltonian crosses a critical value λ_c. Therefore, it is quite natural to expect that the overlap

$$F(\lambda + \delta\lambda) \equiv \left|\left\langle\Psi(\lambda + \delta\lambda)|\Psi(\lambda)\right\rangle\right| \tag{2.154}$$

between the ground states corresponding to two slightly different values of the parameter λ, should manifest an abrupt drop when the small variation $\delta\lambda$ crosses λ_c. Thus, such an overlap, which has been named *ground-state fidelity* in the literatur. We consider the crossover problem, that is, a many-body system for which a substantial change in the nature of its ground state occurs over a finite range of the controlling parameter λ, rather than abruptly at a critical value. On physical grounds, we expect that the sudden drop of the ground-state fidelity at a critical value should in this case be replaced by a minimum, located in the region of λ where the ground state is changing more rapidly, namely, in the crossover region. In terms of the fidelity susceptibility which will be defined, the divergence at a critical point should correspondingly be replaced by a peak, whose width should be associated with the width of the crossover region. [18] In this section we will introduce fidelity susceptibility an derive its expression for the BCS wave function for the three-dimensional system. This quantity is calculated explicitly for the BCS-BEC crossover with model square well potential interaction. We also show the evolution of the condensate fraction duruing he BCS-BEC crossover process.

2.7.1 Fidelity susceptibility

Ground state fidelity depends on control parameter λ and its variation $\delta\lambda$. However, the dependence on the $\delta\lambda$ can be eliminated by the considering its small value

$$F(\lambda+\delta\lambda)^2 = \left[\langle\psi(\lambda)| + \delta\lambda + \frac{(\delta\lambda)^2}{2}\frac{\partial^2\langle\psi(\lambda)|}{\partial\lambda^2}\right]|\Psi(\lambda)\rangle \tag{2.155}$$

$$= 1 - \frac{(\delta\lambda)^2}{2}\frac{\partial\langle\psi(\lambda)|}{\partial\lambda}\frac{\partial|\psi(\lambda)\rangle}{\partial\lambda} \tag{2.156}$$

where the state $|\Psi(\lambda)\rangle$ is assumed to be real and normalized. A sudden drop of the ground-state fidelity at the critical point will then correspond to a divergence of the *fidelity susceptibility*:

$$\chi(\lambda) \equiv -\frac{1}{\Omega}\lim_{\delta\lambda\to 0}\frac{4\ln[F(\lambda+\delta\lambda)]}{(\delta\lambda)^2} \tag{2.157}$$

$$= \frac{1}{\Omega}\frac{\partial\langle\psi(\lambda)|}{\partial\lambda}\frac{\partial|\psi(\lambda)\rangle}{\partial\lambda} \tag{2.158}$$

where Ω is the volume of the system. The BCS wavefunction provides a reasonably good approximation for the ground-state wavefunction over the whole BCS-BEC crossover, from the weak-coupling limit of highly overlapping Cooper pairs to the strong-coupling limit of tightly bound dilute composite bosons. That's why we will calculate the fidelity susceptibility $\chi(\lambda)$ for the BCS wavefunction:

$$|\Psi_{\mathbf{BCS}}\rangle = \prod_{\mathbf{k}}(u_{\mathbf{k}}(\lambda) + v_{\mathbf{k}}(\lambda)\hat{c}^{\dagger}_{\mathbf{k}\uparrow}\hat{c}_{-\mathbf{k}}\downarrow)|0\rangle \tag{2.159}$$

When the BCS wavefynction is inserted in Eq. (2.158), $\chi(\lambda)$ is obtained as

$$\chi(\lambda) = \int\frac{d\mathbf{k}}{(2\pi)^d}\left[\left(\frac{du_k}{d\lambda}\right)^2 + \left(\frac{dv_k}{d\lambda}\right)^2\right] \tag{2.160}$$

where d is the spatial dimension and after taking the derivatives it can be written for 3D system as

$$\chi(\lambda) = \int\frac{4\pi k^2 dk}{(2\pi)^3}\frac{1}{4E_k^4}\left[\Delta_k\frac{d\mu}{d\lambda} + \xi_k\frac{d\Delta_k}{d\lambda}\right]^2 \tag{2.161}$$

$$\chi(\lambda) = k_F^3\frac{1}{2\pi^2}\sum_i\omega_i\tilde{k}_i^2\frac{1}{4\tilde{E}_i^4}\left[\tilde{\Delta}_i\frac{d\tilde{\mu}}{d\lambda} + \tilde{\xi}_i\frac{d\tilde{\Delta}_i}{d\lambda}\right]^2 \tag{2.162}$$

We calculate the $\chi(\lambda)$ against each one of the small variations over the controlling parameter from the BCS to BEC state.

2.7.2 Condensate fraction in the BCS-BEC crossover

As the interaction is turned on and gradually increased, the system evolves continuously from the ideal Fermi gas, to the BCS state of extremely wide and weakly

bound Cooper pairs, to a gas of increasingly tightly bound "molecular" bosonic dimers, to finally reach the limit of an ideal Bose gas in its Bose-Einstein condensed state. The condensate fraction is a thermodynamic property characterizing the superfluid or superconducting state. In a Fermi gas it is possible to work out the condensate fraction through mean field theory [19] which shows good agreement with the experiment [9]. Here we calculated the condensate fraction which is strictly related to the off-diagonal long-range order (ODLRO) of the system. We use the following mean field description of the condensate fraction

$$n_c = \sum_k \left[\frac{\Delta_k}{2E_k}\right]^2 \tag{2.163}$$

in thermodynamic limit

$$n_c = \frac{k_F^3}{2\pi^2}\int d\tilde{k}\tilde{k}^2 \left[\frac{\tilde{\Delta}_k}{2\tilde{E}_k}\right]^2 \tag{2.164}$$

$$n_c = \frac{k_F^3}{2\pi^2}\sum_i \omega_i \tilde{k}_i^2 \left[\frac{\tilde{\Delta}_i}{2\tilde{E}_i}\right]^2 \tag{2.165}$$

2.8 Discussions on 3D Results

In this section we present the results for 3D system. In three dimension with the existence of the Fermi sea there is always a bound state between two fermions for very weak interactions. However this is not true for all interaction strength in free space for three dimensional systems. There must be threshold value for attractive interaction in order to construct a bound state. In our calculations we fix the range of the potential with one hundredth of the interparticle distance, $r_0 = 0.01n^{-1/3}$, (the diluteness conditions $nr_0^3 \ll 1$ are $(k_0/k_F)^3 \gg 1$ satisfied) and control the interaction strength with scattering length. Typically, this corresponds to depth of the potential well values $U_0 \propto 1/r_0^2 \approx 10^4\varepsilon_F$ and $k_0 \approx 100k_F$ (see App. B).

In the BCS limit the chemical potential of the system equals to Fermi energy and the maximum value of the superconducting gap function is almost zero. In Fig. 2.10 it is shown that when you increase the interaction between particles the chemical potential of the system decreases whereas the maximum value of the superconducting gap increases. In the BEC limit, there only exist the binding energies in the system. After tightly bound pairs are constructed, they weakly interact each other. Because of the Pauli exclusion principle the particle with same spin in the dimers can not come side by side. It is depicted in Fig. 2.6. On the one hand, the momentum

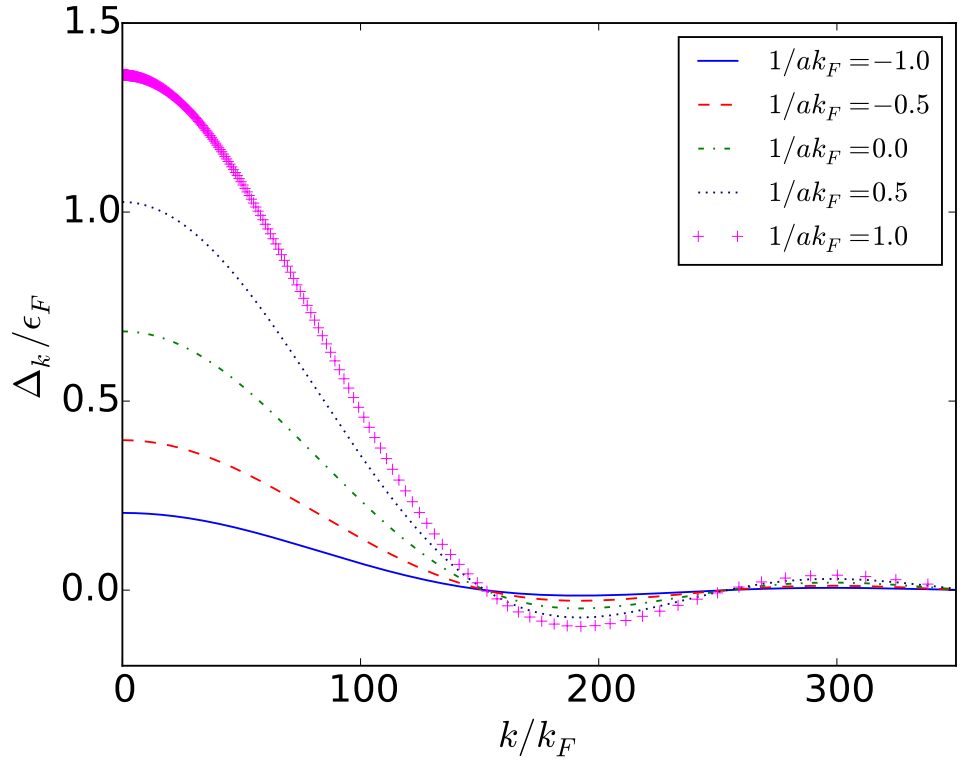

Figure 2.5 : Evolution of the gap as a function of k states for different interaction parameters from weakly interactin BCS limit to strongly interacting BEC limit.

distribution is a step function in the low interaction limit, but on the other hand, it tilts with the increasing interaction. In the BCS regime, the Fermi surface is only slightly smoothened due to pairing around the Fermi momentum. Towards the BEC regime, the distributions become flatter and flatter; more and more momentum states are needed to build up tightly bound pairs. Changing of the gap function with respect to the momentum is depicted in Fig. 2.5. The gap function starts to oscillate in the a certain k-state. First oscillation of the gap corresponds to the inverse of the range of the potential. Under conditions the main contribution to scattering comes from states with an $l = 0$ component of the angular momentum. The delta function up to $2k_F$ is constant. Beacuse of this, the oscillations are not important under diluteness conditions. In Fig. 2.7 it is shown that the evolution of the quasi-particle excitation energies during the BCS-BEC crossover process. The gap on the spectrum of $E_{\mathbf{k}}$ onto Fermi momentum corresponds to value of $\Delta_{\mathbf{k}}$ in Fig. 2.5. As the interaction is increased the effect of gap on the quasi-particle energies is increased. The pair wave function is depicted in Fig. 3.4. In the weak interacting limit the most contribution to pair formation is in the vicinity of k_F momentum. With the increasing of the interaction,

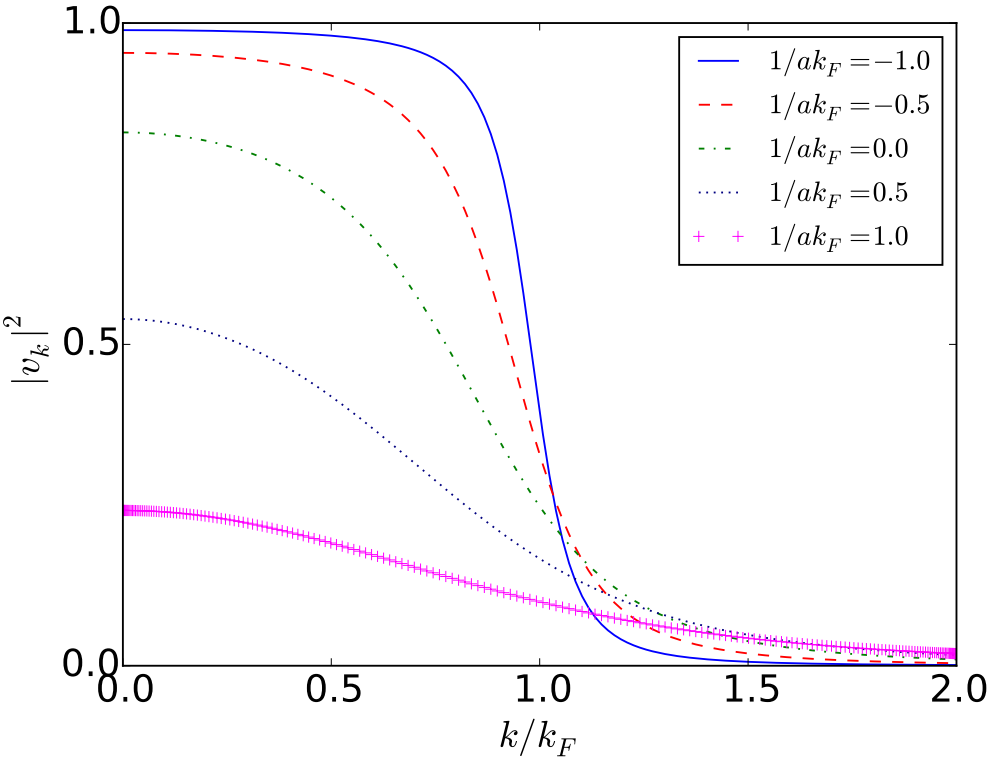

Figure 2.6 : Occupation of momentum states for different interaction parameters in the BCS-BEC crossover.

strength the contribution from other states starts to come for pairing formation. In the BCS limit, the minimum of the quasi-particle energies and the maximum of the gap function are equal each other. In Fig. 2.9 when the interaction increases, the equality breaks after the unitarity with the formation of the bound states. Fig. 2.11 shows the behavior of the energy per particle, chemical potential and binding energy from weakly interacting limit to strongly interacting limit. In BCS limit, the chemical potential of the system is in the Fermi energy level and energy per particle is sixty percent of the chemical potential. With the increasing of the interaction both chemical potential and energy per particle goes to one half of the binding energy and difference between them vanishes. This means that there is only weakly interacting or non-interacting bosonic molecules in the system and all energy is in their binding. Fig. 2.12 shows the fidelity susceptibility from BCS limit to BEC limit. Fidelity susceptibility shows a peak in the middle. This means the maximum changing of the ground state occurs in the unitarity. The evolution of the condensate fraction of the system is depicted in Fig. 2.13. As the interaction is increased the fraction approaches to one which means all dimers condense into the lowest energy state.

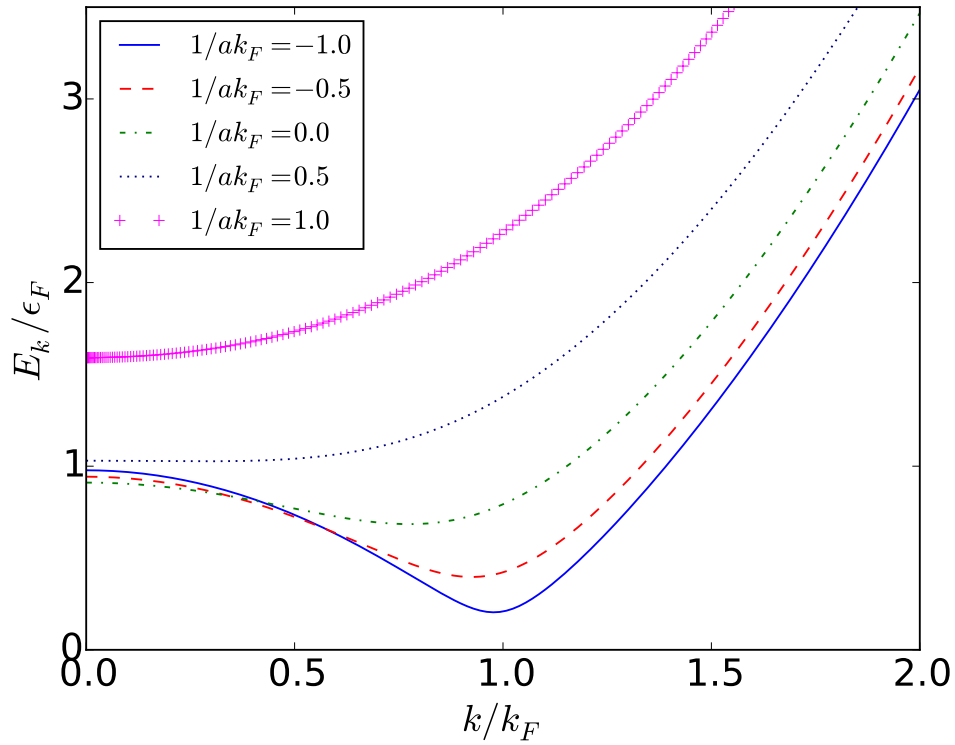

Figure 2.7 : Evolution of the quasi-particle excitation energies as a function of momentum for different interaction parameters during the BCS-BEC crossover.

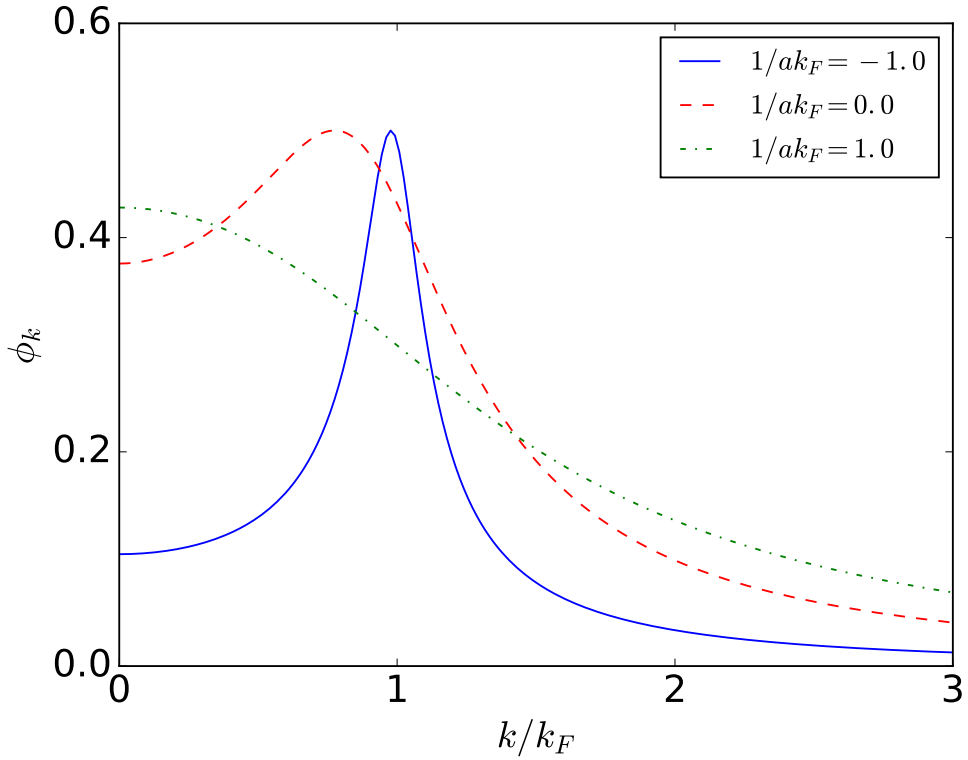

Figure 2.8 : Evolution of pair-correlation wave function as a function of momentum for different interaction parameters during the BCS-BEC crossover.

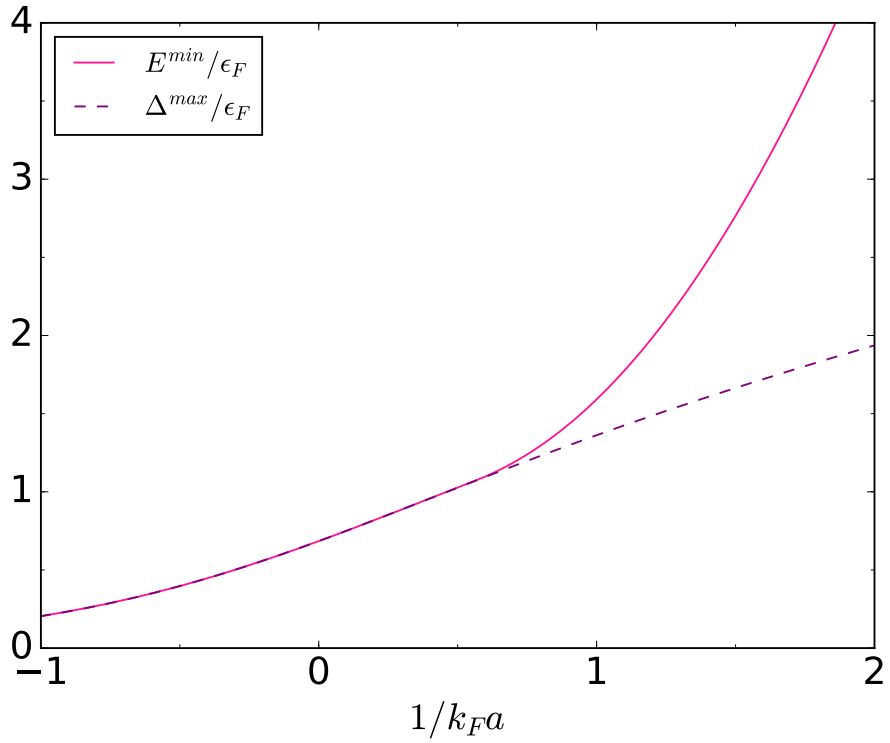

Figure 2.9 : Changing of minimum excitation energy and maximum values of the gap with respect to dimensionless interaction parameter.

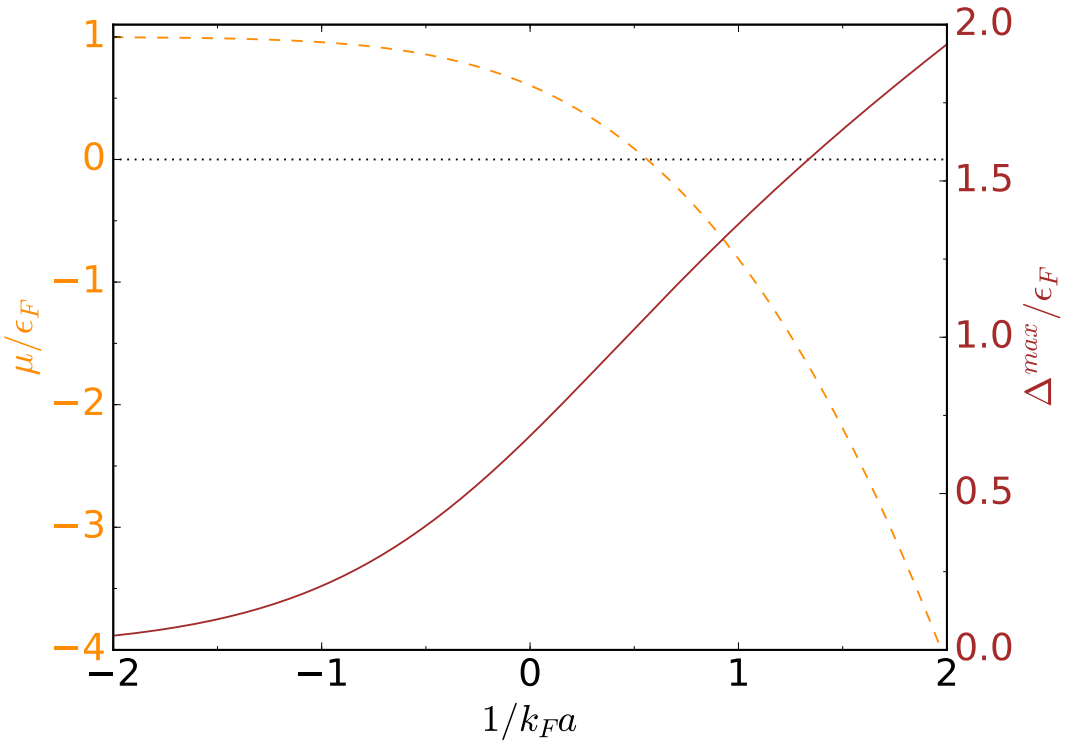

Figure 2.10 : Chemical potential (dashed line) and gap (solid line) in the BCS- BEC crossover as a function of the interaction parameter $1/k_Fa$. The BEC limit of positive $1/k_Fa$ is to the right hand side of the graph.

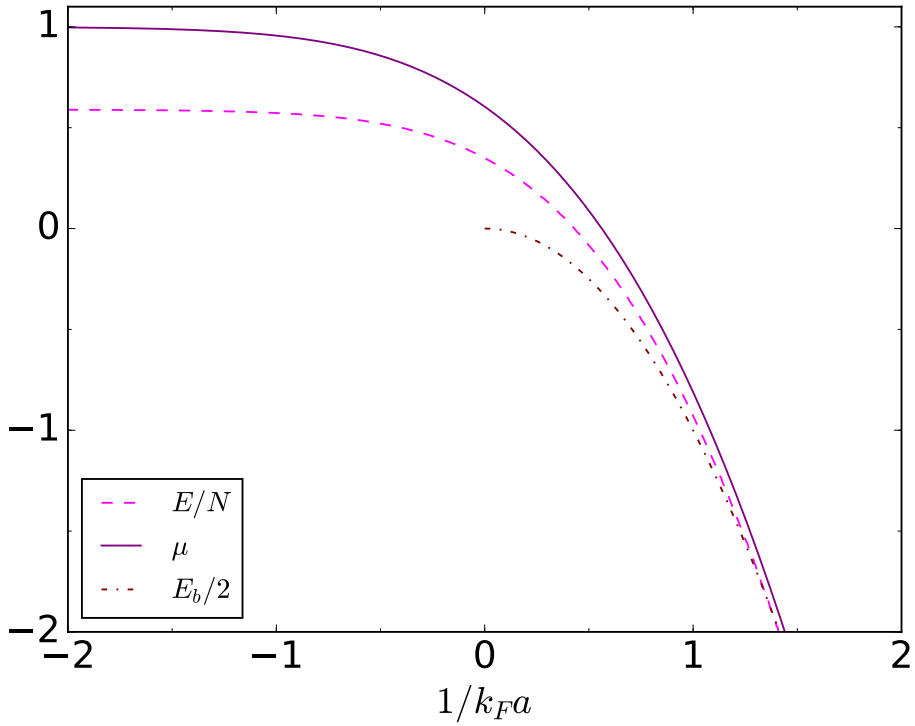

Figure 2.11 : The energy per particle and the chemical potential as a function of the interaction parameter in the process of BCS-BEC crossover in three dimensional system.

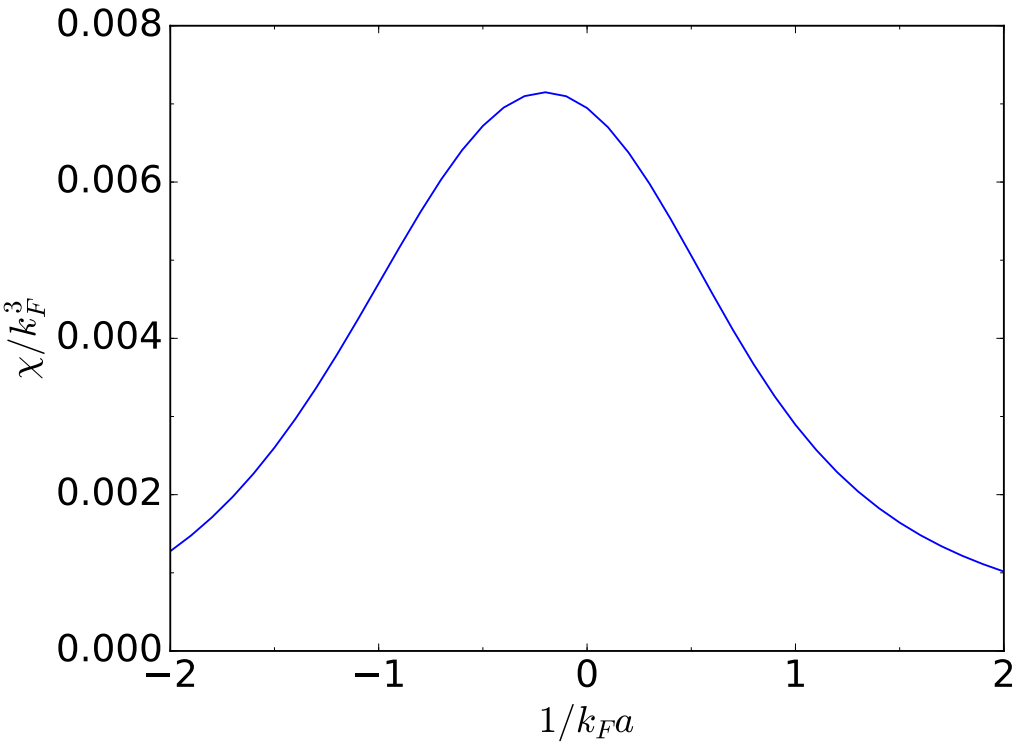

Figure 2.12 : Changing of the fidelity susceptibility for three dimensional square well potential as a function of the dimensionless coupling strength during the BCS-BEC crossover.

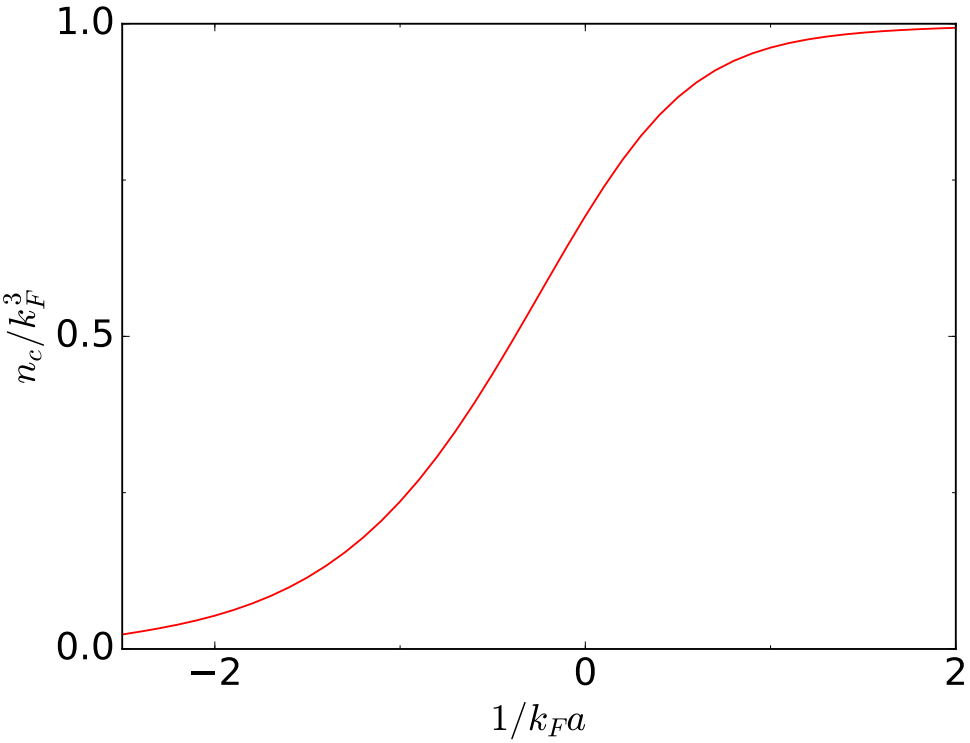

Figure 2.13 : Condensate fraction of Fermi pairs in the uniform two-component dilute Fermi gas as a function of the controlling parameter during the BCS-BEC crossover.

3. BCS-BEC Crossover in 2D

Quantum fluctuations play a crucial role in low-dimensional systems. In the analysis of the two-dimensional attractive Fermi gas one must remember that, contrary to the 3D case, 2D realistic interatomic attractive potentials have always a bound state. Unlike 3D, a two-body bound state always exists in 2D even though the attraction is arbitrarily weak. We obtain and solve numerically the self consistency equation for 2D system. In this case we drive the crossover by changing the depth of the model square well interaction potential U_0 at fixed range of the well $nr_0^2 = 10^{-4}$. We show the evolution of gap function, momentum distributions, quasi-particle excitation energies and chemical potential with respect to the interaction strength.

3.1 Non-interacting Fermi gas in 2D

Consider a large sheet of area

$$A = L_x L_y \tag{3.1}$$

and the particle inside the sheet are confined in a two dimensional infinite zero potential well and infinite potential outside the sheet.

$$V(\vec{r}) = \begin{cases} 0 & ; \qquad |\vec{r}| < (L_x^2 + L_y^2)^{1/2} \\ \infty & ; \qquad |\vec{r}| > (L_x^2 + L_y^2)^{1/2} \end{cases} \tag{3.2}$$

The particle states inside the sheet are given by the solution of Schrödinger equation. Using periodic boundary conditions, the eigenfuction are written as

$$\Psi_{\mathbf{k}}(x,y) = \frac{1}{\sqrt{A}} e^{i(k_x x + k_y y)} \tag{3.3}$$

The boundary conditions dictate that the allowed values of k_x and k_y are quantized as in in Eq. (2.7). The single particle energies are

$$\varepsilon_{\mathbf{k}} = \frac{\hbar^2 k^2}{2m} = \hbar^2 \frac{k_x^2 + k_y^2}{2m} \tag{3.4}$$

$$= \frac{2\hbar^2 \pi^2}{m} \left(\frac{n_x^2}{L_x^2} + \frac{n_y^2}{L_y^2} \right) \tag{3.5}$$

3.1.1 Balanced populations

The number of particles in 2D system is

$$N = 2\frac{\pi k_F^2}{(\frac{2\pi}{L})^2} = A\frac{{k_F}^2}{2\pi} \tag{3.6}$$

where two factor comes from spin and the particle density is

$$\frac{N}{A} = n = \frac{{k_F}^2}{2\pi} \tag{3.7}$$

In the thermodynamic limit the total internal energy Eq. (2.12) for this system

$$\sum_{\mathbf{k}} \quad \rightarrow \quad \frac{A}{(2\pi)^2}\int d^2k \tag{3.8}$$

$$E = \frac{A}{2\pi m}\int_0^{k_F} k^3 dk \tag{3.9}$$

$$= \frac{A}{2\pi m}\frac{k_F^4}{4} \tag{3.10}$$

$$= \frac{A}{2} n\varepsilon_F \tag{3.11}$$

the energy density and energy per particle are

$$\frac{E}{V} = e = \frac{n}{2}\varepsilon_F \tag{3.12}$$

$$\frac{e}{n} = \frac{E}{N} = \frac{\varepsilon_F}{2} \tag{3.13}$$

3.1.2 Imbalanced populations

The particle densities for spin up and down particles are

$$n_\uparrow = \frac{k_{F\uparrow}^2}{4\pi} \qquad n_\downarrow = \frac{k_{F\downarrow}^2}{4\pi} \tag{3.14}$$

and the total number of particles is given by

$$n = n_\uparrow + n_\downarrow = \frac{k_{F\uparrow}^2}{4\pi} + \frac{k_{F\downarrow}^2}{4\pi}. \tag{3.15}$$

From Eq. (2.11)

$$k_F^2 = \frac{1}{2}(k_{F\uparrow}^2 + k_{F\downarrow}^2) \tag{3.16}$$

and also from Eq. (3.14) and Eq. (2.22)

$$k_{F\uparrow} = k_F(1+\eta)^{1/2} \qquad k_{F\downarrow} = k_F(1-\eta)^{1/2} \tag{3.17}$$

The single particle energies of the spin-up particles is given

$$E_\uparrow = \frac{A}{4\pi m}\int_0^{k_{F\uparrow}} k^3 dk \tag{3.18}$$

$$= \frac{A}{4\pi m}\frac{{k_{F\uparrow}}^4}{4} \tag{3.19}$$

energy density for spin-up particles

$$e_\uparrow = \frac{\varepsilon_F}{4} n(1+\eta)^2 \tag{3.20}$$

and similarly for spin-down particles

$$e_\downarrow = \frac{\varepsilon_F}{4} n(1-\eta)^2 \tag{3.21}$$

so from Eq. (3.20) and Eq. (3.21) the energy per total particle is

$$\frac{e}{n} = \frac{E}{N} = \frac{\varepsilon_F}{4}\left[(1+\eta)^2 + (1-\eta)^2\right] \tag{3.22}$$

3.2 Solution of the Gap Equation in 2D

For the gap energy we have

$$\Delta_{\mathbf{k}} = -\frac{1}{2A}\sum_{\mathbf{k}'} U_{\mathbf{q}} \frac{\Delta_{\mathbf{k}'}}{E_{\mathbf{k}'}} \tag{3.23}$$

and the Fourier transform of the square well potential in strictly 2D system

$$U_{\mathbf{q}} = \int_0^\infty U(\mathbf{r}) e^{-i\mathbf{q}\mathbf{r}}\, d\mathbf{r} \tag{3.24}$$

$$= -U_0 \int_0^{r_0} r dr \int_0^{2\pi} e^{-iqr\cos\phi} d\phi \tag{3.25}$$

$$= -2\pi U_0 \int_0^{r_0} r J_0(qr) dr \tag{3.26}$$

$$= -2\pi U_0 r_0 \frac{J_1(qr_0)}{q} \tag{3.27}$$

where $\mathbf{q} = \mathbf{k} - \mathbf{k}'$ and ϕ is the angle between vectors $\mathbf{k}$ and $\mathbf{k}'$. In the thermodynamic limit we can write the sum as an integral

$$\sum_{\mathbf{k}} \quad \rightarrow \quad \frac{A}{(2\pi)^2}\int d^2k$$

In the calculation of $\Delta_{\mathbf{k}}$,

$$\frac{1}{A}\sum_{\mathbf{k}'} U_{\mathbf{k}\mathbf{k}'} F(k') \quad \rightarrow \quad \frac{1}{(2\pi)^2}\int dk' k' U(k,k') F(k')$$

where we assume that $\xi_{\mathbf{k}}, \Delta_{\mathbf{k}}$ only depends on the magnitude of $\mathbf{k}$ and $U(k,k^{'})$ is the $U_{\mathbf{kk}^{'}}$ integrated over the angle ϕ.

$$U(k,k^{'}) = -2\pi U_0 r_0 \int_0^{2\pi} \frac{J_1(r_0\sqrt{k^2+k'^2-2kk'\cos\phi})}{\sqrt{k^2+k'^2-2kk'\cos\phi}} d\phi \tag{3.28}$$

and the gap energy can be rewritten as

$$\Delta_k = \frac{U_0 r_0}{4\pi} \int_0^{\infty} dk'k' \left[\int_0^{2\pi} \frac{J_1(r_0\sqrt{k^2+k'^2-2kk'\cos\phi})}{\sqrt{k^2+k'^2-2kk'\cos\phi}} d\phi \right] \frac{\Delta_{k'}}{\sqrt{\xi_{k'}^2+\Delta_{k'}^2}} \tag{3.29}$$

In dimensionless units, the interaction term can be written as

$$\tilde{U}(\tilde{k},\tilde{k'}) = -\frac{k_F^2}{4\pi^2\varepsilon_F} U(k,k^{'}) \tag{3.30}$$

$$= \tilde{U}_0\tilde{r}_0 \int_0^{2\pi} \frac{J_1(\tilde{r}_0\sqrt{\tilde{k}^2+\tilde{k'}^2-2\tilde{k}\tilde{k'}\cos\phi})}{\sqrt{\tilde{k}^2+\tilde{k'}^2-2\tilde{k}\tilde{k'}\cos\phi}} d\phi \tag{3.31}$$

and the gap equation is

$$\tilde{\Delta}_k = \frac{1}{2}\int d\tilde{k'}\ \tilde{k'}\tilde{U}(\tilde{k},\tilde{k'}) \frac{\tilde{\Delta_{k'}}}{\sqrt{(\tilde{k'}^2-\tilde{\mu})^2+\tilde{\Delta}_{k'}^2}} \tag{3.32}$$

$$\tilde{\Delta}_i = \frac{1}{2}\sum_j \omega_j \tilde{k_j'} \tilde{U}(\tilde{k}_i,\tilde{k_j'}) \tilde{F}(\tilde{k_j'}) \tag{3.33}$$

where

$$\tilde{F}(\tilde{k_j'}) = \frac{\tilde{\Delta}_j}{\sqrt{(\tilde{k}_j'^2-\tilde{\mu})^2+\tilde{\Delta}_j^2}} \tag{3.34}$$

The number and density operators in 2D can similarly be calculated as

$$\langle \hat{\mathrm{N}} \rangle = 2\sum_k |v_k|^2 \tag{3.35}$$

$$\langle \hat{\mathrm{n}} \rangle = \frac{2}{A}\sum_k |v_k|^2 \tag{3.36}$$

$$= \frac{2}{A}\frac{A}{(2\pi)^2} 2\pi \int_0^{\infty} dk\ k |v_k|^2 \tag{3.37}$$

$$= \frac{1}{\pi}\sum_i \omega_i k_i |v_i|^2 \tag{3.38}$$

$$\langle \tilde{\hat{\mathrm{n}}} \rangle = \frac{1}{\pi}\sum_i \omega_i \tilde{k}_i |\tilde{v}_i|^2 \tag{3.39}$$

and energy density operator is

$$\langle \hat{\mathrm{h}} \rangle = \frac{1}{A}\sum_{\mathbf{k}} \left[2\varepsilon_{\mathbf{k}} |v_{\mathbf{k}}|^2 - \frac{1}{2}\frac{{\Delta_{\mathbf{k}}}^2}{E_{\mathbf{k}}} \right] + \frac{1}{2} Nn \int d\mathbf{r}\, U(\mathbf{r}) \tag{3.40}$$

$$= \frac{1}{A}\frac{A}{(2\pi)^2} 2\pi \int_0^\infty dk\, k \left[2\varepsilon_{\mathbf{k}} |v_{\mathbf{k}}|^2 - \frac{1}{2}\frac{{\Delta_{\mathbf{k}}}^2}{E_{\mathbf{k}}} \right] - \frac{N}{2}\frac{1}{2\pi}\pi {r_0}^2 U_0 \tag{3.41}$$

$$= \frac{1}{2\pi}\sum_i \omega_i k_i \left[2\varepsilon_i |v_i|^2 - \frac{1}{2}\frac{{\Delta_{\mathrm{i}}}^2}{E_{\mathrm{i}}} \right] - N\frac{U_0 {r_0}^2}{4} \tag{3.42}$$

finally energy per particle in 2D is given by the following expression.

$$\frac{\langle \tilde{\hat{\mathrm{h}}} \rangle}{\langle \tilde{\hat{\mathrm{n}}} \rangle} = \frac{\sum_i \omega_i {\tilde{k}_i}^2 \left[2\tilde{k}_i |\tilde{v}_i|^2 - \frac{1}{2}\frac{\tilde{\Delta}_i^2}{\tilde{E}_i} \right]}{2\sum_i \omega_i \tilde{k}_i |\tilde{v}_i|^2} - \frac{U_0 {r_0}^2}{4} \tag{3.43}$$

3.3 Discussions on 2D Results

In this section we show the results for 2D system. We notice that the crossover occurs at lower interactions with respect to the 3D system and solving the gap equations starts from lower interactions to obtain true density which is associated with the Fermi momentum. We change the depth of the model square well potential in order to change the interaction strength by keeping the range of the potential constant. We have chosen the fixed range of the potential to be one hundredth of the interparticle separation ($nr_0^2 = 10^{-4}$). Thus the diluteness conditions $nr_0^2 \ll 1$ and $(k_0/k_F)^2 \gg 1$ is satisfied.

In two dimension, there is always a bound state and the Cooper pairs appear in much low interaction strength with respect to the three dimensional. In the BCS limit the chemical potential of the system equals to Fermi energy and the maximum value of the superconducting gap function is almost zero. In Fig. 3.6 it can be seen that when you increase the interaction between particles the chemical potential of the system decrease while the maximum values of the superconducting gap increase. The crossover occurs at weaker interactions with respect to the three dimensional case. The momentum distribution of the system becomes flat as the interaction strength between particles increases in Fig. 3.2. In the BCS regime, the Fermi surface is only slightly smoothened due to pairing for momenta around the Fermi momentum. Towards the BEC regime, the distributions become flatter and flatter; more and more momentum states are needed to build up tightly bound pairs. The gap parameter is plotted as a function of momentum in Fig. 3.1 for different values of the interaction. The gap function

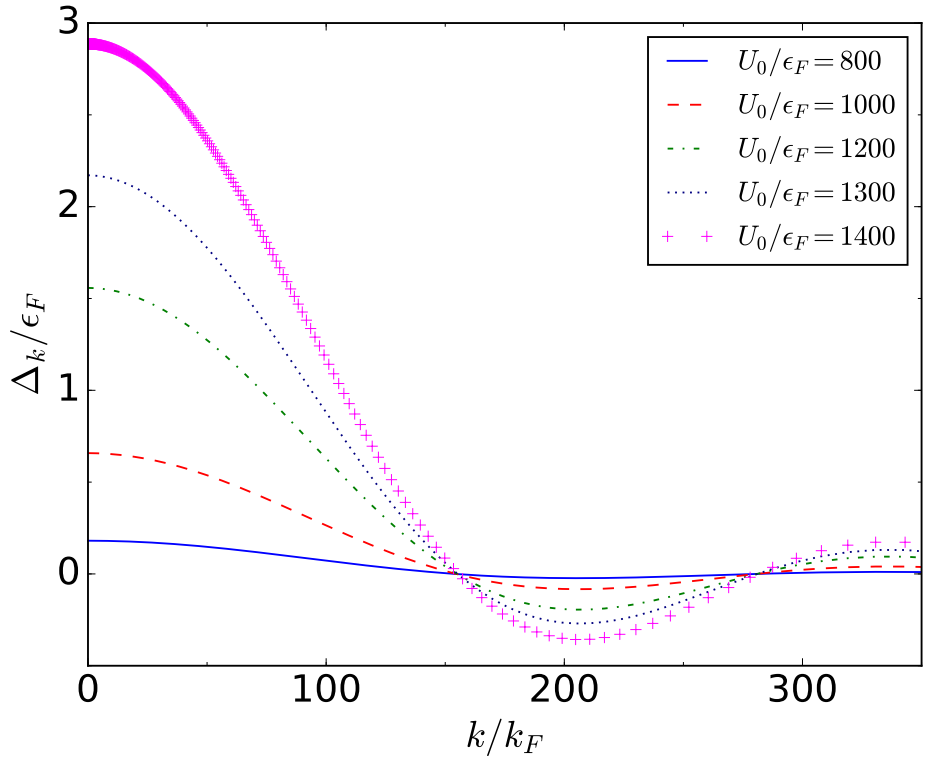

Figure 3.1 : Evolution of the gap as a function of k states for different scattering lengths from BCS to BEC in 2D. The gap function starts to oscillate the order of $1/r_0$.

oscillates with a large period corresponding to the inverse of the range of the potential. In Fig. 3.3 the evolution of the quasi-particle excitation energies is shown during the BCS-BEC crossover process. In the weak interacting limit the most contribution to pair formation is in the vicinity of k_F momentum. With the increasing of the interaction strength the contribution from the other states starts to come for pairing formation. In the BCS limit, the minimum of the quasi-particle energies and maximum of the gap function is equal each other. In Fig. 3.5 when the interaction increases, the minimum of the excitation energy and the maximum of the gap parameter start to differ after the unitarity point. In Fig. 3.7 behavior of the energy per particle, chemical potential and binding energy is plotted from weakly interacting limit to strongly interacting limit. In BCS limit chemical potential of the system is equal to the Fermi energy and energy per particle is fifty percent of the chemical potential. With the increasing of the interaction both chemical potential and energy per particle goes to one half of the binding energy and difference between them is vanish. This means that there is only weakly interacting bosonic molecules in the system and all energy is in their binding.

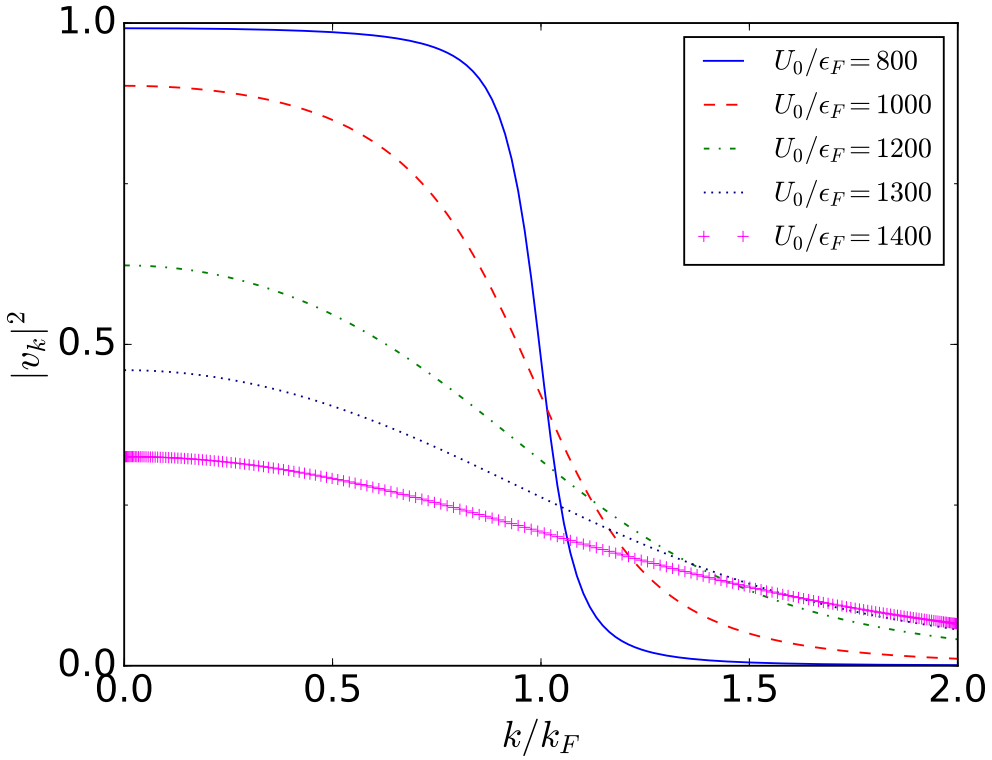

Figure 3.2 : Occupaton of momentum states for different interaction parameters in the 2D BCS-BEC crossover.

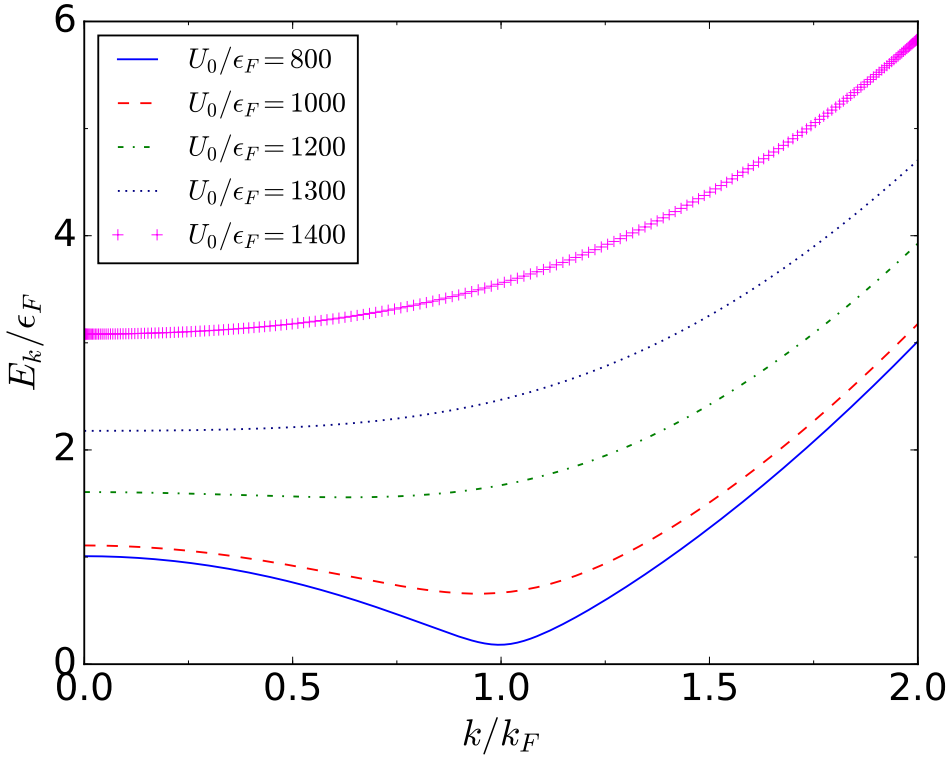

Figure 3.3 : Evolution of the single-particle excitation spectrum for different interaction parameters during the 2D BCS-BEC crossover.

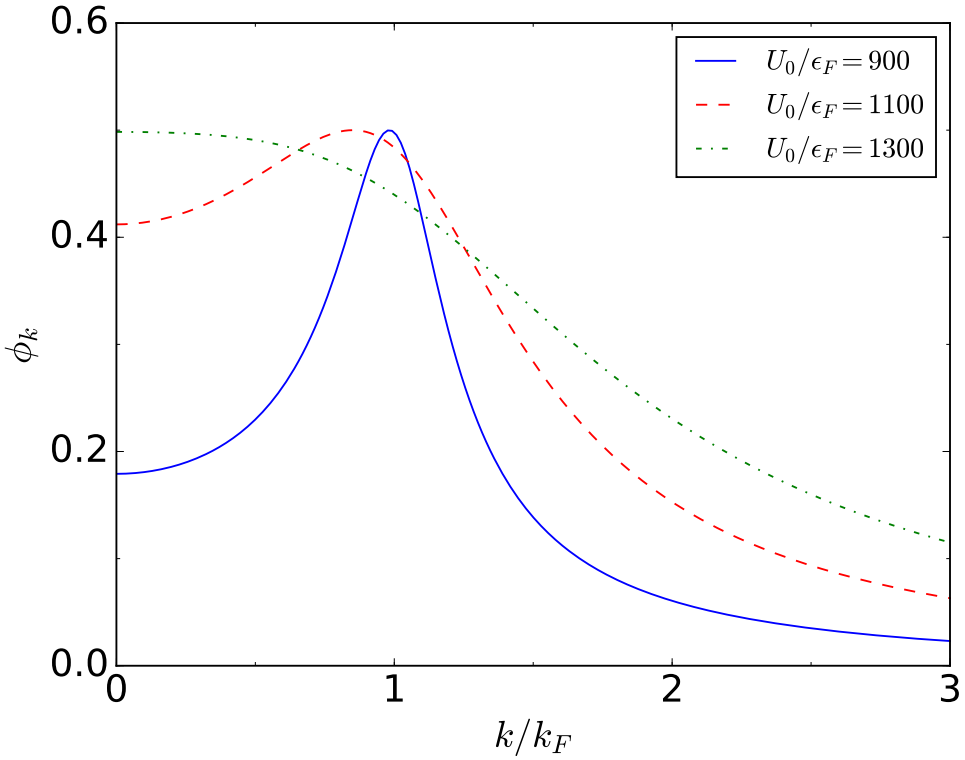

Figure 3.4 : Evolution of pair-correlation wave function for different interaction parameters during the BCS-BEC crossover in 2D.

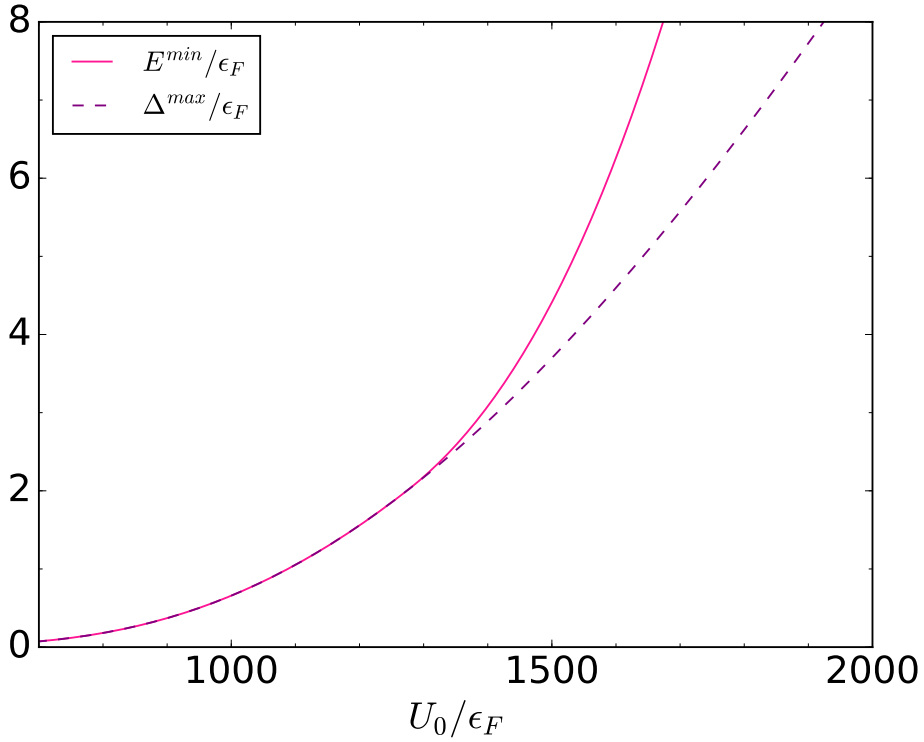

Figure 3.5 : Changing of minimum excitation energy and maximum values of the gap with respect to the inverse of the scattering length in 2D BCS-BEC Crossover.

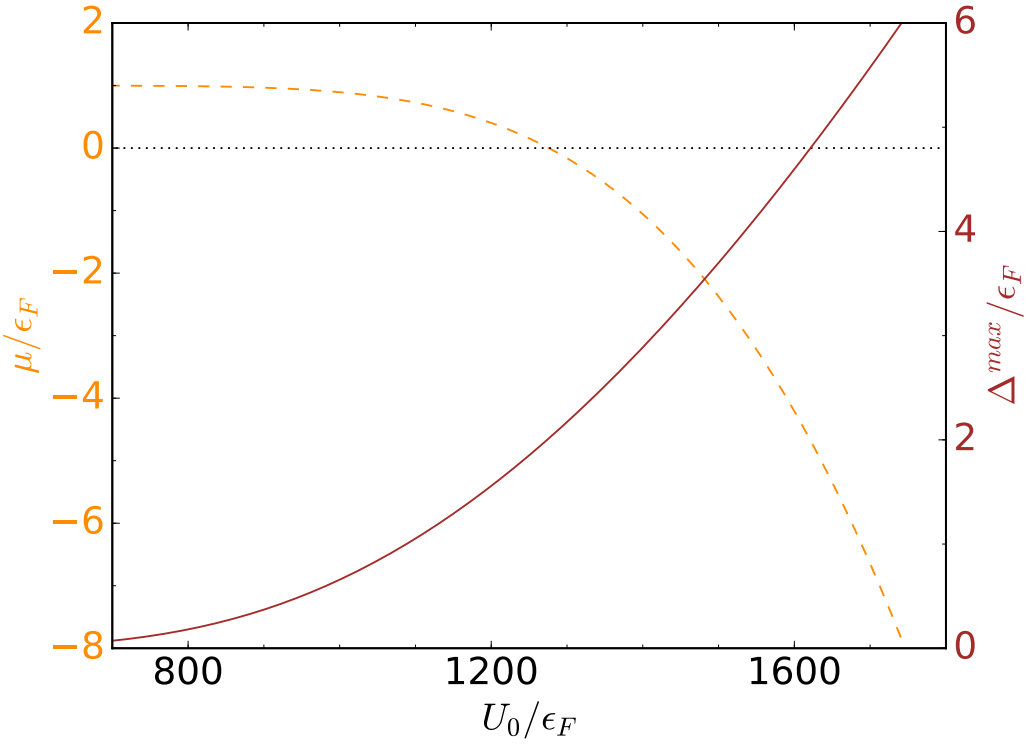

Figure 3.6 : Chemical potential (dashed line) and gap (solid line) during the BCS-BEC crossover in a 2 dimensional fermionic system as a function of the interaction parameter $1/k_F a$. The BEC-limit of is to the right hand side of the grap.

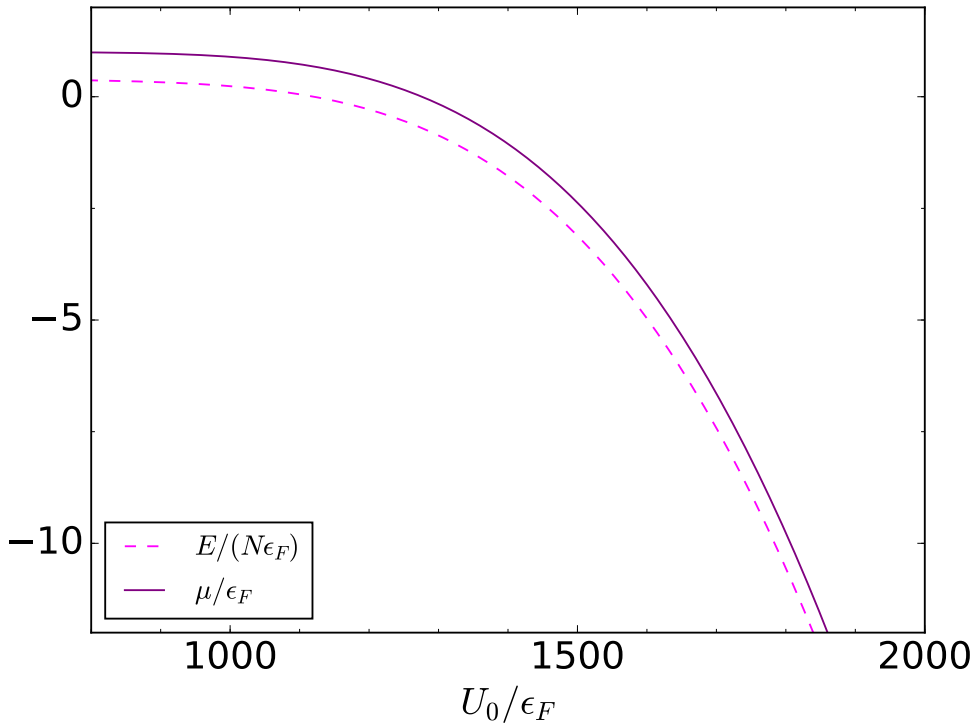

Figure 3.7 : Changing of energy per particle (solid line) and chemical potential (dashed line) throughout the BCS-BEC crossover in 2D.

3.4 Interaction in Reduced Dimensions

In this section we examine Fourier transformation of the square well potential in a infinite slab of thickness w (Fig.3.8). w is chosen so small that the particles are located in the lowest energy level, ϕ_0 of transverse motion, and in the other levels are so high in energy as to be practically irrelevant. Therefore, the only relevant wave functions have the form [20]

$$\phi_{\vec{k}_{||}\sigma}(\vec{r}_{||},\vec{r}_{\perp}) = \phi_0(\vec{r}_{\perp})\frac{e^{i\vec{k}_{||}\cdot\vec{r}_{||}}}{\sqrt{L^d}}\delta_{s\sigma} \tag{3.44}$$

where $\vec{r}_{||}$ and $\vec{r}_{||}$ are the components of $\vec{r}$ and similarly $\vec{k}_{||}$, $\vec{k}_{||}$ are those of $\vec{k}$ (e.g $\vec{r}_{\perp} = z$ and $\vec{r}_{||} = (x,y)$). Note that these states are labelled by quantum numbers $\vec{k}_{||}$ and σ. The interaction can be expressed within the subspace spanned by the states of the form given above. For this purpose, we consider the matrix element of the interaction between two states formed from the product of wave functions in the lowest level of the vertical trap.

$$U_{q_{||}} = -U_0\big\langle i,\vec{k}_{||1}+\vec{q}_{||}\sigma_1\big|\big\langle j,\vec{k}_{||2}-\vec{q}_{||}\sigma_2\big|\theta(r_0-|\vec{r}_{ij}|)\big|j,\vec{k}_{||2}\sigma_2\big\rangle\big|i,\vec{k}_{||1}\sigma_1\big\rangle \tag{3.45}$$

where $\vec{r}_{ij} = |\vec{r}_i - \vec{r}_j|$. Using the three dimensional Fourier representation of our model interaction Eq. (2.38) we can write

$$U_{q_{||}} = \int \frac{dq_{\perp}}{2\pi}\frac{4\pi U_0}{\sqrt{q_{||}^2+q_{\perp}^2}}\left[\frac{r_0\cos(\sqrt{q_{||}^2+q_{\perp}^2}r_0)}{\sqrt{q_{||}^2+q_{\perp}^2}} - \frac{\sin(\sqrt{q_{||}^2+q_{\perp}^2}r_0)}{q_{||}^2+q_{\perp}^2}\right]|F(q_{\perp})|^2 \tag{3.46}$$

where

$$|F(q_{\perp})|^2 = \int d\vec{r}_{\perp}|\phi_0(\vec{r}_{\perp})|^2 e^{-i\vec{q}_{\perp}\cdot\vec{r}_{\perp}} \tag{3.47}$$

is the *form factor* associated with the transverse density distribution $|\phi_0(\vec{r}_{\perp})|^2$. Let us assume for definiteness that ϕ_0 has the Gaussian form such as

$$\phi_0(r_{\perp}) = \left(\frac{2}{\pi w^2}\right)^{\frac{3-d}{4}} e^{-r_{\perp}^2/w^2} \tag{3.48}$$

where d is the dimensionality to reduce (e.g. $d = 2$ for a slap). For the slap the form factor is

$$F(\vec{q}_{\perp}) = e^{-q_{\perp}^2 w^2/2} \tag{3.49}$$

Substituting this Eq. (3.46) we obtain

$$U_{q_{||}} = \int \frac{dq_\perp}{2\pi} \frac{4\pi U_0}{\sqrt{q_{||}^2 + q_\perp^2}} \left[\frac{r_0 \cos(\sqrt{q_{||}^2 + q_\perp^2} r_0)}{\sqrt{q_{||}^2 + q_\perp^2}} - \frac{\sin(\sqrt{q_{||}^2 + q_\perp^2} r_0)}{q_{||}^2 + q_\perp^2} \right] e^{-q_\perp^2 w^2} \quad \textbf{(3.50)}$$

After scaling the momenta with respect to the r_0 i.e.

$$q \quad \rightarrow \quad \frac{\tilde{q}}{r_0} \quad \textbf{(3.51)}$$

$$w \quad \rightarrow \quad \tilde{w} r_0 \quad \textbf{(3.52)}$$

$$U_{q_{||}} = 2U_0 r_0^2 \int \frac{d\tilde{q}_\perp}{\sqrt{\tilde{q}_{||}^2 + \tilde{q}_\perp^2}} \left[\frac{\cos(\sqrt{\tilde{q}_{||}^2 + \tilde{q}_\perp^2})}{\sqrt{\tilde{q}_{||}^2 + \tilde{q}_\perp^2}} - \frac{\sin(\sqrt{\tilde{q}_{||}^2 + \tilde{q}_\perp^2})}{\tilde{q}_{||}^2 + \tilde{q}_\perp^2} \right] e^{-\tilde{q}_\perp^2 \tilde{w}^2} \quad \textbf{(3.53)}$$

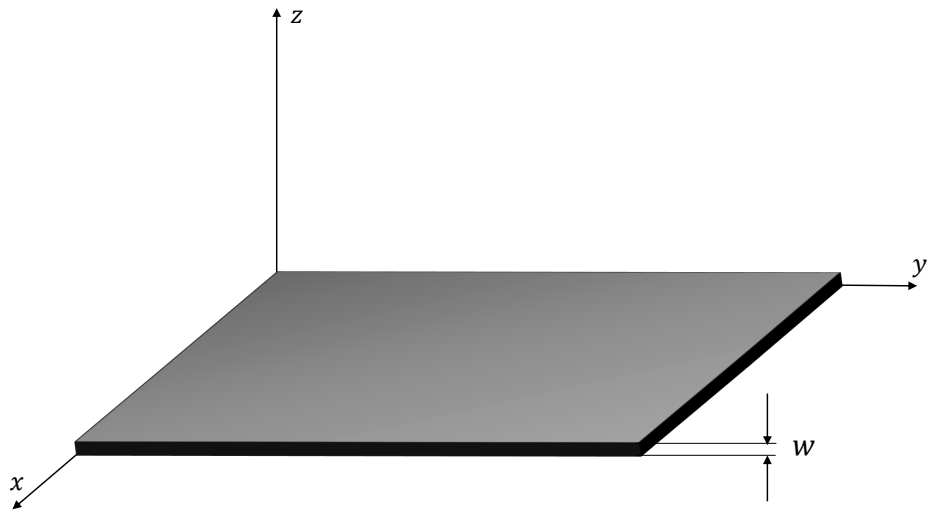

Figure 3.8 : Skecth of a model $2D$ slap as a reduced dimensional sytem. The motion of the particles is restricted by choosing a Gaussian wavefunction in the vertical direction.

In dimensionless form, we have

$$\tilde{U}_{q_{||}} = \frac{k_F^2}{4\pi^2 \varepsilon_F} U_{q_{||}} \quad \textbf{(3.54)}$$

$$\tilde{U}_{q_{||}} = \tilde{U}_0 \tilde{r}_0^2 \int \frac{d\tilde{q}_\perp}{\sqrt{\tilde{q}_{||}^2 + \tilde{q}_\perp^2}} \left[\frac{\cos(\sqrt{\tilde{q}_{||}^2 + \tilde{q}_\perp^2})}{\sqrt{\tilde{q}_{||}^2 + \tilde{q}_\perp^2}} - \frac{\sin(\sqrt{\tilde{q}_{||}^2 + \tilde{q}_\perp^2})}{\tilde{q}_{||}^2 + \tilde{q}_\perp^2} \right] e^{-\tilde{q}_\perp^2 \tilde{w}^2} \quad \textbf{(3.55)}$$

Now, we put the Fourier transform of the potential into the gap equation.

$$\tilde{\Delta}_k = -\frac{1}{2}\int d\tilde{k}'\ \tilde{k}'\tilde{U}(\tilde{k},\tilde{k}')\frac{\tilde{\Delta_{k'}}}{\sqrt{(\tilde{k}'^2-\tilde{\mu})^2+\tilde{\Delta}_{k'}^2}} \tag{3.56}$$

$$\tilde{\Delta}_i = -\frac{1}{2}\sum_j \omega_j \tilde{k}_j'\tilde{U}(\tilde{k}_i,\tilde{k}_j')\tilde{F}(\tilde{k}_j') \tag{3.57}$$

3.5 Discussions on Quasi-2D Results

We have constructed a mean-field theory for the quasi-2D Fermi gas that is able to capture the deviations from 2D and 3D behaviors resulting from confinement. We expect it to provide a benchmark for further investigations into quasi-2D Fermi systems. In this case we use the same relation between depth of the well and scattering length in case of 3D. We fix the range of potential well at one hundredth of interparticle separation.

In Fig. 3.9 it is shown that since the width of the slap is increased the initial amplitude of superconducting gap function is decreased. $(k_F a)^{-1} = -90$ corresponds to BEC limit in 2D system and when the thickness of the system is increased gap starts to vanish i.e. system approaches the BCS limit of 3D system. $w = 0$ cases are the results of the strictly 2D calculation with the same interaction potential parameters (r_0 and U_0) as finite with cases. Also momentum distributions change with the increasing of thickness in the z direction of the slap. When we increase the width in perpendicular at $(k_F a)^{-1} = -150$ -BEC region in 2D system- it is depicted that the momentum distribution of the particles changes from smooth function to a step function like in the BCS limit of 3D system in Fig. 3.13. Similarly, quasi-particle excitation energies change with the thickness w. For instance, in Fig. 3.11, it is demonstrated that as the thickness w increases, the effects of the energy gap diminish and the results converge to BCS limit of 3D system. Also, when we continue to increase the thickness of the system almost near $2.424r_0$ the system approaches to 3D limit. In Fig. 3.12 it is demonstrated that for $(k_F a)^{-1} = -1$ -BCS region in 3D- increasing of the width at z-direction causes the delta function in quasi-2D system to resemble that of the 3D system. On the other hand, in Fig. 3.13 it is illustrated the changing of the excitation energies and it is depicted in Fig. 3.14 the evolution of the momentum with respect to the increasing thickness values distribution.

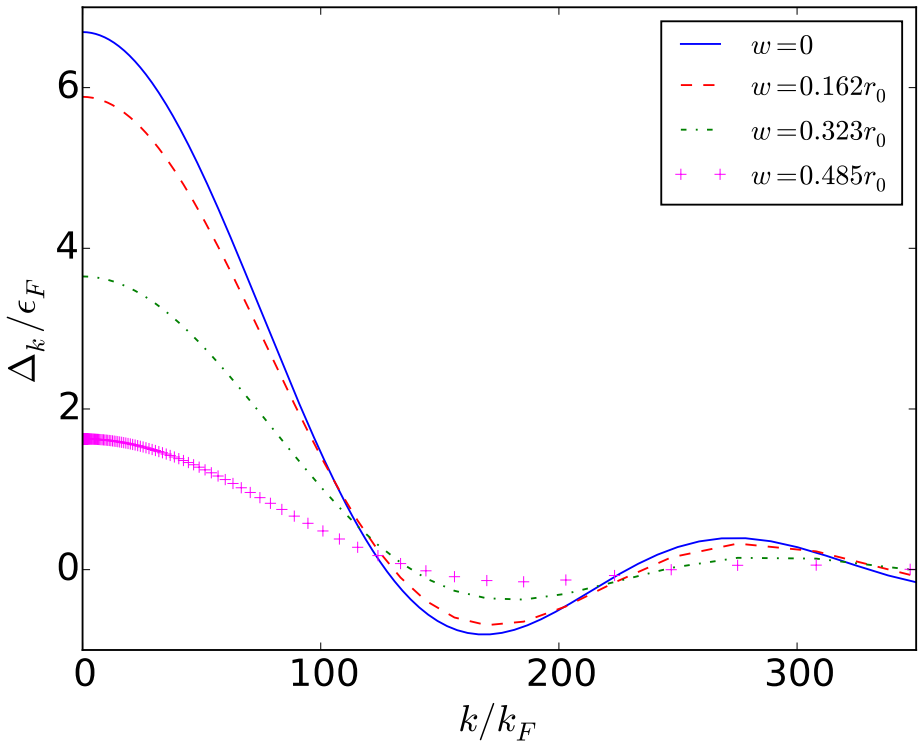

Figure 3.9 : The gap as a function of k states for different thickness of the system at a given controlling parameter $(k_F a)^{-1} = -90$ for increasing width w.

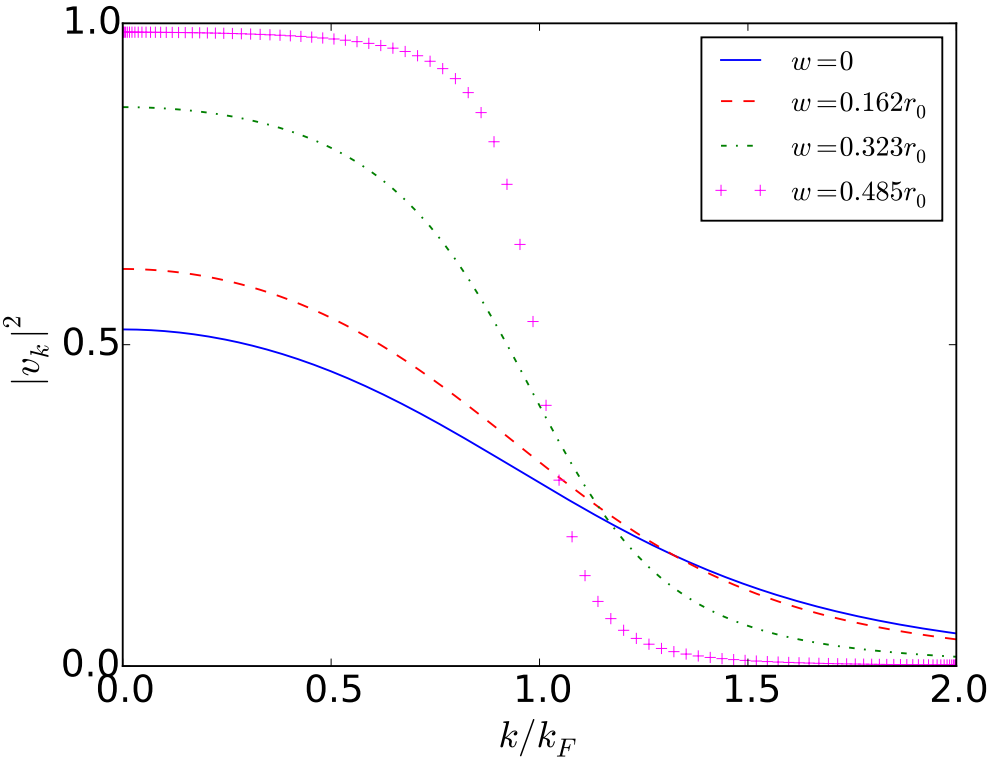

Figure 3.10 : The momentum distribution for different values of thickness of the system at $(k_F a)^{-1} = -150$.

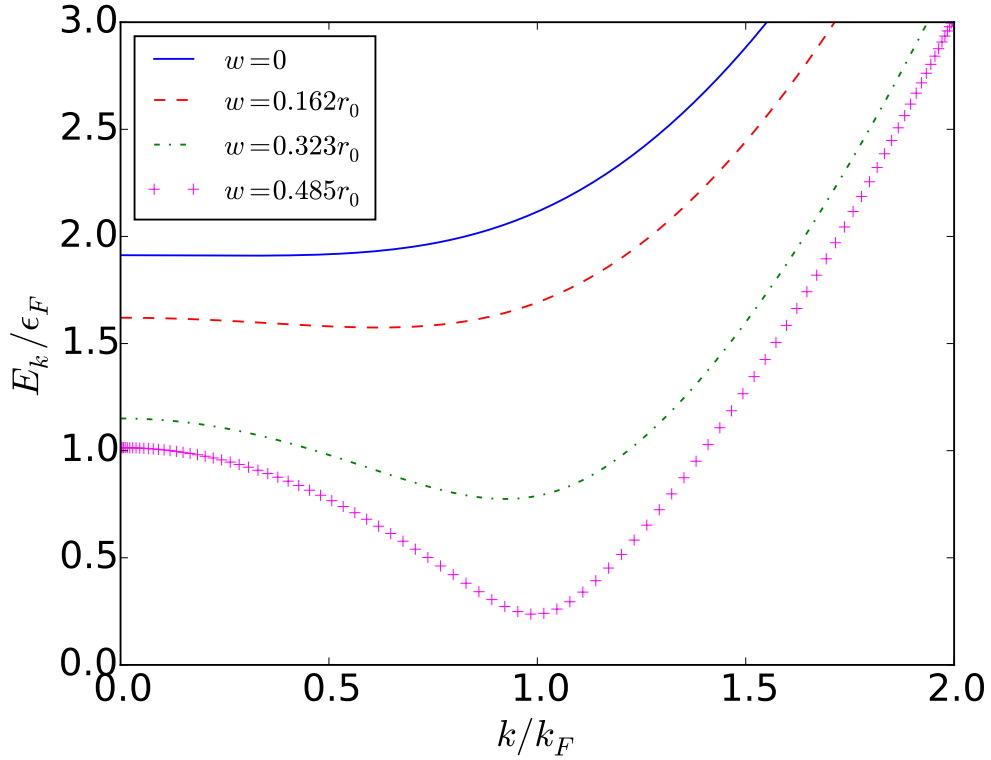

Figure 3.11 : The energy spectrum as a function of momentum states for different values of the thickness of the system at a certain tuning parameter $(k_F a)^{-1} = -150$.

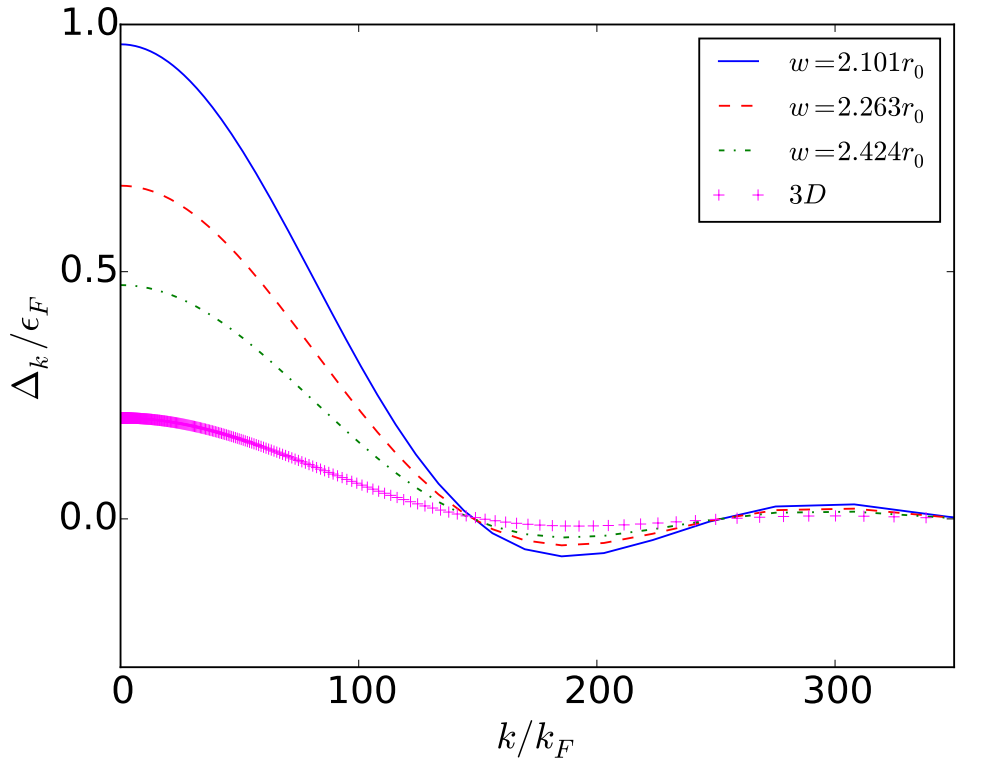

Figure 3.12 : The superconducting gap parameter with respect to the thickness of the system at a certain tuning parameter $(k_F a)^{-1} = -1$.

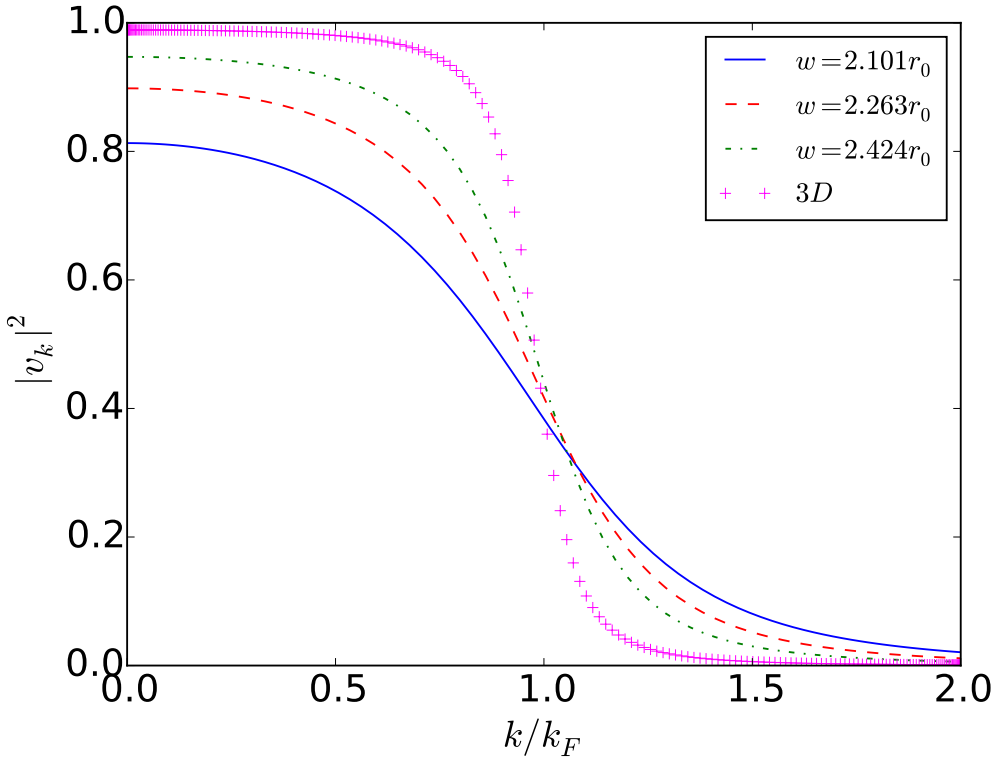

Figure 3.13 : The momentum distribution for different values of the thickness of the system at a given controlling parameter $(k_F a)^{-1} = -1$.

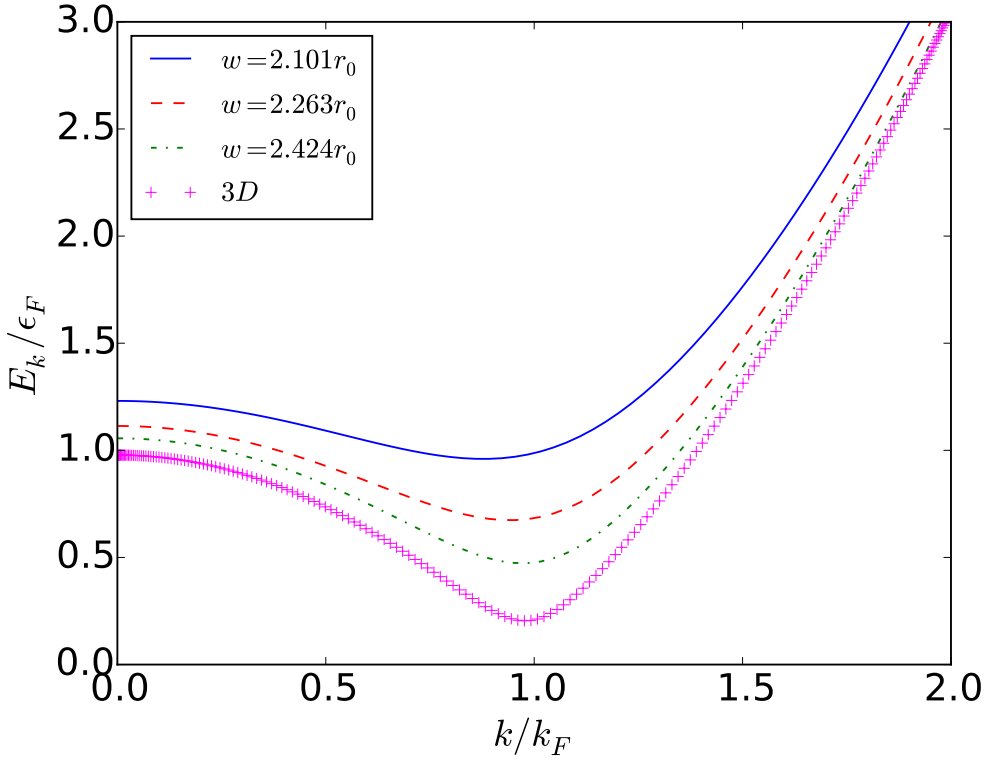

Figure 3.14 : The energy spectrum with respect to the thickness of the system at a certain tuning parameter $(k_F a)^{-1} = -1$.

4. CONCLUSIONS AND OUTLOOK

In this thesis we focused on the the fermionic superfluidity which can be seen in superconductors, neutron stars, nuclear matter, and ultracold atoms. We first examined that fermions with opposite spins and zero center of mass momentum on top of the non-interacting Fermi level can form a bound state if there is an attractive interaction between them. Secondly, we studied the BCS theory that proposes variational wavefunction describing the weakly interacting Cooper pairs at ground state. When we increase the interaction we can smoothly pass from the weakly interacting and largely overlapping Cooper pairs to BEC regime of the tightly bound bosonic molecules. There is no a phase transition in this process and it's called BCS-BEC crossover for balanced case where number of the spin-up and spin-down particles is equal.

We studied the crossover from the BCS state to BEC in a Fermionic gas at zero temperature by changing the interaction between fermions and used mean field approximation. We examined the the BCS-BEC crossover in a 3 dimensional(3D) fermionic gas. We showed that there is a smoothly crossover between two limits in the case of s-wave pairing and calculated the physical quantities such as momentum distribution, energy per particle, excitation energies, changing of the chemical potential of the system and superconducting gap parameter with respect to the interaction parameter or scattering length. In the second part we studied a strictly 2D and a quasi-2D system. We show that the crossover occurs much lower interactions with respect to the 3D system. Finally, the BCS-BEC crossover can be studied for the different model interaction such as Coulomb, dipole-dipole interaction potentials. Also, linear dispersive of energy cases can be examined with this given numerical framework.

It's very important to extend the analysis presented in this thesis. In the case of polarized Fermi gas there is a phase transition rather than a smoothly crossover. Studies in this thesis can be generalized in the case of a spin-polarized Fermi gas. Also, recently materials with linear dispersion relation have been reported [21] [22] and

the numerical implementation in this thesis can easily be generalized to study such systems. For example, it is possible to study the situation in the Joglekar's article [23] by choosing the model Coulomb interaction and linear energy dispersion. In this thesis we used the mean field approximation however there are other approaches to the the theoretical investigation of the ground-state properties of the gas along the BCS-BEC crossover such as the fixed-node diffusion Monte Carlo (FN-DMC) technique [24], diagrammatic methods based on the T-matrix approach and Bose-Fermi model in which the Hamiltonian includes interaction terms involving both fermionic and bosonic degrees of freedom [12].

REFERENCES

[1] **Pethick, C.J. and Smith, H.** (2008). *Bose–Einstein Condensation in Dilute Gases*, Cambridge University Press.

[2] **Moerdijk, A.J.**, **Verhaar, B.J. and Axelsson, A.** (1995). Resonances in ultracold collisions of ^{6}Li, ^{7}Li, and ^{23}Na, *Phys. Rev. A*, *51*, 4852–4861.

[3] **Cornish, S.L.**, **Claussen, N.R.**, **Roberts, J.L.**, **Cornell, E.A. and Wieman, C.E.** (2000). Stable ^{85}Rb Bose-Einstein Condensates with Widely Tunable Interactions, *Phys. Rev. Lett.*, *85*, 1795–1798.

[4] **London, F.** (1938). The λ-Phenomenon of Liquid Helium and the Bose-Einstein Degeneracy, *Nature*, *141*, 643–644.

[5] **Cooper, L.N.** (1956). Bound Electron Pairs in a Degenerate Fermi Gas, *Phys. Rev.*, *104*, 1189–1190.

[6] **Bardeen, J.**, **Cooper, L.N. and Schrieffer, J.R.** (1957). Theory of Superconductivity, *Physical Review*, *108*(5), 1175–1204.

[7] **Bardeen, J.**, **Cooper, L.N. and Schrieffer, J.R.** (1957). Microscopic Theory of Superconductivity, *Physical Review*, *106*(1), 162–164.

[8] **Comte, C. and Nozières, P.** (1982). Exciton Bose condensation : the ground state of an electron-hole gas - I. Mean field description of a simplified model, *Journal de Physique*, *43*(7), 1069–1081.

[9] **Zwierlein, M.W.**, **Stan, C.A.**, **Schunck, C.H.**, **Raupach, S.M.F.**, **Kerman, A.J. and Ketterle, W.** (2004). Condensation of Pairs of Fermionic Atoms near a Feshbach Resonance, *Phys. Rev. Lett.*, *92*, 120403.

[10] **Parish, M.M.**, **Mihaila, B.**, **Timmermans, E.M.**, **Blagoev, K.B. and Littlewood, P.B.** (2005). BCS-BEC crossover with a finite-range interaction, *Physical Review B*, *71*(6), 064513.

[11] **Randeria, M. and Taylor, E.** (2014). Crossover from Bardeen-Cooper-Schrieffer to Bose-Einstein Condensation and the Unitary Fermi Gas, *Annual Review of Condensed Matter Physics*, *5*(1), 209–232.

[12] **Giorgini, S.**, **Pitaevskii, L.P. and Stringari, S.** (2008). Theory of ultracold atomic Fermi gases, *Reviews of Modern Physics*, *80*(4), 1215–1274.

[13] **Stoof, H.T.C.**, **Gubbels, K.B. and Dickerscheid, D.B.M.** (2009). *Ultracold Qunatum Fields*, Springer Science+Business Media B.V.

[14] **Ortiz, G. and Dukelsky, J.** (2005). BCS-to-BEC crossover from the exact BCS solution, *Physical Review A*, *72*(4), 043611.

[15] **Landau, R.H.** (2004). *QUANTUM MECHANICS II A Second Course in Quantum Theory*, WILEY-VHC.

[16] **Annett, J.F.** (2004). *Superconductivity, Superfluids and Condensates*, Oxford University Press.

[17] **Martin, P.A.**, **Rothen, F. and Goldfarb, S.** (2002). *Many Body Problems and Quantum Field Theory: An Introduction*, Springer-Verlag.

[18] **Khan, A. and Pieri, P.** (2009). Ground-state fidelity in the BCS-BEC crossover, *Physical Review A*, *80*(1), 012303.

[19] **Salasnich, L.**, **Manini, N. and Parola, A.** (2005). Condensate fraction of a Fermi gas in the BCS-BEC crossover, *Physical Review A*, *72*(2), 023621.

[20] **Giuliani, G., V.G.** (2008). *Quantum Theory of the Electron Liquid*, Cambridge University Press.

[21] **Young, S.M. and Kane, C.L.** (2015). Dirac Semimetals in Two Dimensions, *Physical Review Letters*, *115*(12), 126803.

[22] **Wang, J.**, **Deng, S.**, **Liu, Z. and Liu, Z.** (2015). The rare two-dimensional materials with Dirac cones, *National Science Review*, *2*(1), 22–39.

[23] **Zhang, C.H. and Joglekar, Y.N.** (2008). Excitonic condensation of massless fermions in graphene bilayers, *Phys. Rev. B*, *77*(23), 233405.

[24] **Astrakharchik, G.E.**, **Boronat, J.**, **Casulleras, J. and Giorgini, S.** (2004). Equation of State of a Fermi Gas in the BEC-BCS Crossover: A Quantum Monte Carlo Study, *Phys. Rev. Lett.*, *93*, 200404.

APPENDICES

APPENDIX A: Scaling of Energy, Length and Mass
APPENDIX B: Scattering length and Fourier transform of square well potential
APPENDIX C: Python source codes for numerical calculations

APPENDIX A: Scaling of Energy, Length and Mass

We work in dimensionless units such that $\hbar = 1$, $m = 1/2$, $k_F = 1$.

$$\varepsilon_F = \frac{\hbar^2 k_F^2}{2m} \qquad \rightarrow \qquad \tilde{\varepsilon}_F = 1$$

$$k = k_F \tilde{k} \qquad \rightarrow \qquad k = \tilde{k}$$

$$\Delta_k = \varepsilon_F \tilde{\Delta}_k \qquad \rightarrow \qquad \Delta_k = \tilde{\Delta}_k$$

$$r_0 = \frac{\tilde{r}_0}{k_F} \qquad \rightarrow \qquad r_0 = \tilde{r}_0$$

$$\varepsilon_k = \frac{\hbar^2 k^2}{2m} = \varepsilon_F \tilde{k}^2 \quad \rightarrow \quad \tilde{\varepsilon}_k = \tilde{k}^2$$

$$\xi_k = \varepsilon_k - \mu \qquad \rightarrow \qquad \tilde{\xi}_k = \tilde{k}^2 - \tilde{\mu}$$

$$U_0 = \frac{\hbar^2 k_0^2}{2m_r} \qquad \rightarrow \qquad \tilde{U}_0 = 2\tilde{k}_0^2$$

$$n = \frac{k_F^3}{3\pi^2} \qquad \rightarrow \qquad \tilde{n} = \frac{1}{3\pi^2}$$

APPENDIX B: Scattering length and Fourier transform of the square well potential

We desire to find the corresponding value of U_0 of the potential for a given range r_0 and a given scattering length a. In this thesis, we consider a dilute system and fix r_0 to be small compared to the interparticle distance such that $nr_0^3 \ll 1$. In order for the potential with fixed r_0 to give rise to a scattering length a the following transcendental equation has to be solved [1, 13].

$$\frac{1}{a} = \frac{1}{r_0\left(1 - \frac{\tan(k_0 r_0)}{k_0 r_0}\right)} \tag{A.1}$$

This equation can be written as

$$\tan x = \alpha x \tag{A.2}$$

where $x = k_0 r_0$ and $\alpha = 1 - a/r_0$ or in terms of dimensionless quantities

$$\alpha = 1 - \frac{k_F a}{k_F r_0} = 1 - \frac{\tilde{a}}{\tilde{r_0}}. \tag{A.3}$$

For $\alpha > 1$ (negative scattering length $a < 0$) the solution for x is between 0 and $\pi/2$. For $\alpha < 1$ (positive scattering length) the solution is between $\pi/2$ and $3\pi/2$. Note that in the weakly interacting limit, the scattering length $a \to 0^-$ and $\alpha \to 1^+$, the root finding problem becomes $\tan x = 1^+ x$ and the solution gives $k_0 \to 0$ and $U_0 \to 0$. Also note that for $1/\alpha \approx r_0/a = 0$, when the scattering length diverges, the solution is $x = k_0 r_0 = \pi/2$. In general we can use a root finding method to find a numerical solution for given a and r_0. The roots of the above equation are indicated in Fig. B.1. From the root x, we obtain

$$k_0 = \frac{x}{r_0} \qquad \text{and} \qquad U_0 = \frac{\hbar^2 {k_0}^2}{2m_r}, \tag{A.4}$$

where $m_r = m/2$ is reduced mass.

For small values of U_0, *i.e* $k_0 r_0 < \pi/2$, the scattering length a is negative. In this case the interaction is weak to have a bound state in the potential well. When the depth of the well U_0 increases, we find that scattering length goes to infinity as $k_0 r_0 \to \pi/2$, the point when the potential is large enough to constitute a bound state. For a stronger interaction, the binding energy is given by $E_b = -\hbar^2/ma^2$. If the depth of the well U_0 is slightly lower than the threshold for the construction of a bound state the scattering length a is large and negative. On the other hand, if U_0 is slightly larger than this threshold, a is large and positive.

The depth of the well U_0 is plotted in Fig. B.2 as a function of the inverse of the scattering length for three different values of nr_0^3. At fixed r_0, U_0 increases as inverse of the scattering length increases from negative to positive values. When the width r_0 of the square well decreases the depth of the potential increases for fixed a. For $nr_0 \ll 1$ we find that $U_0 \gg \varepsilon_F$.

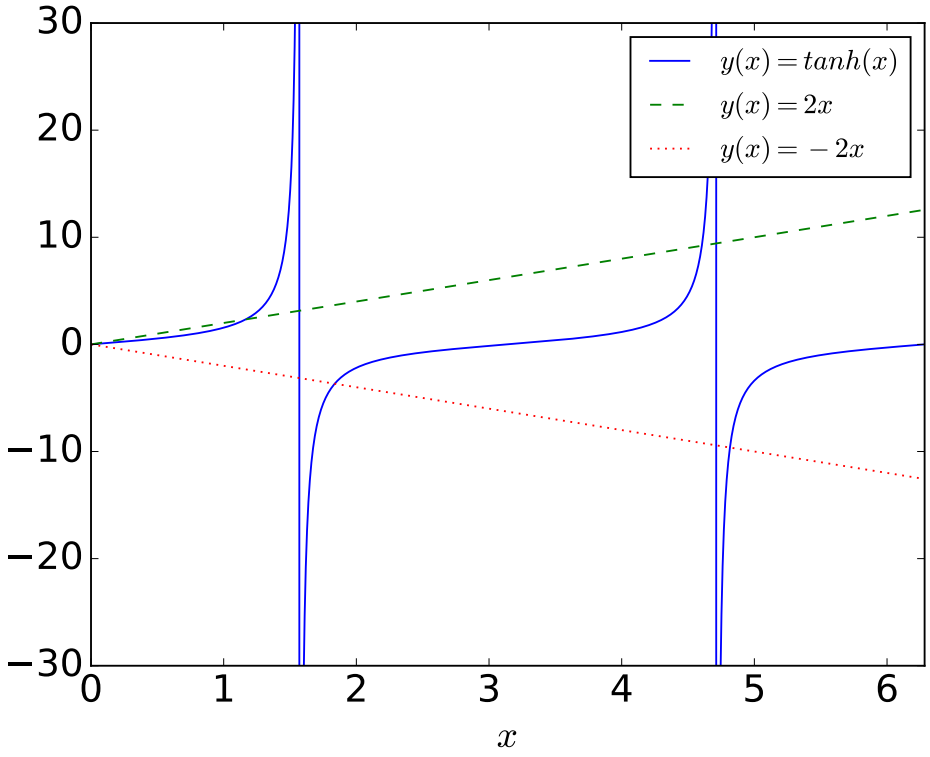

Figure B.1 : Plotting of the tan$x$ and αx for $\alpha = 2$ (dashed-green) line and $\alpha = -2$ (dotted red) line.

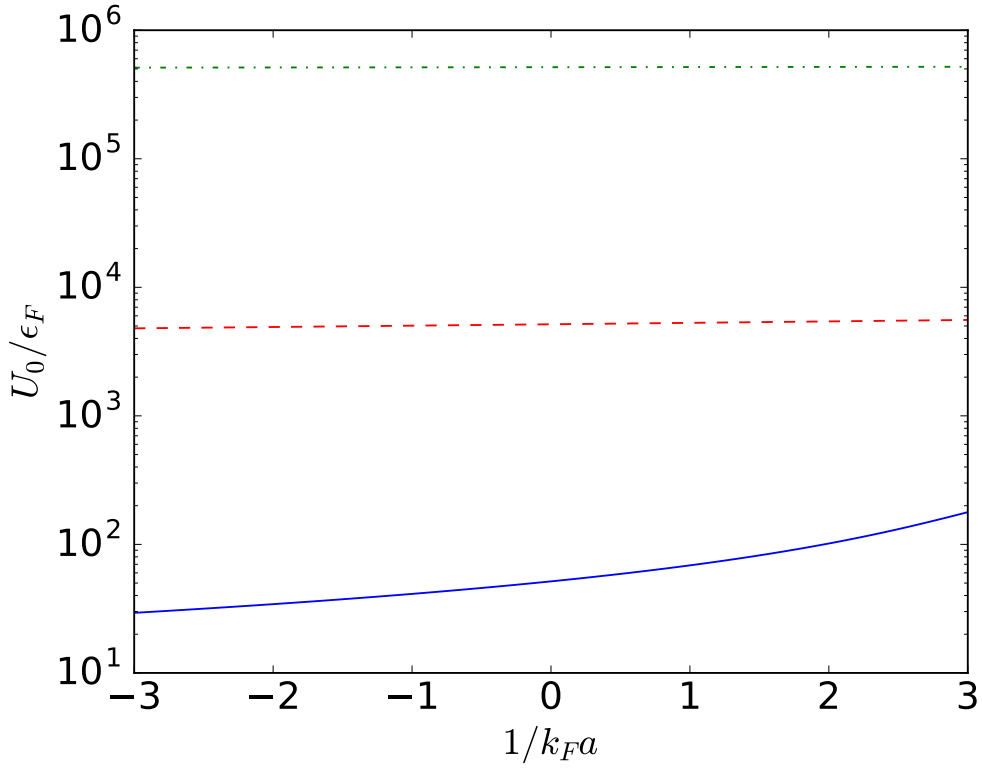

Figure B.2 : The depth U_0 of the model square well interaction for different nr_0^3 as a function of the inverse scattering length. Blue (solid), red (dashed) and green (dotted-dashed) curves correspond to $nr_0^3 = 10^{-3}, 10^{-6}, 10^{-9}$ respectively.

In our numerical calculations the Fourier transform of the square well potential enters which is plotted in Fig. B.3 for different r_0 values at fixed scattering length using two different scaling. The upper figure shows the oscillations as a function of qr_0 and $(k_F a)^{-1} = 0$ is fixed. The lower panel shows the k_F scaling used in the main text. When the width of the well is decreased, the period of the oscillations increases and the Fourier transform of the potential goes to a constant. In the limit of contact interaction, $U(\mathbf{r}) = -g\delta(\mathbf{r})$, where g is called the coupling constant, U_0 will diverge. Fig. B.4 shows the Fourier transform of the potential for different values of the scattering length and at the fixed value of $nr_0 = 10^{-6}$ used in the calculations. As the inverse scattering length increases, so does the amplitude of the Fourier transform.

Comparison with contact interaction

For an ultra cold gas of atoms the s-wave scattering length is the single parameter describing the interactions and can be measured experimentally. In Fig. B.5 we plot the maximum of the gap and the chemical potential for different values of $k_F r_0$. It is seen that the data points for a fixed scattering length value are very similar and approach the contact interaction limit as the width of the potential decreases to zero.

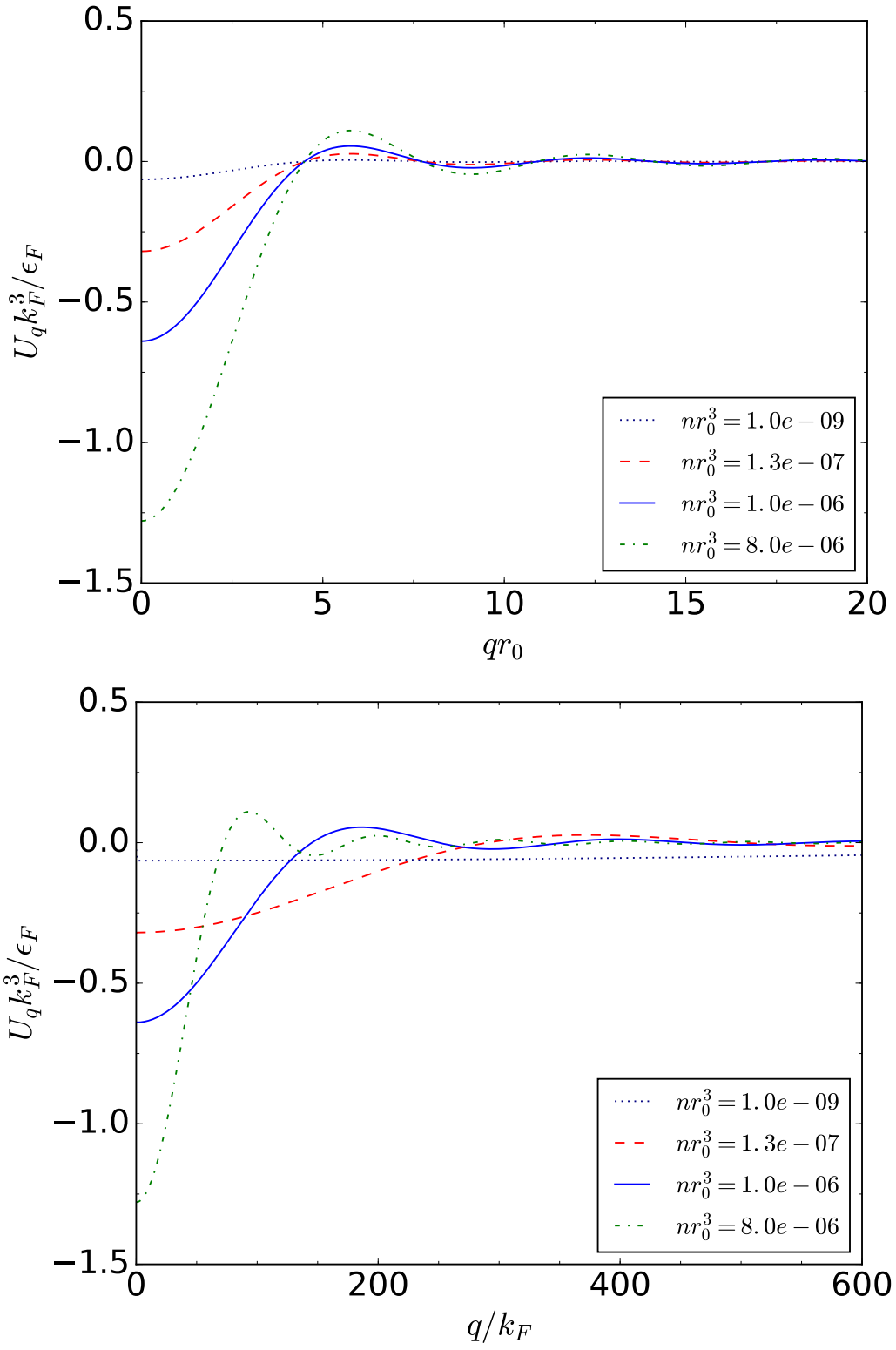

Figure B.3 : Fourier transform $U(q)$ of the square well potential for different values of the well width r_0. The value of the scattering length is fixed to be $1/(k_F a) = 0$ for all curves. The upper panel displays oscillations as a function of qr_0, whereas the lower panel plot shows k_F scaling used in the main text.

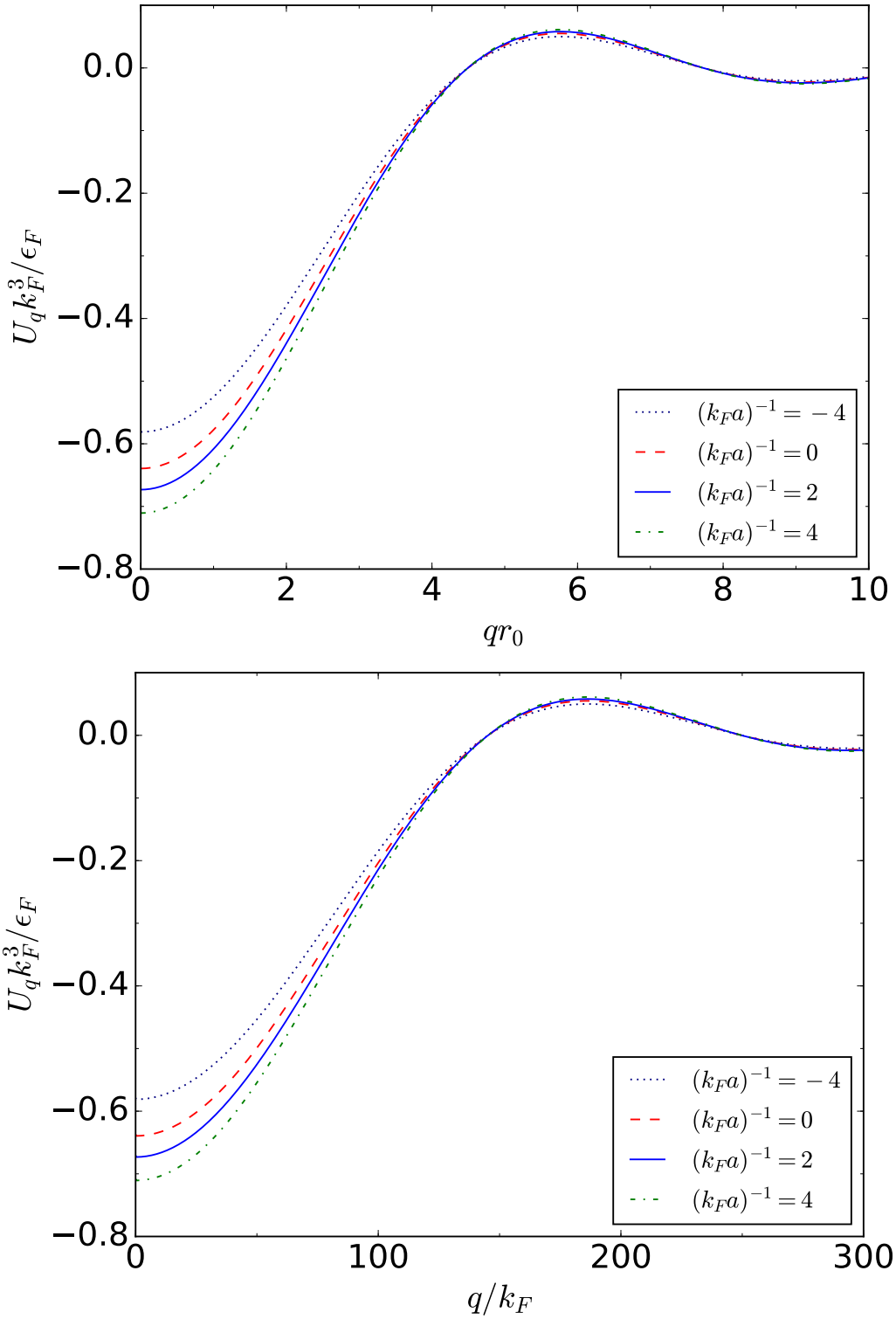

Figure B.4 : Fourier transform $U(q)$ of the square well potential for different values of the scattering length a. The value of the width of the potential well is fixed through $nr0^3 = 10^{-6}$ for all curves. The upper panel displays oscillations as a function of qr_0, whereas the lower panel plot shows k_F scaling used in the main text.

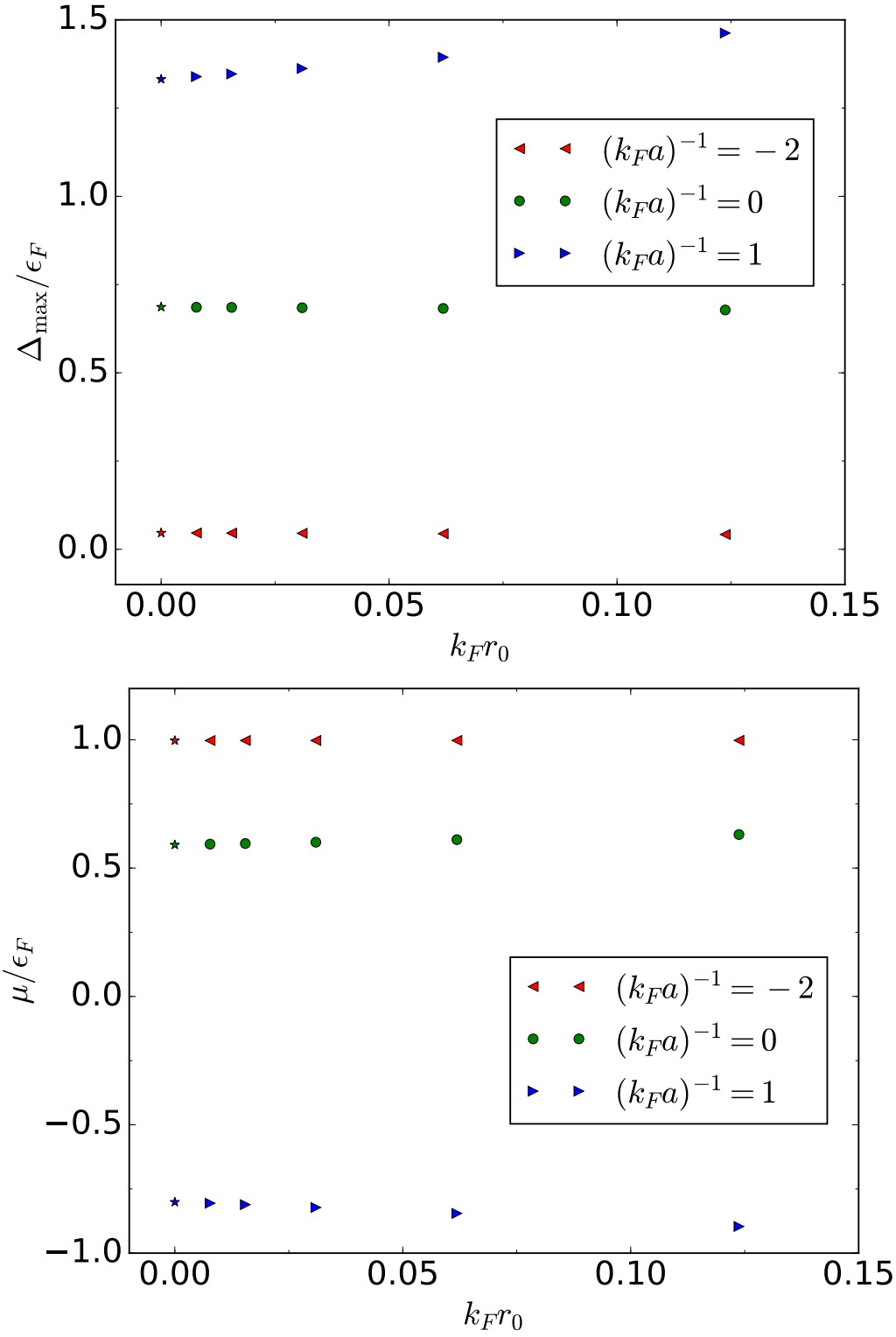

Figure B.5 : The maximum values of superconducting gap parameter (upper panel) and the chemical potential (lower panel) as a function $k_F r_0$ for various interaction strengths. The $r_0 = 0$ points are from an independent calculation with contact interaction. (Data provided by A. Levent Subaşı)

APPENDIX C: Python source codes for numerical calculations

```
# -*- coding: utf-8 -*-
"""
Created on Tue Aug 18 18:02:28 2015

-------Main Program-------

@author: Hasan Huseyin Somek
"""
import numpy as np
import three_bal_sr as sr

sr.create_grid()
sr.xmu = np.loadtxt(sr.mu_file, unpack = True)
mu = sr.opt_mu(sr.xmu)
n = sr.particle_den( sr.v2_k )
h = sr.energy_den( sr.E_k, sr.v2_k )
EPP = h / n - 2. * sr.fU0() * sr.r_0 ** 3 / (9. * np.pi)
if sr.a_inv > 0:
    half_E_b=-sr.a_inv**2
else:
    half_E_b=0
print ("Particle Density= ",3. * n * np.pi**2)
print ("Chemical Potential= ", mu /sr.E_FG)
print ("Energy per Particle= ", EPP / sr.E_FG)
print ("E_b/2= ", half_E_b)
print ("U_0= ", sr.fU0())
print ("Delta_max= ", np.max(sr.delta_i))
```

```
# -*- coding: utf-8 -*-
"""
Created on Fri Oct  2 16:05:09 2015

In this computer code we implement the solution of self
consistency equations for a model suqare well interaction.
Using the initial guess of chemical potential we iterate
the gap function up to convergence and optimize the
density function.

@author: Hasan Huseyin Somek
"""
import numpy as np
from scipy import optimize
import os
Niter = 2000
# r_0 is the range of the model square well
c=1.e-2
r_0 = ((3.*np.pi**2)**(1./3.))*c
a_inv = 0.        # Inverse of the scattering length
nc=0.
U_0 = 0.
E_FG =  3./5.
xmu = 1*np.ones(1)      # Initial guess for chemical potential.
```

```
Nk_list = np.array([200, 300])
Nk = np.sum(Nk_list)
k_i=np.array([])
w_i=np.array([])
Uk_kp = np.zeros([Nk, Nk])
U2k_kp = np.zeros([Nk, Nk])
U_mat = np.zeros([Nk, Nk])
U2_mat = np.zeros([Nk, Nk])
ek_i=np.zeros([Nk])
delta_i=np.zeros([Nk])
xi=np.zeros([Nk])
E_k=np.zeros([Nk])
E_k_0 = np.zeros([Nk])
v2_k=np.zeros([Nk])
Dk_file="Dk_temp_Nk="+str(Nk_list[0])+"+"+str(Nk_list[1])+".txt"
U_file = "U_file_Nk="+str(Nk_list[0])+"+"+str(Nk_list[1])+".txt"
U2_file = "U2_file_Nk="+str(Nk_list[0])+"+"+str(Nk_list[1])+".txt"
mu_file="mu_temp_Nk="+str(Nk_list[0])+"+"+str(Nk_list[1])+".txt"

def U(x):           # Scattering length equation.
    alpha = 1. - 1. / ( a_inv * r_0 )
    y = np.tan(x) - alpha*x
    return y

def fU0():       # Determination of depth of model square well.
    if a_inv < 0:
        x = optimize.bisect(U, 1e-5, np.pi/2-1e-5)
    elif a_inv > 0 :
        x = optimize.bisect(U, np.pi/2+1e-5, np.pi-1e-5)
    elif a_inv == 0:
        x = np.pi / 2.
    k_0 = x / r_0
    return 2 * k_0 ** 2
def create_grid():  # Choosing a meshgrid for integrals
    global k_i,w_i,xi,ek_i,U_0,xmu,Uk_kp,U2k_kp,epp
    (q_i, wq_i) = np.polynomial.legendre.leggauss(Nk_list[0])
    q_i = ( q_i + 1. )
    k_i = np.append( k_i, q_i )
    w_i = np.append( w_i, wq_i )
    (q_i, wq_i) = np.polynomial.legendre.leggauss(Nk_list[1])
    q_i = ( q_i + 1 ) * np.pi / 4.
    wq_i = wq_i * np.pi / 4.
    q_0 = 1. / r_0
    wq_i = wq_i * q_0 / np.cos( q_i ) ** 2
    q_i = 2. + q_0 * np.tan(q_i)
    k_i = np.append( k_i, q_i )
    w_i = np.append( w_i, wq_i )
    ek_i = k_i**2
    xi  = ek_i - xmu
    epp = energy_den(E_k, v2_k)/particle_den(v2_k)\
    - 2.*U_0*r_0 ** 3/( 9.*np.pi )
    if not os.path.exists(mu_file):
        np.savetxt(mu_file, xmu, fmt='%12.5e',
                   delimiter = ' ', newline=os.linesep)
    if not os.path.exists(Dk_file):
        delta_i = np.ones(Nk)
        np.savetxt(Dk_file, np.transpose([delta_i]),
                   fmt='%12.5e', delimiter = ' ',
                   newline=os.linesep)
```

```
    if not os.path.exists(U_file):
        import three_bal_inter as im
        im.U_k_kp(Nk, k_i)
        np.savetxt(U_file, np.transpose([U_mat]),
               fmt='%12.5e', delimiter = ' ',
               newline=os.linesep)
    if not os.path.exists(U2_file):
        import three_bal_inter as im
        im.U2_k_kp(Nk, k_i)
        np.savetxt(U2_file, np.transpose([U2_mat]),
           fmt='%12.5e', delimiter = ' ', newline=os.linesep)
    U_0 = fU0()
    Uk_kp = fU0()*np.loadtxt(U_file, unpack = True)
    U2k_kp = fU0()*np.loadtxt(U2_file, unpack = True)

def iterate(Nit):   # Iteration of gap equation
    global delta_i,E_k_0,nc
    # Initial guess for gap func.
    delta_i = np.loadtxt(Dk_file, unpack = True)
    # Interaction model
    Uk_kp=fU0()*np.loadtxt(U_file, unpack = True)
    for i in range(Nit):
       delta0_i = delta_i
       E_k_0 = np.sqrt(xi ** 2 + delta0_i ** 2)
       delta_i = -np.dot(Uk_kp, w_i*k_i*
       delta0_i / E_k_0)/(2*np.pi)
       tolerance = sum(abs(delta_i - delta0_i))
       if (tolerance <= 1.e-8) :
           np.savetxt(Dk_file, np.transpose([delta_i]),
            fmt='%12.5e', delimiter=' ', newline=os.linesep)
           break # Stopping the iteration after convergence
    print (i,"iteration")

def my_den(mu):   # Density equation
    global xi,E_k,v2_k
    xi = ek_i - mu
    iterate(Niter)
    E_k = np.sqrt(xi ** 2 + delta_i ** 2)
    v2_k = 0.5*(1.-( xi / E_k ))
    n = particle_den( v2_k )
    y = n - 1./(3. * np.pi ** 2)
    return y

def opt_mu(xmu): # Searching of true density
    (mu, infodict, ier, mesg)=\
         optimize.fsolve(my_den, xmu, full_output=1)
    print (mu, ier, mesg)
    print (infodict["fvec"])
    np.savetxt(mu_file, mu, fmt='%12.5e',
               delimiter=' ', newline=os.linesep)
    return mu

def particle_den(v2_k):
    return 2*int_k(v2_k)

def energy_den( E_k, v2_k  ):
    return int_k(( 2. * ek_i * v2_k - .5 * delta_i**2 / E_k ))

def int_k(fk_i): # Common integration function for integrals
```

```
    return np.sum( w_i*k_i**2*fk_i )/(2*np.pi**2)
```

```
# -*- coding: utf-8 -*-
"""
Created on Fri Oct 09 21:06:16 2015

----- The interaction module -----
In this module we calculate the model interaction
in k-space using the meshgrid points.

@author: Hasan Huseyin Somek
"""
import numpy as np
import three_bal_sr as sr
from numba import jit
@jit
def U_k_kp( Nk, k_i ):
    for i in range(Nk):
        for j in range(Nk):
            k = k_i[i]
            kp = k_i[j]
            if k == kp:
                sr.U_mat[i][j]=(1./k)*\
                (np.sin(sr.r_0*(k + kp))/(k+kp)-sr.r_0)
            else:
                sr.U_mat[i][j]=(1./k)*\
                (np.sin(sr.r_0*(k + kp))/(k+kp)
                - np.sin(sr.r_0*(k-kp))/(k-kp))

@jit
def U2_k_kp( Nk, k_i ):
    for i in range(Nk):
        for j in range(Nk):
            k = k_i[i]
            kp = k_i[j]
            if k == kp:
                sr.U2_mat[i][j]=(kp/k)*\
                (np.sin(sr.r_0*(k+kp))/(k+kp)-sr.r_0)
            else:
                sr.U2_mat[i][j]=(kp/k)*\
                (np.sin(sr.r_0*(k+kp))/(k+kp)
                - np.sin(sr.r_0*(k-kp))/(k-kp))
```

```
# -*- coding: utf-8 -*-
"""
Created on Sun Nov 29 01:27:03 2015

@author: Hasan Huseyin Somek
"""
import three_bal_sr as sr
import numpy as np
import os
a_inv_certain=[-2.5,-2,-1.5,-1,-0.7,-0.5,-0.4,-0.3,-0.2,-0.1,
               -0.2,0.,0.1,0.2,0.3,0.5,0.7,0.8,0.9,1.,1.5,2.,
               2.5,3,3.5,4,4.5,5,5.5,6]

a_inv_arr=np.linspace(-2.5,2.5,1001)
Ek_min_arr=np.zeros([len(a_inv_arr)])
delta_max_arr=np.zeros([len(a_inv_arr)])
```

```
epp_arr=np.zeros([len(a_inv_arr)])
mu_arr=np.zeros([len(a_inv_arr)])
mu_minus_epp_arr=np.zeros([len(a_inv_arr)])
half_E_bind_arr=np.zeros([len(a_inv_arr)])
difdelta=np.zeros([sr.Nk])
dmu_dlam=np.zeros([sr.Nk])
ddelta_dlam=np.zeros([sr.Nk])
my_path=os.getcwd()

for i in range(len(a_inv_arr)):
    print (i)
    sr.a_inv=a_inv_arr[i]
    exec(open('./three_bal_main.py').read())
    Ek_min_arr[i]=np.min(sr.E_k)
    delta_max_arr[i]=np.max(sr.delta_i)
    mu_arr[i]=sr.xmu
    epp_arr[i]=sr.epp
    mu_minus_epp_arr[i]=mu_arr[i]-epp_arr[i]
    if sr.a_inv>0:
        half_E_bind_arr[i]=-sr.a_inv**2
    else:
        half_E_bind_arr[i]=0
    if sr.a_inv in a_inv_certain:
        deltak_vs_k = "delta_k_ainv="+str(sr.a_inv)+\
        "_Nk="+str(sr.Nk_list[0])+"+"+str(sr.Nk_list[1])+".txt"
        np.savetxt(deltak_vs_k, np.transpose([sr.k_i,sr.delta_i]),
                   fmt='%12.5e', delimiter=' ', newline=os.linesep)
        v2k_vs_ainv="v2_k_ainv="+str(sr.a_inv)+\
        "_Nk="+str(sr.Nk_list[0])+"+"+str(sr.Nk_list[1])+".txt"
        np.savetxt(v2k_vs_ainv, np.transpose([sr.k_i,sr.v2_k]),
                  fmt='%12.5e', delimiter=' ', newline=os.linesep)
        Ek_vs_ainv="Ek_vs_ainv="+str(sr.a_inv)+\
        "_Nk="+str(sr.Nk_list[0])+"+"+str(sr.Nk_list[1])+".txt"
        np.savetxt(Ek_vs_ainv, np.transpose([sr.k_i,sr.E_k]),
                   fmt='%12.5e', delimiter=' ', newline=os.linesep)

mu_minus_epp="mu_minus_epp_Nk="+str(sr.Nk_list[0])+"+"\
+str(sr.Nk_list[1])+".txt"
np.savetxt(mu_minus_epp, np.transpose([mu_minus_epp_arr]),
           fmt='%12.5e', delimiter=' ', newline=os.linesep)
mu_vs_ainv="mu_vs_ainv_Nk="+str(sr.Nk_list[0])+"+"\
+str(sr.Nk_list[1])+".txt"
np.savetxt(mu_vs_ainv, np.transpose([a_inv_arr,mu_arr]),
           fmt='%12.5e', delimiter=' ', newline=os.linesep)
epp_vs_ainv="epp_vs_ainv_Nk="+str(sr.Nk_list[0])+"+"\
+str(sr.Nk_list[1])+".txt"
np.savetxt(epp_vs_ainv, np.transpose([a_inv_arr,epp_arr]),
           fmt='%12.5e', delimiter=' ', newline=os.linesep)
Ek_min_vs_ainv="Ek_min_vs_ainv_Nk="+str(sr.Nk_list[0])+"+"\
+str(sr.Nk_list[1])+".txt"
np.savetxt(Ek_min_vs_ainv, np.transpose([a_inv_arr, Ek_min_arr]),
           fmt='%12.5e', delimiter=' ', newline=os.linesep)
delta_max_vs_ainv="delta_max_vs_ainv_Nk="+str(sr.Nk_list[0])+"+"\
+str(sr.Nk_list[1])+".txt"
np.savetxt(delta_max_vs_ainv,
np.transpose([a_inv_arr,delta_max_arr]),
fmt='%12.5e', delimiter=' ', newline=os.linesep)
Eb_vs_ainv="Ebind_vs_ainv_Nk="+str(sr.Nk_list[0])+"+"\
+str(sr.Nk_list[1])+".txt"
```

```
np.savetxt(Eb_vs_ainv, np.transpose([a_inv_arr, half_E_bind_arr]),
           fmt='%12.5e', delimiter=' ', newline=os.linesep)
```

```
# -*- coding: utf-8 -*-
"""
Created on Sun Nov 29 13:23:01 2015

@author: Hasan
"""
"""
We plot all results of our study in this module.
"""
import matplotlib.pylab as plt
from matplotlib.ticker import MultipleLocator
import three_bal_sr as sr
import numpy as np
import os
my_path=os.getcwd()
sr.a_inv=1.
deltak_vs_ainv = "delta_k_ainv="+str(sr.a_inv)+\
"_Nk="+str(sr.Nk_list[0])+"+"+str(sr.Nk_list[1])+".txt"
v2k_vs_ainv="v2_k_ainv="+str(sr.a_inv)+\
"_Nk="+str(sr.Nk_list[0])+"+"+str(sr.Nk_list[1])+".txt"
Ek_vs_ainv="Ek_vs_ainv="+str(sr.a_inv)+\
"_Nk="+str(sr.Nk_list[0])+"+"+str(sr.Nk_list[1])+".txt"
mu_vs_ainv="mu_vs_ainv_Nk="+str(sr.Nk_list[0])+"+"\
+str(sr.Nk_list[1])+".txt"
epp_vs_ainv="epp_vs_ainv_Nk="+str(sr.Nk_list[0])+"+"\
+str(sr.Nk_list[1])+".txt"
Ek_min_vs_ainv="Ek_min_vs_ainv_Nk="+str(sr.Nk_list[0])+"+"\
+str(sr.Nk_list[1])+".txt"
delta_max_vs_ainv="delta_max_vs_ainv_Nk="+str(sr.Nk_list[0])+"+"\
+str(sr.Nk_list[1])+".txt"
Eb_vs_ainv="Ebind_vs_ainv_Nk="+str(sr.Nk_list[0])+"+"\
+str(sr.Nk_list[1])+".txt"
fidsus_vs_ainv="fidsus_vs_ainv_Nk="+str(sr.Nk_list[0])+"+"\
+str(sr.Nk_list[1])+".txt"
nc_vs_ainv="nc_vs_ainv_Nk="+str(sr.Nk_list[0])+"+"\
+str(sr.Nk_list[1])+".txt"

def plotting_delta_k(line_type,cl):
    plt.figure(1, figsize = (8,6))
    plt.xlim(0, 10)
    plt.ylim(-0.2, 1.5)
    plt.axes().xaxis.set_minor_locator(MultipleLocator(50))
    plt.axes().yaxis.set_minor_locator(MultipleLocator(0.25))
    plt.tick_params( axis = 'both', labelsize = 20 )
    plt.locator_params(axis='both',nbins=4)
    x,y=np.loadtxt(deltak_vs_ainv, unpack = True)
    plt.plot(x,y,line_type,color=cl,label='$1/ak_F=%4.1f$'%sr.a_inv)
    plt.xlabel('$ k/k_F $',fontsize = 20)
    plt.ylabel('$\Delta_k / \epsilon_F$', fontsize = 20 )
    plt.legend( prop = {'size':15} )
    delta_fig="delta_k3d.pdf"
    plt.savefig(my_path+'/Delta/'+delta_fig,bbox_inches='tight')

def plotting_vk2(line_type,cl):
    plt.figure(2, figsize = (8,6) )
    plt.xlim(0, 2)
```

```
    plt.tick_params( axis = 'both', labelsize = 20 )
    x,y=np.loadtxt(v2k_vs_ainv, unpack = True)
    plt.plot(x,y,line_type,color=cl,label='$1/ak_F=%4.1f$'%sr.a_inv)
    plt.xlabel( '$ k / k_F $', fontsize = 20 )
    plt.ylabel( '$ |v_k|^2 $', fontsize = 20 )
    plt.locator_params(axis='both',nbins=4)
    plt.legend( prop = {'size':15} )
    v2k_fig="vk2_3d.pdf"
    plt.savefig(my_path+'/v2_k/'+v2k_fig,bbox_inches='tight')

def plotting_phi_k(line_type,cl):
    plt.figure(7, figsize = (8,6) )
    plt.xlim(0, 3)
    plt.tick_params( axis = 'both', labelsize = 20 )
    x,y=np.loadtxt(v2k_vs_ainv, unpack = True)
    plt.plot(x, np.sqrt(y*(1-y)),line_type,color=cl,
             label='$1/ak_F=%4.1f$'%sr.a_inv)
    plt.xlabel( '$ k / k_F $', fontsize = 20 )
    plt.ylabel( '$ \phi_k $', fontsize = 20 )
    plt.locator_params(axis='both',nbins=4)
    plt.legend( prop = {'size':15} )
    phi_k_fig="phi_k_3d.pdf"
    plt.savefig(my_path+'/phi_k/'+phi_k_fig,bbox_inches='tight')
    plt.show()

def plotting_E_k(line_type,cl):
    plt.figure(3, figsize = (8,6) )
    plt.xlim(0, 2)
    plt.ylim(0, 3)
    plt.tick_params( axis='both', labelsize = 20 )
    plt.locator_params(axis='both',nbins=4)
    x,y=np.loadtxt(Ek_vs_ainv, unpack = True)
    plt.plot( x, y, line_type,color=cl,
             label='$1/ak_F=%4.1f$'%sr.a_inv)
    plt.xlabel('$ k/k_F $',fontsize = 20)
    plt.ylabel('$E_k / \epsilon_F$', fontsize = 20)
    plt.legend( prop = {'size':13}, loc=2 )
    Ek_fig="Ek_3d.pdf"
    plt.savefig(my_path + '/E_k/'+Ek_fig,
                bbox_inches='tight' )

def plotting_Ek_min_and_max_gap():
    plt.figure(9, figsize = (8,6) )
    plt.tick_params( axis = 'both', labelsize = 20 )
    plt.axes().xaxis.set_minor_locator(MultipleLocator(0.5))
    plt.axes().yaxis.set_minor_locator(MultipleLocator(0.5))
    x1,y1=np.loadtxt(Ek_min_vs_ainv, unpack = True)
    plt.plot(x1,y1,'-',color='deeppink',
             label='${E}^{min}/\epsilon_F$' )
    x2,y2=np.loadtxt(delta_max_vs_ainv, unpack = True)
    plt.plot(x2,y2,'--',color='purple',
             label='$\Delta^{max}/\epsilon_F$')
    plt.xlabel('$ 1/k_Fa $', fontsize = 20)
    plt.xlim(-1,2)
    plt.ylim(0,4)
    plt.locator_params(axis='both',nbins=4)
    plt.tick_params( axis = 'both', labelsize = 20 )
    plt.legend( prop = {'size':15}, loc=2)
    plt.savefig(my_path+'/E_k/'+"Ek_min_and_Gap3d.pdf",
```

```
                bbox_inches='tight')


def plotting_EPP_and_mu():
    plt.figure(2, figsize = (8,6) )
    plt.tick_params( axis = 'both', labelsize = 20 )
    plt.axes().xaxis.set_minor_locator(MultipleLocator(0.5))
    plt.axes().yaxis.set_minor_locator(MultipleLocator(0.5))
    plt.xlim(-2.,2.)
    plt.ylim(-2.,1.1)
    plt.xlabel('$ 1/k_Fa $', fontsize = 20)
    plt.locator_params(axis='x',nbins=4)
    plt.locator_params(axis='y',nbins=4)
    x1,y1=np.loadtxt(epp_vs_ainv, unpack = True)
    plt.plot( x1,y1, '--', color = 'magenta',label='$E/N$' )
    x2,y2=np.loadtxt(mu_vs_ainv, unpack = True)
    plt.plot( x2,y2,'-', color = 'purple',label='$\mu$' )
    x3,y3=np.loadtxt(Eb_vs_ainv, unpack = True)
    plt.plot( x3,y3,'-.', color = 'maroon',label='$E_b/2$' )
    plt.legend(prop={'size':15},loc=3)
    plt.savefig(my_path+'/E_k/'+"Epp_and_mu3d.pdf",
                bbox_inches='tight')

def plotting_chem_and_max_gap():
    fig, ax1 = plt.subplots(figsize = (8,6))
    plt.tick_params( axis = 'both', labelsize = 20 )
    x1,y1=np.loadtxt(mu_vs_ainv, unpack = True)
    ax1.plot(x1,y1, '--',color='darkorange' )
    ax1.plot(x1,np.zeros(len(y1)), ':',color='black' )
    ax1.set_xlabel('$ 1/k_Fa $', fontsize = 20)
    ax1.set_ylabel('$\mu/\epsilon_F$',fontsize = 20,
                   color='darkorange')
    plt.locator_params(axis='y',nbins=4)
    plt.ylim(-4, 1.1)
    plt.gca().yaxis.set_minor_locator(MultipleLocator(0.5))
    plt.locator_params(axis='both',nbins=9)
    for tl in ax1.get_yticklabels():
        tl.set_color('darkorange')
    ax2 = ax1.twinx()
    plt.tick_params( axis = 'both', labelsize = 20 )
    x2,y2=np.loadtxt(delta_max_vs_ainv, unpack = True)
    ax2.plot(x2,y2,color='brown' )
    ax2.set_ylabel('$\Delta^{max}/\epsilon_F$',fontsize = 20,
                   color='brown')
    for tl in ax2.get_yticklabels():
        tl.set_color('brown')
    plt.xlim(-2, 2)
    plt.ylim(0, 2)
    plt.gca().xaxis.set_minor_locator(MultipleLocator(0.5))
    plt.gca().yaxis.set_minor_locator(MultipleLocator(0.25))
    plt.locator_params(axis='both',nbins=4)
    fig.savefig(my_path+'/E_k/'+"Chem_pot_and_Gap3d.pdf",
                bbox_inches='tight')

def plotting_fid_sus():
    plt.figure(1, figsize = (8,6))
    plt.tick_params( axis = 'both', labelsize = 20)
    plt.gca().xaxis.set_minor_locator(MultipleLocator(0.5))
    plt.gca().yaxis.set_minor_locator(MultipleLocator(0.001))
```

```
    x,y=np.loadtxt(fidsus_vs_ainv, unpack = True)
    plt.plot(x, y, color='blue')
    plt.xlabel('$ 1/k_Fa $', fontsize = 20)
    plt.ylabel('$\chi / k^3_F$',fontsize = 20)
    plt.xlim(-2,2)
    plt.ylim(0,0.008)
    plt.locator_params(axis='both',nbins=6)
    plt.tick_params( axis = 'both', labelsize = 20 )
    plt.legend(prop = {'size':15})
    plt.savefig("fid_sus3d.pdf", bbox_inches = 'tight')

def plotting_cond_frac():
    plt.figure(2, figsize = (8,6))
    plt.tick_params( axis = 'both', labelsize = 20 )
    plt.gca().xaxis.set_minor_locator(MultipleLocator(1))
    plt.gca().yaxis.set_minor_locator(MultipleLocator(0.25))
    x,y=np.loadtxt(nc_vs_ainv, unpack = True)
    plt.plot(x, y, color='red')
    plt.xlabel('$ 1/k_Fa $', fontsize = 20)
    plt.ylabel('$n_c/k^3_F$',fontsize = 20)
    plt.xlim(-2.5,2)
    plt.locator_params(axis='both',nbins=4)
    plt.tick_params( axis = 'both', labelsize = 20 )
    plt.legend( prop = {'size':15})
    plt.savefig("cond_frac3d.pdf", bbox_inches = 'tight')

#cl='blue'
#lt='-'
#plotting_vk2(lt,cl)
#plotting_delta_k(lt,cl)
#plotting_E_k(lt,cl)
#plotting_fid_sus('-','blue')
#plotting_cond_frac('-','red')
#plotting_phi_k(lt,cl)
```

CURRICULUM VITAE

Name Surname: Hasan Hüseyin Sömek

Place and Date of Birth: Zeytinburnu/Istanbul 10.10.1990

Adress: Istanbul Technical University
Faculty of Science and Letters
Physics Engineering Department
B4-101 34469
Istanbul/Turkey

E-Mail: somek@itu.edu.tr

B.Sc.: Selçuk University

M.Sc.: Istanbul Technical University

Professional Experience and Rewards: Research Assistant in Istanbul Technical University (2013 -)